# Molecular Characterization of the Hsp70/Hsp90 Organizing Protein (Hop): Phosphorylation, Subcellular Localization and Interaction with Hsp90

A Thesis Submitted in Fulfillment of the Requirements for the Degree of

**DOCTOR OF PHILOSOPHY**

(BIOCHEMISTRY)

in the

DEPARTMENT OF BIOCHEMISTRY, MICROBIOLOGY AND BIOTECHNOLOGY

FACULTY OF SCIENCE

**RHODES UNIVERSITY**

by

**SHERIL DANIEL**

June 2007

# Declaration

I hereby declare that this submission is my own unaided work and that, to the best of my knowledge and belief, it contains no material previously published or written by another person, nor material which to a substantial extent has been accepted for the award of any other degree of the university or other institute of higher learning, except where due acknowledgement has been made in the text.

SHERIL DANIEL

This 19 day of NOVEMBER 2007

# ABSTRACT

Hop (Hsp70-Hsp90 Organizing Protein) is a co-chaperone of two major molecular chaperones, Hsp70 and Hsp90, and acts by transferring substrates from Hsp70 to Hsp90. Although under normal conditions Hop is predominantly localized within the cytosol, Hop has been detected in the nucleus under certain conditions including cell cycle arrest. A putative nuclear localization signal (NLS) has been identified within Hop, which overlaps with the TPR2A domain (previously shown to be critical for Hop-Hsp90 interactions). Hop is phosphorylated *in vitro* by two cell cycle kinases, namely, casein kinase II (CKII) at S189 and cdc2-kinase at T198; both residues are found upstream of the putative NLS and TPR2A domain. Mimicking phosphorylation at either phosphorylation site appeared to affect the subcellular localization of Hop. The aim of this study was to characterize Hop with respect to its phosphorylation status *in vivo*, as well as its subcellular localization pattern under heat stress and determine how these properties affected its interaction with Hsp90 as a co-chaperone. Dephosphorylation of proteins under normal and heat shock conditions changed the isoform composition of Hop, providing strong evidence that Hop was phosphorylated *in vivo*. Surface plasmon resonance (SPR) and glutatione-S-transferase (GST) co-precipitation studies showed that a cdc2-kinase phosphorylated mimic of Hop disrupted Hop-Hsp90 binding. A full length Hop-EGFP construct, as well as substitution mutants of the predicted NLS residues within the Hop-EGFP construct, were transfected into baby hamster kidney (BHK)-21 cells in order to establish the subcellular localization of Hop under heat stress and to test whether predicted residues were critical for nuclear localization of Hop. Under normal conditions, both Hop-EGFP and the NLS mutants were predominantly cytosolic, but

when the cells were subjected to heat stress, Hop and its NLS-mutants were localized to both the cytosol and the nucleus. SPR and GST co-precipitation studies showed that substitution of the residues within the major arm of the putative NLS abrogated Hop-Hsp90 interactions. The data obtained from this study, showed for the first time, that Hop was phosphorylated *in vivo* and suggested that phosphorylation of Hop by cdc2-kinase could inhibit Hop-Hsp90 interactions. Moreover, these results suggested that the subcellular localization of Hop was dependent on stress levels of the cell, particularly heat stress. We propose that the nuclear localization of Hop may be primarily regulated by stress and secondarily by cell cycle arrest. The major arm of the putative NLS did not affect the localization of Hop directly, but was shown to be critical for Hop-Hsp90 binding *in vitro*. The results of this study suggested that binding of Hop to Hsp90 sequestered Hop within the cytosol and that Hsp90 acted as a cytosolic retention factor for Hop. Both phosphorylation of Hop, and its subcellular localization, appeared to be intimately related to its interaction with Hsp90 as a co-chaperone.

*For Ammachi (Mrs. Mariamma George)*

*And*

*In remembrance of a beloved Appachan*
*(Shri. P.P. George).*

*Two roads diverged in a yellow wood*
*and sorry I could not travel both*
*And be one traveller, long I stood*
*and looked down one as far as I could*
*to where it bent in the undergrowth;*

*Then took the other, as just as fair,*
*and having perhaps the better claim*
*because it was grassy and wanted wear;*
*though as for that, the passing there*
*had worn them really about the same,*

*And both that morning equally lay*
*in leaves no feet had trodden black.*
*Oh, I kept the first for another day!*
*Yet knowing how way leads on to way,*
*I doubted if I should ever come back.*

*I shall be telling this with a sigh*
*Somewhere ages and ages hence:*
*Two roads diverged in a wood, and I --*
*I took the one less travelled by,*
*and that has made all the difference*

*- Robert Frost*

# ACKNOWLEDGEMENTS

I acknowledge, with deep gratitude, my supervisor, Prof. Gregory L. Blatch, who has been a guide and mentor to me in the science profession. His enthusiasm and dedication as a researcher has inspired me, and this project would certainly not have been possible without his expert advice and insight at every stage of the process. Furthermore, his approachable nature and unparalleled support of his students has made this journey that much easier and memorable.

I thank my co-supervisor, Dr. Graeme Bradley whose expertise in 2D-gel electrophoresis, and all things technical, has contributed indispensably to the practical aspect of this work. Moreover, his useful suggestions with respect to the written part of the work has added to it, and is sincerely appreciated.

This project was funded by the following sources, which are thankfully acknowledged:

- The Department of Biochemistry, Microbiology and Biotechnology (Rhodes University)
- The Andrew Mellon Prestigious scholarship (Rhodes University)
- The Wellcome Trust Fund
- The NRF-Grant holder bursary
- The NRF-Hungary Grant.

I also acknowledge the following contributions:

- Prof. Peter Csermely and Dr. Csaba Söti, for the provision of various reagents and the use of the Biacore X apparatus with which all the SPR studies were conducted. Thank you also to Dr. Söti whose technical expertise in SPR provided valuable contributions to this part of the project.
- The Natal EM unit and Prof. Edith Elliott for the kind use of the confocal microscope facilities.
- Dr. Caroline Knox and Ms. Lindsay Murray, for their input into the cell culture and microscopic work conducted, as well generously providing various reagents for this work.
- Dr. Vicky Longshaw (my “Crisis Buddy”), who lent her technical expertise to many experiments and who has been a source of inspiration, support and encouragement to me throughout this project. Thank you also, for meticulously proof-reading this thesis and for your valuable input and additions that have contributed significantly to improving the final product!
- The Rhodes University Graphics Unit for their expertise with the figures generated.
- Sam McCann, Dani Marais and Layle Henderson for kindly proof-reading various sections of this work and for the much appreciated feedback!

- ALL past and present members of the Chaperone Research Laboratory (Lab 301). Lab 301 has been a source of advice, support and many memorable moments of comic relief!
- The staff and all fellow colleagues of the department of Biochemistry, Microbiology and Biotechnology (Rhodes University) for their support and encouragement during my project.

I express my deepest gratitude to my family! Thank you especially, to my parents (Mr. and Mrs. Mary and George Daniel) and my sister, Shija Daniel, for their unwavering belief in me and for helping me to stand strong during the storm. Thank you to my incredibly supportive husband, Abraham Thomas, who came right in time to rescue me from academic insanity! I am indebted to the Longshaw family (Geoff, Jenny and Vicky Longshaw), who generously opened their homes to me during the initial and final stages of this thesis, and supported me in every way possible. I thank all my friends from the bottom of my heart for their encouragement, support and companionship! Above all, I thank God, for bringing opportunities my way, for courage and wisdom to make difficult choices and for giving me a glimpse of His beauty and skill.

# TABLE OF CONTENTS

DECLARATION……ii
ABSTRACT……iii
DEDICATION……v
ACKNOWLEDGEMENTS……vi
TABLE OF CONTENTS……viii
LIST OF FIGURES……xii
LIST OF SYMBOLS AND STANDARD ABBREVIATIONS……xiv
LIST OF RESEARCH OUTPUTS……..xvi

## CHAPTER ONE
### INTRODUCTION

TITLE PAGE 1

1.1 LITERATURE REVIEW 2
1.1.1 The ‘Crowded’ Cell 2
1.1.2 Protein Folding and Molecular Chaperones 3
1.1.3 Subcellular Protein Translocation 5
1.1.4 Protein Translocation into the Nucleus 7
1.1.5 Regulation of Nuclear Protein Import 11
1.1.6 The Cell Cycle Control System 14
1.1.7 The Heat Shock Response 16
1.1.8 Heat Shock Proteins 17
1.1.9 Hsp70 18
1.1.10 Hsp90 24
1.1.11 Hop (**H**sp70-Hsp90-**O**rganizing **P**rotein) 29
1.1.12 Hop Modulates Hsp70 and Hsp90 Chaperone Pathways 32
1.1.13 Hop’s Interactions Beyond Hsp70 and Hsp90 35

1.2 MOTIVATION FOR THIS STUDY AND PROBLEM STATEMENTS THEREOF 39

1.3 PRIMARY HYPOTHESIS 42

1.4 SECONDARY HYPOTHESES 42

## CHAPTER TWO
### THE PHOSPHORYLATION STATUS OF HOP


TITLE PAGE 43

2.1 INTRODUCTION 44
2.2 EXPERIMENTAL PROCEDURES 45
2.2.1 Tissue Culture and Heat Shock of NIH 3T3 Mouse Fibroblast Cells 45
2.2.2 Harvesting Cells for One-Dimensional (1D) and Two-Dimensional (2D) Gel Electrophoresis 45
2.2.3 SDS-PAGE 46
2.2.4 2D Gel Electrophoresis 46
2.2.4.1 Protein Quantitation 46
2.2.4.2 Protein Clean-Up 47
2.2.4.3 Isoelectric Focusing (IEF) 47
2.2.5 Western Analysis 48
2.2.5.1 Protein Transfer/Blotting onto Nitrocellulose 48
2.2.5.2 Chemiluminescence-Based Immunodetection 48
2.2.5.3 Primary and Secondary Antibody Dilutions 49
2.2.6 Analysis of the Phosphorylated State of Hop *In Vivo* 49
2.3 RESULTS 51
2.3.1 Heat Shock Response Was Induced at 42$^{o}$C But Hop Protein Levels Did Not Change 51
2.3.2 Acidic Isoforms of Hop Emerged After Heat Shock 51
2.3.3 Hop was Phosphorylated *In Vivo* at 37$^{o}$C 54
2.3.4 Hop was Phosphorylated Differently *In Vivo* at 42$^{o}$C Versus 37$^{o}$C 54
2.4 DISCUSSION 58


## CHAPTER THREE
### THE SUBCELLULAR LOCALIZATION OF HOP


TITLE PAGE 62

3.1 INTRODUCTION 63
3.2 EXPERIMENTAL PROCEDURES 65
3.2.1 The Subcellular Localization of Hop-EGFP and Derivatives of the Putative NLS Under Normal Conditions, Heat Shock and G1/S Arrest, Using Confocal Fluorescence Microscopy 65
3.2.1.1 Generation and Analysis of Plasmid Constructs Encoding Hop-EGFP and its Mutant Derivatives 65
3.2.1.2 The Subcellular Localization of Hop-EGFP and its Mutant Derivatives Under Various Treatments by Confocal Laser Scanning Fluorescence Microscopy 66

3.2.1.2.1 Tissue Culture and Heat Shock of Baby Hamster Kidney (BHK)-21 Cells 66
3.2.1.2.2 Transient Transfection of BHK-21 Cells and Preparation of Cells For Confocal Microscopy 66
3.2.1.2.3 Confocal Laser Scanning Fluorescence Microscopy 67
3.2.2 The Subcellular Localization of Hop, Hsp70 and Hsp90 Under Normal and Heat Shock Conditions Using Biochemical Fractionation 67
3.3 RESULTS 69
3.3.1 pB-mSTI1-EGFP and its Derivative Constructs Were Successfully Generated 69
3.3.2 Hop-EGFP and its Derivative Constructs were Predominantly Localized to the Cytosol Under Normal Conditions 74
3.3.3 Hop-EGFP and its Derivative Proteins Localized to the Nucleus Under Heat Shock 74
3.3.4 Hop-EGFP and its NLS Mutants Showed Increased Incidence of Nuclear Localization Under Conditions of G1/S Arrest 79
3.3.5 β-actin Localizes Predominantly to the Cytosol Under Normal and Heat Shock Conditions 79
3.3.6 Hsp70 Translocated to the Nucleus After Heat Shock 81
3.3.7 Endogenous Hop Co-localized With Hsp70 and Hsp90 to the Cytosol, Membranes and Cytoskeletal Fractions Under Normal Conditions and After Heat Shock 81
3.3.8 Endogenous Hop Co-localized With Hsp70 But Not Hsp90 in Heat Shocked Nuclear Fractions 83
3.4 DISCUSSION 84

## CHAPTER 4
## AN INVESTIGATION INTO THE POSSIBLE INTERACTIONS OF THE PUTATIVE NLS AND *IN VITRO* PHOSPHORYLATION SITES OF HOP IN HOP-HSP90 BINDING

TITLE PAGE 90

4.1 INTRODUCTION 91
4.2 EXPERIMENTAL PROCEDURES 93
4.2.1 Generation and Analysis of Plasmid Constructs Encoding GST-Hop and its Derivative Proteins 93
4.2.2 Expression and Purification of GST-Tagged Proteins 93
4.2.3 Surface Plasmon Resonance Spectroscopy (SPR) Analysis 93
4.2.4 GST-Co-Precipitation Assays 94
4.3 RESULTS 96
4.3.1 pGEX3X2000 and its Derivatives Were Successfully Generated 96
4.3.2 GST-Hop and its Derivative Proteins Were Successfully Expressed and Purified 97

4.3.3 The Interaction of GST-Hop and Derivative Proteins With Hsp90 Using SPR Analysis 101
4.3.4 The Interaction of GST-Hop Derivative Proteins With Hsp90 Using GST-Co-Precipitation Assays 101
4.4 DISCUSSION 105

**CHAPTER 5**
**CONCLUSION**

TITLE PAGE 109

5.1 CHAPTER 2 110
5.2 CHAPTER 3 110
5.3 CHAPTER 4 111
5.4 DISCUSSION 112

**REFERENCES** 126

**APPENDIX**
A1 Special Reagents and Chemicals 139
A2 Technical Data Obtained from Amersham 142
A3 Preparation of Supercompetent Cells 143
A4 Transformation of Supercompetent Cells 143
A5 Induction Studies 144
A6 Expression and Purification of GST-Tagged Proteins 144
A7 Bradfords Assay 145
A8 Site Directed Mutagenesis 146
A9 Restriction Endonuclease Digestion of Double-Stranded DNA 147
A10 Agarose Gel Electrophoresis 148
A11 DNA Sequencing 148

B1 Generation of a Recombinant Antibody against GST-C334 (C-Terminus of Hop) 150
B1.1 Purification of GST-Fusion Protein GST-C334 150
B1.2 Generation of Recombinant Antibodies 150
B1.3 Recombinant Antibody Against C-terminus of Hop was Generated and Successfully Tested 151

C Oligonucleotide Primers 152

# LIST OF FIGURES


Figure 1.1 Affinity of importin-α for an NLS bearing protein is increased in the presence of importin-β (adapted from Lange *et al.*, 2007). **10**

Figure 1.2 The mechanism of heat shock response in humans (adapted from Kiang and Tsokos, 1999). **19**

Figure 1.3 A summary of known cellular functions of Hop (adapted from Daniel *et al.*, 2006). **38**

Figure 1.4 Partial amino acid sequence of Hop showing the predicted bipartite NLS, the TPR2A domain and a flanking C-terminal helix. **41**

Figure 2.1 Heat shock responses was induced at 42$^{o}$C but the protein levels of Hop were not changed by the heat shock response. **52**

Figure 2.2 Acidic isoforms of Hop emerged after heat shock. **53**

Figure 2.3 Hop was phosphorylated *in vivo* at 37$^{o}$C. **56**

Figure 2.4 Hop was phosphorylated differently *in vivo* at 42$^{o}$C versus 37$^{o}$C. **57**

Figure 3.1 The identity of pSK-mSTI1-EGFP was restriction analyzed with *Not* I and *Xho* I. **71**

Figure 3.2 Codon changes for the K239A and K237/238/239A substitutions were successfully engineered in pSK-mSTI1-EGFP. **72**

Figure 3.3 The coding regions for mSTI1-EGFP, mSTI1-K239A-EGFP and mSTI1-K237/238/239A-EGFP were successfully ligated into the pBCMGSneo (pB) vector. **73**

Figure 3.4 Hop-EGFP and its NLS mutants localized predominantly to the cytosol under normal conditions. **76**

Figure 3.5 Hop-EGFP and its derivatives were predominantly cytosolic under normal conditions but translocated to the nucleus under heat shock conditions. **77**

Figure 3.6 Hop-EGFP and its NLS derivatives localized to the nucleus during heat shock. **78**

Figure 3.7 Hop-EGFP and its NLS mutants localize to the nucleus when the cells are treated with hydroxyurea. **80**

Figure 3.8 Biochemical fractionation analysis of Hop, Hsp70 and Hsp90 under normal conditions and heat shock conditions. **82**

Figure 4.1 pGEX3X2000 and its NLS-mutated derivatives were successfully generated. **98**

Figure 4.2 Phosphorylation mimic constructs pGEX3X2000 (S189E) and pGEX3X2000 (T198E) were successfully generated and confirmed using restriction endonuclease analysis. **99**

Figure 4.3 GST-Hop and its derivative proteins were successfully expressed and purified. **100**

Figure 4.4 Surface plasmon resonance (SPR) spectroscopy was used to determine the apparent affinity of GST-Hop and its derivative proteins for purified Hsp90. **102**

Figure 4.5 Mutations in the major arm of the NLS abrogated Hop-Hsp90 binding whereas cdc2-kinase phosphorylation of Hop may disrupt binding of Hop to Hsp90. **103**

Figure 4.6 Interaction of GST-Hop derivative proteins with purified Hsp90. **104**

Figure 4.7 Ribbon representations of the structure of TPR2A of Hop and the C-terminal TPR acceptor motif of Hsp90. **107**

Figure 5.1 Predicted model for Hop's interaction as an Hsp70-Hsp90 co-chaperone. **113**

Figure 5.2 Minor arm of the putative NLS acts as a Monopartite NLS with a second possible NLS downstream? **117**

Figure B1 Antibody generated toward the C-terminus of Hop successfully detected Hop in positive controls **151**

# LIST OF SYMBOLS AND STANDARD ABBREVIATIONS

| | |
|---|---|
| % | Percentage |
| $A_{260}$ | Absorbance at 260 nanometers |
| $A_{280}$ | Absorbance at 280 nanometers |
| ADP | Adenosine diphosphate |
| ATP | Adenosine triphosphate |
| bp | Base pair |
| $CO_2$ | Carbon dioxide |
| Da | Daltons |
| g $L^{-1}$ | Grams per liter |
| g $mL^{-1}$ | Grams per milliliter |
| g | Gram / relative centrifugal force (gravity) |
| HCl | Hydrochloric acid |
| kDa | kiloDalton |
| L | Litre |
| M | Molar |
| mA | Milliamperes |
| mg | Milligram |
| min | Minutes |
| mL | Milliliter |
| mm | Millimeter |
| mM | Millimolar |
| mol | Mole |
| nm | Nanometer |
| $^oC$ | Degree Celcius |
| pmol | Picomole |
| rpm | Rotations per minute |
| U | Units |
| V | Volts |
| v/v | Volume per volume |
| W | Watts |
| w/v | Weight per volume |
| α | Alpha |
| β | Beta |
| γ | Gamma |
| µg | Microgram |
| µL | Microlitre |
| µM | Micromolar |

| Amino Acids | Abbreviation | Code |
|---|---|---|
| Alanine | Ala | A |
| Arginine | Arg | R |
| Asparagine | Asn | N |
| Aspartate | Asp | D |
| Cysteine | Cys | C |
| Glutamate | Glu | E |
| Glutamine | Gln | Q |
| Glycine | Gly | G |
| Histidine | His | H |
| Isoleucine | Iso | I |
| Leucine | Leu | L |
| Lysine | Lys | K |
| Methionine | Met | M |
| Phenylalanine | Phe | F |
| Proline | Pro | P |
| Serine | Ser | S |
| Threonine | Thr | T |
| Tryptophan | Trp | W |
| Tyrosine | Tyr | Y |
| Valine | Val | V |

| Nucleotides | Code |
|---|---|
| Adenosine | A |
| Cytosine | C |
| Guanine | G |
| Thymidine | T |

The nomenclature used for the twenty amino acids and the four nucleotides listed above are as outlined by the International Union of Pure and Applied Chemists (IUPAC) and the International Union of Biochemistry and Molecular Biology (IUBMB).

# LIST OF RESEARCH OUTPUTS

## Publications

**Daniel S**., Bradley G., Longshaw V.M., Söti C., Csermely P. and Blatch G.L. 2007. Nuclear translocation of the phosphoprotein Hop (Hsp70/Hsp90 organizing protein) occurs under heat shock, and its proposed nuclear localization signal is involved in Hsp90 binding. *Biochimica et Biophysica Acta* (Molecular Cell Research). **Under Review**.

Gordon, A., Blatch, G.L., **Daniel, S**. and Muller, W. 2007. Stress protein responses in South African freshwater invertebrates exposed to detergent surfactant linear alkylbenzene sulfonate (LAS). Environmental Toxicology. **Under Review**.

**Daniel S**., Söti C., Csermely P., Bradley G. and Blatch G.L. 2006. Hop: an Hsp70/90 co-chaperone that functions within and beyond Hsp70-Hsp90 protein folding pathways. In: Blatch G.L. ed. Networking of Chaperones by Co-Chaperones. Austin: Landes Bioscience; New York: Springer Science + Business Media, 26-37.

Boshoff A., Nicoll W.S., Hennessy F., Ludewig M., **Daniel S**., Modisakeng K.W., Shonhai A., McNamara C., Bradley G., and Blatch G.L. 2004. Molecular chaperones in biology, medicine and protein biotechnology. South African Journal of Science (Rhodes Centenary Issue), 100: 665-677.

**Daniel S.**, Limson J., Dairam A., Watkins, G. and Daya S. 2004. Through metal binding, curcumin protects against lead- and cadmium-induced lipid peroxidation in rat brain homogenates and against lead-induced tissue damage in rat brain; Journal of Inorganic Biochemistry. 98: 266 – 275.

Pillay R., Maharaj D.S., **Daniel S.** and Daya S. 2003. Acetylcholine reduces cyanide-induced superoxide anion generation and lipid peroxidation in rat brain homogenates; Progress in Neuro-Psychopharmacology and Biological Psychiatry. 27: 61 – 64;

## International Conference Proceedings

Daniel S., Bradley, B., Söti C., Csermely P., Blatch, G.L. 2005. Mapping of functional residues in the Hsp70/Hsp90 organizing protein, mSTI1. FEBS J. 272: G1-013P. Joint 30'th FEBS/9'th IUBMB conference, Budapest, Hungary.

## Local Conference Proceedings

Daniel S., Bradley, B., Söti C., Csermely P., Blatch, G.L. 2005. The regulatory effects of cell cycle kinases on localization and function of the murine stress inducible protein 1 (mSTI1). SASBMB XIX Conference, Stellenbosch, South Africa.

# CHAPTER 1

# INTRODUCTION

*"The pure and simple truth is rarely pure and never simple."*

*- Anon*

# 1.1 LITERATURE REVIEW

## 1.1.1 The 'Crowded' Cell

The biological cell is a membrane-bound unit composed of a concentrated aqueous solution of chemicals and is capable of duplicating itself through the process of cell division (Alberts *et al.*, 1998). The total percentage of the volume occupied by macromolecules present within a cell is approximately 20-30% (i.e. within a concentration range of 200-300 g $L^{-1}$). The steric significance of this proportion results in a large volume of the cell being unavailable to other molecules, and allows the interior environment of the cell to be designated as 'crowded' (as reviewed by Ellis, 2001b, 2007). Thus most biomolecules have evolved to function within crowded environments and the functioning of protein machineries within the cell reflects this appropriately.

Almost all the major processes that take place in a cell are driven by the assembly of a number of protein molecules, which interact with each other to form 'protein machineries'. These protein machineries may eventually interact with other protein complexes such that they form networks of interactions and interwoven functions within the cell (reviewed in Alberts, 1998; Ellis, 2007). This is particularly fascinating, in light of the crowded environments that they function in. For example, in the case of a single cell of *Escherichia coli* (*E. coli*) the total concentration of protein and RNA is estimated to be in the range of 300-400 g $L^{-1}$ (Zimmermann and Minton, 1991). A measurement of the diffusion coefficients for large molecules such as green fluorescent protein (GFP) and small molecules like carboxyfluorescein within the cytoplasm, have shown a three to tenfold reduction compared to their values in water (Kao *et al.*, 1993; Elowitz *et al.*, 1999).

Although crowding reduces the rate of diffusion as shown by the above-mentioned examples, it increases the thermodynamic activities of various biochemical reactions within the cell (Burg, 2000). As a result, some biochemical effects caused by the crowded cellular environment include an increase in macromolecular association

reactions, oligomerization of various molecular components, the formation of multicomponent complexes within specific biological pathways and the unfolding of proteins induced by stress. The increased proximity of polypeptide chains during the process of folding and the associated increase in the thermodynamic activity of partly folded polypeptides, thus poses the danger of misfolding and the binding of these polypeptide chains to one another causing aggregation (Ellis, 2001b, 2007). Since the diffusion rate may be slowed down to a greater extent in the case of larger polypeptides, than that of small polypeptides, this may mean that the increase in aggregation may be more predominant in smaller polypeptide chains. Aggregation of proteins into non-functional bodies is seen in various forms, for e.g. inclusion bodies in a bacterial system and plaques in human amyloid disease (Burg, 2000; Ellis, 2001b, 2007).

### 1.1.2 Protein Folding and Molecular Chaperones

The folding of proteins into their three-dimensional structures is fundamental for efficient functionality, long-term stability in crowded biological environments as well as their correct subcellular localization. Moreover, protein folding is a process that is coupled to the regulation of cellular growth, cell cycle events and differentiation (Radford and Dobson, 1999). Early work in this field showed that all the information required for a protein to fold into its basic structural elements was contained within its amino acid sequence. Despite the large number of total possible conformations into which a protein can fold, the native state most proteins usually assume is the lowest thermodynamic energy conformation possible under the physiological conditions. The more stable native-like interactions between residues are preferred over non-native ones, thus achieving its lowest possible energy three-dimensional structure (reviewed in Dobson, 2003; Pauwels *et al.*, 2007).

It is believed that a smaller number of amino acid residues within the protein interact to form a ‘folding nucleus’ and the remainder of the structure condenses around it. The final structure is achieved when all the side chains become occupied in a closely packed arrangement and water is excluded from the core of the protein (Fersht, 2000; Cheung *et*

*al.*, 2002; Dobson, 2003). Partially folded proteins may unavoidably expose certain residues, which are otherwise buried within the native structure, to the solvent and thus be prone to aggregation or inappropriate interactions with other molecules within the cell (as reviewed by Ellis, 2001a, 2007). Protein damage may not always be induced by environmental stress, and sometimes may be caused by some of its inherent properties such as mutations that disrupt its native structure. Using a *Caenorhabditis elegans* polyglutamine aggregation model, it was shown that mutation of a single protein that caused misfolding, disrupted the general protein homeostasis within the cellular environment (Gidalevitz *et al.*, 2006). Failure within protein folding pathways is linked to a wide variety of pathological conditions, including cystic fibrosis, Alzheimer's and Parkinson's disease, the spongiform encephalopathies and type II diabetes (reviewed by Thomas *et al.*, 1995; Horwich, 2002; Dobson, 2003).

The cell employs various strategies to counteract this problem of protein misfolding and aggregation. One such strategy lies in the form of a class of proteins termed 'molecular chaperones', which assists other proteins in assembling and disassembling and which removes itself from the final functional structure of the proteins they assist (Ellis, 2007). Molecular chaperones are known to interact with nascent polypeptide chains, as they emerge from the ribosome (co-translational), as well as assist proteins in later stages of folding processes (post-translational). Molecular chaperones can not only prevent the misfolding of proteins, but sometimes are involved in the rescue of misfolded and aggregated proteins, and usually require ATP for efficient functioning. A classic example of well-studied chaperone machinery is the bacterial GroEL/GroES system, which belongs to the family of chaperonins. This system operates by the sequestering of incompletely folded polypeptides within a cage-like structure in GroEL, so that the polypeptide is shielded from the complex outer environment (reviewed in Bukau and Horwich, 1998; Hartl and Hayer-Hartl, 2002; Ellis, 2007).

Although chaperones increase the efficiency of protein folding, they normally do not increase the folding rate constants significantly. There is, however, a second strategy

employed by the cell to prevent the misfolding of proteins. Folding catalysts such as the peptidylprolyl isomerases and protein disulphide isomerases operate by speeding up potentially slow steps in the folding process. The former acts by increasing the rate of *cis-trans* isomerization of peptide bonds involving proline residues and the latter enhances the rate of formation and reorganization of disulphide bonds (Schiene and Fischer, 2000). Outer membrane proteins (OMP) of bacteria, such as PhoE in E.*coli*, have been shown to fold *in vivo* at a comparatively faster rate than other proteins (Jansen *et al.*, 2000; Tamm *et al.*, 2004). A proposed folding catalyst for such OMPs is SurA, a periplasmic peptidyl-prolyl isomerase whose peptidyl-prolyl activity lies in a parvulin-like domain in the C-terminus. However, SurA also has chaperone-like activity in its N-terminus, and it appears that both domains play a part in its protein folding activity (Lazar and Kolter, 1996; Behrens *et al.*, 2001).

A third strategy employed by the cell in combating problems arising from protein misfolding is in the form of the steric chaperones (Ellis, 1998). These are proteins that are synthesized with a prosequence, which is essential for the correct folding of the rest of the chain but is then proteolytically removed. Examples of proteases that fall under the category of steric chaperones are subtilisin and α-lytic protease. Lipase-specific foldases are specific for lipases, as the name obviously suggests and are active within extracellular medium. Fimbrial chaperones provide an otherwise missing β-strand to a folding fibrila subunit, which otherwise aggregates in the periplasm and are degraded by proteases (as reviewed in Ellis, 1998; Pauwels *et al.*, 2007).

### 1.1.3 Subcellular Protein Translocation

Due to the differences in specificity of the environment offered by each subcellular compartment that affects the physiological and enzymatic activities of proteins as well as the particular localization of protein-interaction partners, many proteins are targeted toward specific subcellular compartments. Thus proteins are not functional until they are accurately transported to their destination after synthesis on ribosomes in the cytoplasm (Simon and Blobel, 1991). The ‘signal hypothesis’ was first put forward by Gunter

Blobel, who postulated the presence of 'codes' i.e. short peptide motifs present in the amino acid sequence of the proteins that directed these proteins to their various subcellular compartments such as the ER, nucleus, mitochondria etc. (Simon and Blobel, 1991; Sheilds, 2001).

Proteins that are destined for secretion to the extracellular environment are first translocated to the ER, which contains a range of molecular chaperones and folding catalysts (Zimmermann *et al.*, 2006). Transport into the ER usually occurs through the recognition of an N-terminal cleavable signal sequence on the protein and the subsequent transport of the protein through a hydrophilic channel that is part of the protein translocation machinery. This is usually the Sec61 pathway in eukaryotes (Zimmermann *et al.*, 2006). The Sec61 complex consists of three units which together form a heterotrimeric complex. A number of heterotrimers are strategically located around a central aqueous pore through which the proteins are translocated. Proteins that have a less hydrophobic signal sequence are transported by another membrane protein complex known as the Sec62/63 complex. In addition, the molecular chaperones, Hsp70 (heat shock protein) and its co-chaperone Hsp40 (these are discussed in sections 1.1.7-1.1.10) along with nucleotide exchange factors, are also involved in this protein translocatory process (reviewed by Osborne *et al.*, 2005; Dudek *et al.*, 2006; Zimmermann *et al.*, 2006; Flower, 2007).

Most mitochondrial proteins are synthesized in the cytosol and then transported to the mitochondria via translocatory protein complexes found in the inner and outer mitochondrial membranes (Hoogenraad *et al.*, 2002). The receptors found on the surface of the outer mitochondrial membrane (Tom) including Tom20, Tom22, Tom70 and the channel protein Tom40, comprise the translocatory machinery at this site, whereas a suite of proteins comprising the Tim translocases are found on the inner mitochondrial membrane (Hoogenraad *et al.*, 2002). Tom70 recognizes internal targeting signals within the amino acid sequences of mitochondrial proteins and is now known to possess a chaperone-binding region. A number of molecular chaperones such as Hsp70 and Hsp90

(discussed in detail in sections 1.1.7-1.1.10) are implicated along with TOM 70 in mitochondrial protein recognition and translocation (Young *et al.*, 2003).

A number of diseased conditions are associated with mislocalization of proteins within the cell. BARD1 (breast cancer-associated protein) and BRCA1 (breast and ovarian cancer susceptibility protein 1) are binding partners and both shuttle between the nucleus and cytoplasm by means of individual nuclear export signals (NES) that direct proteins out of the nucleus and into the cytosol. BARD1 is proapoptotic within the cytoplasm. Interestingly, both BARD1 and BRCA1, in binding to one another, can mask their respective NES, and their resulting nuclear compartmentalization can lead to cell cycle arrest and the promotion of breast cancer (Fabbro *et al.*, 2002; Schüchner *et al.*, 2005). Similarly, in the case of the adenomatous polyposis coli (APC), protein which is a tumor suppressor, the loss of a functional NES within the amino acid sequence resulted in the arrest of the protein within the nucleus and this phenomenon was observed in colorectal cancer cells (Henderson and Fagotto, 2002; Rosin-Arbesfeld *et al.*, 2003).

### 1.1.4 Protein Translocation into the Nucleus

Nuclear proteins, or proteins destined to translocate to the nucleus at some point in their lifetime, are synthesized on free ribosomes in the cytoplasm and transported to the nucleus through the nuclear pore complexes (NPCs) found in the nuclear envelope (Lange *et al.*, 2007). The NPC is a proteinaceous structure with a molecular mass of about 125 MDa in mammalian cells and about 60 MDa in yeast. It contains an aqueous diffusion channel that is approximately 10 nm in diameter through which molecules smaller than 40 kDa can passively diffuse. However, larger proteins require the importing transport mechanism and its recognition of intrinsic nuclear localization signals (NLSs) uniquely present in proteins, which are targeted, to the nucleus. NLSs are short peptide sequences that are necessary and sufficient for nuclear localization of their respective proteins (reviewed in Allen *et al.*, 2000; Yoneda, 2000; Chook and Blobel, 2001; Suntharalingam and Wente, 2003; Lange *et al.*, 2007).

Mutation or deletion of the NLS has been shown to lead to cytosolic localization of the protein in question. The NLS has also been shown to be active in nuclear targeting of a normally cytosolically localized carrier protein. Unlike signal sequences that target proteins into the ER or mitochondria, the NLS is not deleted after or during translocation, but remains as part of the protein molecule (reviewed in Yoneda, 1997, 2000). The NLS of simian virus 40 (SV40) large T-antigen was the first example of an NLS to be identified at the level of its amino acid sequence and this NLS contains a basic amino acid cluster, which is thought to be a characteristic feature of most NLSs. Classical NLSs are divided into two main groups, a single basic type like that found in SV40 large T-antigen, and a bipartite basic type, consisting of two series of basic residues separated by a 10 to 12 amino acid spacer such as that found in nucleoplasmin (reviewed in Dingwall and Laskey, 1991; Yoneda, 2000; Lange *et al.*, 2007).

Non-classical NLSs such as the M9 sequence found in hnRNP (heterogenous nuclear ribonucleoprotein) A1, have also been described previously, and these contain both a signal for nuclear import as well as one for nuclear export, both of which are mediated by pathways that are distinctly different from that of the classical NLSs. Another novel nucleocytoplasmic shuttling domain, KNS, was identified in the hnRNP K shuttling protein, which also confers nuclear import and export qualities to hnRNP K but its import pathway appears to be different from that of the M9 or classical NLSs (Michael *et al.*, 1995; Michael *et al.*, 1997; Krebber and Silver, 2000).

The functioning of NLSs is believed to be through recognition/ligand-receptor-like interactions and it has been shown to be only an entry signal having no part to play in the further retention of the protein within the nucleus (Lange *et al.*, 2007). An NLS can however, confer specific regulatory properties associated with active transport to the protein carrying it, such as temperature and/or ATP dependent nuclear transport (Breeuwer and Goldfarb, 1990). Nuclear transport of proteins bearing a classical NLS is mediated by the importin-$\alpha/\beta$ heterodimer, also known as karyopherin-$\alpha/\beta$ (Moroianu *et al.*, 1995). The process of the classical NLS-mediated nuclear import of proteins is

composed of three stages: (a) docking at the NPC (b) translocation through the NPC and (c) deposition of the cargo within the nucleus.

During the first stage the nuclear protein in the cytosol binds to importin-α and this complex is targeted to the NPC. In the second stage, translocation through the NPC requires the small-guanosine 5' triphosphatase (GTPase) Ran, GTP and physiological temperature. Binding of the cargo protein-importin-α complex to importin-β is responsible for the docking of the cargo protein-importin-α complex to the NPC (Moroianu *et al.*, 1995; Mattaj and Englmeier, 1998). Once the protein-importin-α complex is inside the nucleus, importin-β dissociates from the protein complex by binding to Ran loaded with GTP to form a Ran-GTP-importin complex, which then allows importin-α to be taken back to the cytoplasm for further nuclear protein import processes (reviewed in Lange *et al.*, 2007) as shown in figure 1.1.

The 3-D structure of importin-α reveals a short N-terminal binding domain for importin-β, and a large NLS binding domain, which is comprised of 10 tandem armadillo (ARM) repeats. The ARM repeats form a concave binding groove containing a major binding site and a minor binding site for the NLS (Conti *et al.*, 1998; Kobe, 1999; Fontes *et al.*, 2000; Fontes *et al.*, 2005). Monopartite NLS sequences can bind to both sites but only binding to the major site has been shown to be physiologically relevant (Conti *et al.*, 1998; Conti and Kuriyan, 2000). The bipartite NLS sequence binds to both binding sites, with the major binding site of importin-α recognizing the major arm of the NLS and the minor binding site of importin-α recognizing the minor arm of the NLS (Fontes *et al.*, 2000). Interestingly, the importin-β binding domain (IBB) on importin-α mimics an NLS, and binds to the NLS binding domain of importin-α, in the absence of importin-β (Kobe, 1999; Fanara *et al.*, 2000; Catimel *et al.*, 2001). Thus the affinity of importin-α for its NLS bearing substrates is increased in the presence of importin-β, as depicted in figure 1.1.

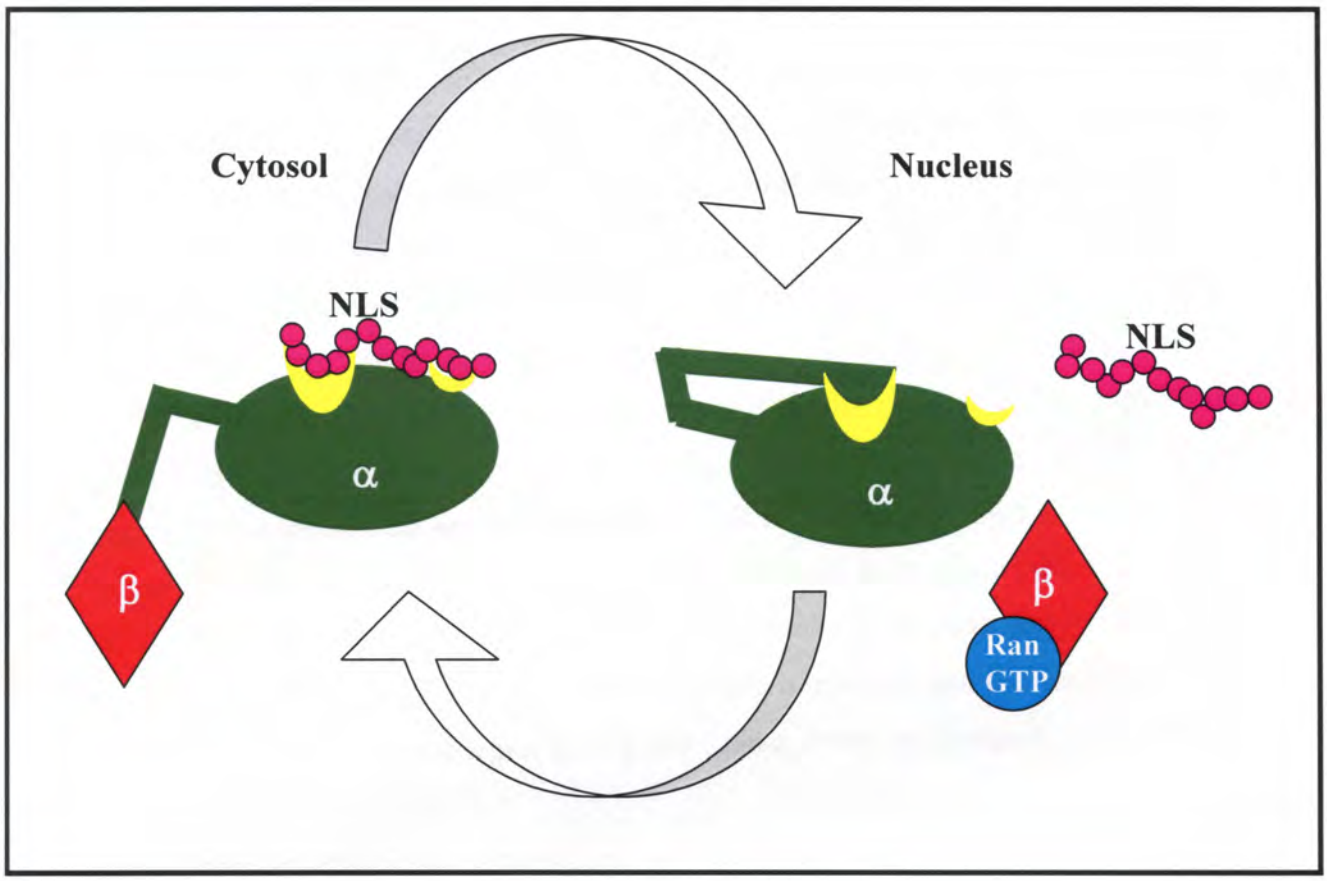


**Figure 1.l: Affinity of importin-α for an NLS bearing protein is increased in the presence of importin-β (adapted from Lange *et al.*, 2007).** A simple schematic showing a bipartite NLS peptide (pink) bound to the major and minor binding domains (yellow) of importin-α (dark green) and the importin-β-binding (IBB) domain of importin-α bound to importin-β (red) in the cytosol. Importin-β facilitates the transport of the importin-NLS complex into the nucleus, after which, its interaction with RanGTP releases it from the flexible IBB. The IBB competes with the NLS peptide for the major binding site on importin-α, which results in a low affinity of importin-α for the NLS peptide, and this facilitates delivery of the NLS-bearing protein cargo into the nucleus.

### 1.1.5 Regulation of Nuclear Protein Import

Various factors have been shown to influence the NLS function of a particular protein. One such factor is the position of the NLS within a protein. The general consensus is that an NLS has to be located on the surface of the protein to be accessible for recognition (Roberts *et al.*, 1997) and studies have shown that the protein context surrounding the NLS can play a role in mediating interactions with importin-α (Friedrich *et al.*, 2006).

The tumour suppressor p53 is linked to DNA repair, apoptotic cell death and genomic stability functions within the cell, and translocates to the nucleus by means of an NLS found at residues 316-322. Moreover, two basic residues, Lys305 and Arg306 also contributed to the nuclear localization of p53, in addition to its NLS. Interestingly, a region of the amino acid sequence proximal to its NLS, residues 326-355, was found to constitute a cytoplasmic sequestration domain (CSD), which also contained an NES (340-351). The CSD was shown to reduce the efficiency of nuclear import of p53 by interfering with the binding of the NLS of p53 with importin-α and this was independent of NES activity in the same region (Liang and Clarke, 1999a, b; Stommel *et al.*, 1999).

Intra- and intermolecular interactions of the NLS (or NLS-containing proteins) (Khokhlatchev *et al.*, 1998) may further regulate nuclear localization (Kaffman and O'Shea, 1999). In the case of the p53 tumour suppressor, it has been suggested that the basic domain comprising of Lys305-Arg306, which is only nine amino acids proximal to its NLS, may interact with the CSD and in doing so present the NLS in a conformation that enhances binding of the NLS to importin α (Liang and Clarke, 1999a, b). The glucocorticoid receptor (GR) belongs to the steroid hormone receptor (SR) family and is generally inactive in the cytosol, while complexed with a number of proteins such as the 90-kDa heat shock protein (Hsp90). In the active state, GR binds to its ligand and accessory proteins like Hsp90 are found to dissociate from the GR-ligand complex, allowing for rapid nuclear translocation and the activation of gene expression. Ligand withdrawal from GR is associated with the export of GR back to the cytosol (Guiochon-Mantel *et al.*, 1996; Kaffman and O'Shea, 1999).

The association of certain proteins that lack a functional NLS, with an NLS-bearing protein, is known as the 'piggy-back' effect. This association may be responsible for the transport of an NLS-devoid protein greater than 40 kDa, into the nucleus (Jans and Hubner, 1996). In the filamentous fungal system (*Aspergillus nidulans*), the Hap complex consisting of subunits B, C and E, are a class of DNA binding transcription factors. HapB was shown to possess an NLS at its C-terminus, outside the conserved region required for both DNA binding and interaction with the other subunits, HapC and HapE. Although HapC and HapE do not carry an NLS, they were shown to translocate to the nucleus in the presence of HapB, suggesting that the mechanism of nuclear entry was by complexing with HapB and "piggy-backing" on the NLS of HapB as a heterotrimeric DNA binding complex (Steidl *et al.*, 2004; Kato, 2005).

Phosphorylation is known to affect the affinity of a cargo protein for its receptor, and thereby influence the outcome of the subcellular localization of the cargo protein. The integrin-linked kinase (ILK), a major signaling integrator in mammalian cells, is phosphorylated by p21-activated kinase 1 (PAK1) at its threonine 173 and serine 246 residues *in vitro* and *in vivo*. ILK is mainly localized in the cytoplasm and cytoskeleton, but has been detected in the nuclei under specific conditions. A functional NLS as well as NES motif was identified in the amino acid sequence of ILK and it was shown that the selective depletion of PAK1 caused an increase in nuclear accumulation of ILK. These results suggested that the ILK shuttles dynamically between the nucleus and cytoplasmic compartments of the cell, and that this subcellular translocation of ILK is regulated by phosphorylation by PAK1 (Chun *et al.*, 2005; Acconcia *et al.*, 2007).

Phosphorylation sites close to the NLS have been shown to enhance or inhibit NLS activity of the protein through phosphorylation – mediated regulatory modules, also known as phosphorylation-regulated NLSs. Phosphorylation of the APC protein at a site immediately adjacent to the C-terminus of an NLS showed to negatively influence the nuclear import of the full- length protein (Zhang *et al.*, 2000). Other studies showed that mimicking phosphorylation at a site adjacent to an NLS could decrease the affinity of the

NLS for importin α (Harreman *et al.*, 2004). The nuclear import of the yeast transcription factor *Swi5* is inhibited by phosphorylation of residues proximal to its two NLSs (Moll *et al.*, 1991) and this was confirmed by Harreman *et al.* (2004).

The nuclear localization of SV40 large T-antigen (T-ag) is subject to regulation by cell cycle-regulatory kinases, casein kinase II (CKII) and cdc2-kinase, at sites that are within the vicinity of the NLS, and this determines both the rate and the absolute amount of T-ag that accumulates in the nucleus (Jans and Hubner, 1996). Phosphorylation at the CKII site at S112 increases the rate of NLS-dependent nuclear import, and phosphorylation by cdc2-kinase at T124 inhibits nuclear import. It is understood that phosphorylation at these sites may modulate the recognition of the NLS by importin-α and that there is no direct interaction of the phosphorylated residues with the importin receptor. This regulatory module for T-ag nuclear transport is referred to as the 'CcN motif' ('C' for CKII, 'c' for cdc2-kinase and 'N' for NLS) and is also found in c-myc (human), B-myb (human) and $p110^{RBI}$ (mouse) (Fontes *et al.*, 2003).

Phosphorylation of the importin transport machinery may be involved in the regulation of nuclear import of proteins. Phosphatase inhibitors okadeic acid and microcystin were shown to inhibit transport mediated by β-importin and this inhibition was partially reversed by the protein kinase inhibitor staurosporine. The phosphatase inhibitors mentioned above, did not have any effect on substrate binding by the α/β importin complex, or the association of this complex with the NPC. This suggested that phosphorylation of a component of the nuclear transport machinery could inhibit nuclear transport of NLS-mediated proteins and that this may be a global mechanism utilized by cells to negatively regulate nucleocytoplasmic trafficking (Kehlenbach and Gerace, 2000). The importin α/β-dependent nuclear transport can also be affected by various cell cycle phases in a manner that is independent of phosphorylation. A decrease in the efficiency of the α/β-transport machinery was observed at the early S, $G_2$/M and $M_1/G_1$ phases (the cell cycle phases are discussed in the next section), thereby suggesting that

the nuclear protein import pathways are also regulated in harmony during cell cycle progression (Yasuhara *et al.*, 2004).

### 1.1.6 The Cell Cycle Control System

The cell cycle control system is a biochemical device comprised of a set of interacting proteins that induce and coordinate the processes involved in the cell cycle. A number of signals exist, which function to stop the cell cycle at specific checkpoints. Signals that arrest the cycle usually act on the $G_1$ control point, which is referred to as the '$G_1$ checkpoint' in higher eukaryotes, whereas in yeast this control point is referred to as 'start'. In a continuously cycling cell the $G_1$ checkpoint is the point where the cell-cycle control system triggers the S phase and the $G_2$ checkpoint is where it triggers the initiation of the M phase (reviewed in Alberts *et al.*, 1994; King and Cidlowski, 1998; Schafer, 1998).

Two main families of proteins participate in the cell cycle control system, namely the cyclin-dependent protein kinases (Cdk) and the cyclins (Kohn, 1999; Kovarova *et al.*, 2003). The Cdks are responsible for inducing the various downstream processes by phosphorylating selected proteins on serines and threonines, whereas the cyclins are a family of specialized Cdk-activating proteins that are known to be highly unstable and continuously 'cycling' during the cell cycle. Four major cyclins (D, E, A and B) are produced sequentially as the cells proceed through the cycle. Entry into mitosis requires the association of cyclin B, with cdc2-kinase (cell division cycle 2, also known as cdk1; Cdc28 in budding yeast), and this results in the activation of cdc2-kinase (also known as $p34^{cdc2}$). In eukaryotic cells, the mitotic phase is initiated by the activation of the $p34^{cdc2}$ protein kinase, which rises to a high level at the onset of M phase and remains high throughout most of this process (Moreno and Nurse, 1990; Kohn, 1999; Kovarova *et al.*, 2003).

In the eukaryotic system the $G_2$ to M phase transition in the cell cycle is controlled by the M-phase promoting factor (MPF). Mitotic cyclin accumulates gradually during the $G_2$

phase and binds to cdc2 to form the MPF complex. Before mitosis, cdc2-Cyclin B1 complexes are held in an inactive state by cdc2 phosphorylation at Thr 14 and Tyr 15. Phosphorylation of the complex is catalyzed by Wee1, Myt1 and related protein kinases. Activation of the MPF complex is initiated by the dephosphorylation of Tyr 15 by cdc25 phosphatase and inhibition of Wee1-like kinases. Other mechanisms that control the dephosphorylation of cdc2 exist and include the protein kinase, Plx, which phosphorylates cdc25 in mitosis (Jin *et al.*, 1998; Kohn, 1999).

Evidence from human cells and starfish oocytes support the possibility that initiation of mitosis is not only accompanied by cdc2 dephosphorylation, but also by changes in the subcellular localization of cyclin B1 (Jin *et al.*, 1998; Porter and Donoghue, 2003). During S phase and $G_2$, cyclin B1 accumulates in the cytoplasm. Just before mitosis, the majority of cdc2-cyclin B1 complexes are found in the nucleus. Since many of the key substrates for the cdc2-Cyclin B1 complex are found in the nucleus, this shuttling of cdc2-Cyclin B1 complexes between nucleus and cytoplasm may be necessary to control mitosis. Interestingly, Cyclin B1 does not have an NLS, but has a leucine rich NES which binds to an export mediator, CRM1, and enables its export from the nucleus to the cytosol. The NES is found within a CSD and phosphorylation of four specific serine residues found within the NES inhibited binding of the NES to CRM1. The mechanism of nuclear localization of the cyclin B1-cdc2 complex is speculated to involve a “piggy-back” mechanism, through the interaction of the cyclin B1-cdc2 complex with cyclin F which translocates into the nucleus through two functional NLSs (Kong *et al.*, 2000; Yang *et al.*, 2001; Porter and Donoghue, 2003).

A protein that plays a significant role in the transition of cells from the $G_0$ phase to the $G_1$ phase of the cell cycle, and in the continuing passage through the early $G_1$ phase is CKII (Pyerin, 1994). CKII is a widely distributed cyclic-AMP-independent protein kinase, which phosphorylates proteins on their serine and threonine residues (Dingwall and Laskey, 1991) and which is itself phosphorylated extensively in mitotic cells, as well as likely to be regulated by cdc2-kinase (Bosc *et al.*, 1995). The regulation of CKII by cdc2-

kinase may mean that CKII is regulated during cell division, and is thus, likely to mediate some effects of MPF (Mulner-Lorillon *et al.*, 1990).

### 1.1.7 The Heat Shock Response

The challenges cells face during their life cycle include starvation, infection, changes in their physical or chemical condition and genotoxic damage, all of which can induce acute and/or chronic stress. Studies in Drosophila salivary glands showed that an increase in temperature of a few degrees above the physiological level caused the induction of a specific group of molecular chaperones termed 'heat shock proteins' (Hsp) and the protective mechanism was termed the heat shock response (Sørensen *et al.*, 2003). Both prokaryotic and eukaryotic systems react to the heat shock response, which is required to preserve cellular function and homeostasis. Although chronic exposure of extreme stress is harmful to the cell, the resultant induction of Hsps is beneficial in instilling stress tolerance as well as providing cytoprotection against stress-induced molecular damage. Moreover, transient exposure to high temperatures was found to bring about a cross-protective effect to the cell against sustained, normally lethal exposures to other forms of stress (as reviewed in Santoro, 2000; Pockley, 2003; Sørensen *et al.*, 2003).

Under normal non-stressful conditions the heat shock transcription factor (HSF) exists as a cytoplasmic, transcriptionally inactive, non-DNA binding monomer (Pirkkala *et al.*, 2001; Pockley, 2003). Four forms of HSF have been identified in vertebrates, of which only HSF1 and HSF2 are conserved, with HSF1 being the main heat shock factor involved in stress response, and HSF2 being selectively induced during early developmental stages. As shown in figure 1.2, the heat shock response stimulates the assembly of HSF1 into active homotrimers (oligomerization) and subsequent translocation into the nucleus, where they are capable of binding to the consensus heat shock element (HSE) located in the promoter region of the heat shock genes (Jacquier-Sarlin *et al.*, 1994; Hong *et al.*, 2001; Pirkkala *et al.*, 2001; Pockley, 2003).

HSF is phosphorylated further, and Hsp mRNA is transcribed and leaves the nucleus for the cytosol where new Hsp protein is synthesized (Kiang and Tsokos, 1998; Santoro, 2000). A number of molecular chaperones including the heat shock proteins 70 and 90 (discussed in further sections) play a role in modulating the activation of HSF1 by forming stable complexes with HSF1 and by stabilizing the monomeric conformation of HSF1 (Shi *et al.*, 1998; Zou *et al.*, 1998; Dai *et al.*, 2003). Modulation of the transcription of heat shock genes is also maintained during non-stressful conditions such as during progression through the cell cycle, development and differentiation of the cell, or following exposure of the cell to molecules that regulate cell proliferation (Santoro, 2000; Pockley, 2003).

### 1.1.8 Heat Shock Proteins

Heat shock proteins are highly conserved, ubiquitous, and abundant in nearly all the subcellular compartments. They are divided into different families according to molecular size in kilodaltons (Hsp 100, Hsp 90, Hsp70, Hsp 60, etc) (Santoro, 2000). The Hsps, mainly Hsp70 and Hsp90 play a direct role in the autoregulation of the heat shock response because, as described in section 1.1.7, they are bound to the inert form of HSF within the cytosol under unstressed conditions. It is the stress signal, which is usually in the form of an influx of non-native proteins, that causes the release of HSF from the Hsps, and the resultant stress-induced transcription (Shi *et al.*, 1998; Zou *et al.*, 1998; Santoro, 2000; Pockley, 2003).

Abrupt increases in temperature produced aggregation of non-native proteins within inclusion bodies in an *E. coli* mutant strain that was defective in the heat shock response (Gragerov *et al.*, 1991). This suggested that the Hsps, among other molecular chaperones, were essential elements in the reduction of such intracellular aggregation processes. The Hsps reversibly interact with nascent chains to minimize off-pathway interactions and thereby increase the yield of native folded protein (Smith *et al.*, 1998). Hsps are also involved in the protection of proteins from irreversible denaturation caused by heat and other stressors such as exposure to heavy metals or viral infections, as well as assisting

them in renaturation. In accordance with this conclusion, most members of the Hsp family were found to be over expressed under physiological as well as stressed conditions (as reviewed by Lindquist and Craig, 1988; Santoro, 2000; Sørensen *et al.*, 2003).

Besides their intracellular chaperoning tasks, members of specific heat shock protein families such as Hsp60, Hsp70 and Hsp90, are regarded as highly immunogenic to the host's cellular immune system (Multhoff *et al.*, 1998). An involvement of heat shock proteins in several autoimmune diseases and in anti-cancer immune responses has also been reported (Multhoff *et al.*, 1998). Hsps have also been shown to protect the cell from injury during metabolic stress (Williams *et al.*, 1993), inflammation (Polla *et al.*, 1998), viral infection (Amici *et al.*, 1994) and ischemia (Mestril *et al.*, 1994).

Hsps are also involved in protein translocation across various organelles such as the ER and the mitochondria. A number of mitochondrial proteins are encoded by nuclear genes, synthesized in the cytoplasm, and then transported across one or both mitochondrial membranes as described in section 1.1.3. Proteins are translocated across the mitochondria in a linear manner as unfolded chains, and both cytoplasmic as well as, mitochondrial heat shock proteins participate in the unfolding and refolding pathways (reviewed in Bursac and Lithgow, 2006; Zimmermann *et al.*, 2006).

### 1.1.9 Hsp70

One of the most studied Hsp families is the 70 kDa Hsp (Hsp70), whose structure is widely conserved through evolution from bacteria to man, indicating an important role in the survival of the organism (Lindquist and Craig, 1988). In the mammalian system, the Hsp70 family is composed of four members: Hsc70 (heat shock cognate), which is constitutively expressed, the inducible Hsp70, BiP (immunoglobulin heavy-chain binding protein), and mtHsp70 (mitochondrial Hsp70). For the purposes of this study, 'Hsp70' will be used as a general term indicating the collective family of Hsp70 proteins including Hsc70. Any specific member of the Hsp70 family will be indicated by the appropriate description, e.g. Hsc70.

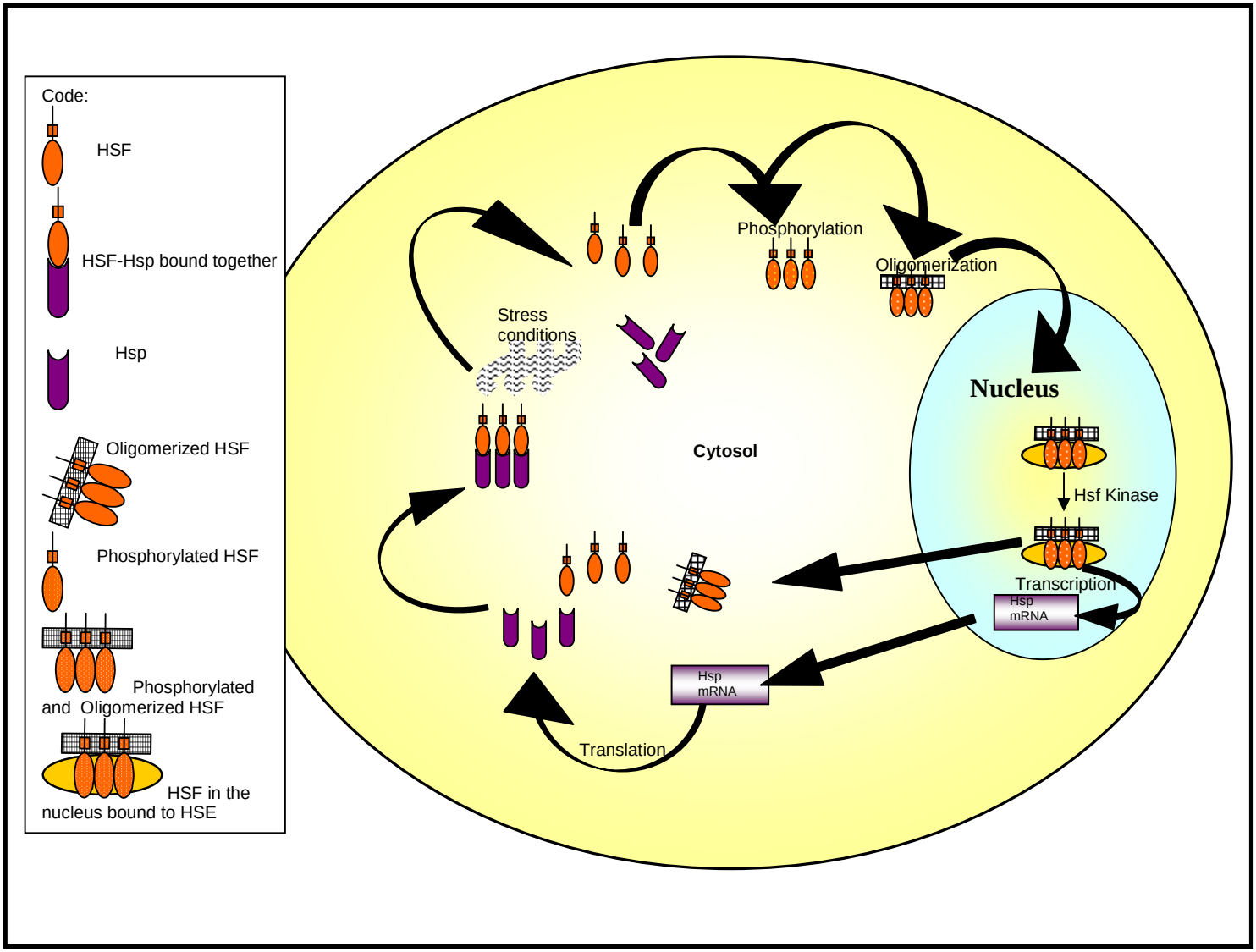


**Figure 1.2: The mechanism of heat shock response in humans (adapted from Kiang and Tsokos, 1999).** Heat shock factor (HSF) that resides in the cytosol under normal conditions is usually found bound to heat shock proteins (Hsp) and inactive. Under stress conditions, HSF separates from Hsp and are phosphorylated by protein kinases. They also oligomerize to form trimers in the cytosol that enter the nucleus and bind to heat shock elements (HSE) in the promoter region of the HSP gene. HSF is further phosphorylated by HSF kinase and the HSP mRNA is transcribed, which translocates to the cytosol and new Hsps are synthesized. HSF also translocates to the cytosol and remains bound to Hsp until the cell undergoes stress again.

The members of the Hsp70 family have been found to be compartment specific; Hsc70 and inducible Hsp70 are localized in the cytosol, whereas BiP and mtHsp70 are found in the ER and mitochondrial matrix, respectively (Fink, 1999). This subcellular localization is essential for the coordinated action of these proteins in the translocation of polypeptides across membranes (Arispe and De Maio, 2000). Hsp70 is known to localize to the nucleus where it regulates the activity of certain nuclear DNA-binding transcription factors (Diehl *et al.*, 2003). The presence of a functional NLS within the C-terminus of Hsp70 has been alluded to, as well as a role for Hsp70 in piggybacking proteins devoid of an NLS into the nucleus. The fusion of a C-terminal Hsp70 peptide and the p50 subunit of NF-κB, a key transcriptional regulator of inflammatory responses, allowed for the nuclear translocation of the NF-κB subunit, and its interaction with DNA (Fujihara and Nadler, 1999). Hsc70 accumulates in the nucleus and nucleolus after heat stress, and a functional NLS and NES have been identified in this heat shock protein. It is suggested that the NLS could be capable of functionally masking the NES, as a mechanism of nucleocytoplasmic traffic regulation of Hsc70 (Tsukahara and Maru, 2004). Hsc70 has also been reported to be involved in the regulation of the subcellular localization of a temperature sensitive p53 mutant $p53^{Val\text{-}135}$. The temperature sensitive mutant accumulated in the nucleus at 32$^{o}$C and acted like the unmutated form, but it was shown to be sequestered in the cytosol at 37$^{o}$C. It was postulated that the association of $p53^{Val\text{-}135}$ with Hsc70 at 32$^{o}$C and not 37$^{o}$C inhibited its interaction with the nuclear import receptor (Akakura *et al.*, 2001).

Hsp70 proteins are composed of two functionally coupled domains. The N-terminal ATPase domain (44 kDa) binds ATP with high affinity in the presence of potassium or magnesium and mediates the hydrolysis of ATP. This process is responsible for the regulation of substrate recognition (Rudiger *et al.*, 1997). The C-terminal domain consists of two functional subdomains, one of which (18 kDa) recognizes and binds substrate polypeptides, and the other (10 kDa) forms a lid over the peptide-binding pocket (Rudiger *et al.*, 1997). The ATP-bound form of Hsp70 binds and releases substrate rapidly, resulting in a low overall affinity of Hsp70 for substrate, whereas the ADP-form

binds substrate slowly but more stably (Palleros *et al.*, 1991). The regulatory motif, EEVD at the C-terminus is conserved among nearly all the eukaryotic cytosolic Hsp70s (Multhoff *et al.*, 1998). Deletion or mutation of EEVD affects the ATPase activity, the ability to interact with substrate, and interferes with the ability of the mutant Hsp70 to interact with HDJ-1 in the refolding of denatured firefly luciferase (Freeman *et al.*, 1998).

Hsc70 is essentially involved in the folding and refolding of proteins, in maintaining their unfolded/transport state, and in the elimination of non-functional proteins through a cycle of ATP binding, hydrolysis and nucleotide exchange (Johnson *et al.*, 1998). The inducible Hsp70, on the other hand, is expressed when cells are exposed to stress and the feedback regulation of inducible Hsp70 contributes to the overall Hsp70 abundance needed to maintain efficient chaperoning activity. The increased abundance of Hsp70 under stress conditions helps to stabilize non-native polypeptides through the binding of exposed hydrophobic peptide segments on partially unfolded proteins, or newly synthesized proteins, as well as during protein translocation and degradation (Rudiger *et al.*, 1997; Tutar *et al.*, 2006). It has been reported that both normal and cancer cells require Hsc70 to be viable, and that cancer cells have an additional requirement for the inducible Hsp70 (Nylandsted *et al.*, 2000; Rohde *et al.*, 2005).

The mammalian Hsp70 is believed to interact with the growing polypeptide chain as it emerges from the ribosome, thus facilitating its exit and preventing premature aggregation (Hartl and Hayer-Hartl, 2002). Hsp70, through its refolding and degradation activities, was shown to reduce the levels of aggregation and toxicity of α-synuclein, a natively unfolded protein that can self-aggregate and form oligomers, which pose a risk in neurons for the development of Parkinson's disease (Klucken *et al.*, 2004). Hsp70 was also shown to associate with newly synthesized Huntingtin protein and play a role in suppressing the aggregation of this protein, which is associated with Huntington's disease (Jana *et al.*, 2000)

Cell surface localization of Hsp70 related proteins is postulated to be involved in chronic inflammatory lesions of several experimental autoimmune diseases, however, contradictory findings have demonstrated that members of the Hsp70 family possess the ability to protect tissues from the deleterious effects of inflammation (Jacquier-Sarlin *et al.*, 1994). Such protection is believed to involve prevention of DNA strand breaks induced by reactive oxygen species and lipid peroxidation as well as protection of mitochondrial structures and functions. The processing and presentation of bacterial and tumoural antigens, is another factor contributing to the protection offered to the immune system by the Hsp70 family (Multhoff *et al.*, 1998).

Evidence is also beginning to suggest a likely role for heat shock proteins, especially Hsp70, in cell cycle control under normal conditions. Studies conducted by Nakamura *et al*. (1999) demonstrate an interaction between Hsc70 and $p27^{Kip1}$, an inhibitor of cyclin-dependent kinase (CDK), during G1/S transition. Cell cycle transitions require the sequential activation of CDKs and inactivation of CDK inhibitors. Complex formation of Hsc70 and $p27^{Kip1}$ was shown to be cell cycle dependent and maximum accumulation occurs at the G1/S transition where levels of $p27^{Kip1}$ were found to be dramatically decreased (Nakamura *et al.*, 1999). Investigations by Diehl *et al*. (2003) suggest the association of Hsc70 with newly synthesised cyclin D1 (the regulatory subunits of the CDK4/6 kinase) and the direct involvement of Hsc70 with cyclin D1 in a mature, catalytically active cyclin D1/CDK4 holoenzyme complex.

Ectopic expression of Hsc70 has been shown to increase the cyclin D1 steady state levels, thereby increasing its availability to activate its catalytic partner CDK4. An Hsc70 mutant lacking ATPase activity, Hsc70 K71E, failed to stabilize cyclin D1, confirming that Hsc70 chaperone function is required for cyclin D1 maturation (Diehl *et al.*, 2003). The same authors also report the identification of a majority of co-purifying Hsc70 found where newly synthesized cyclin D1 is preferentially localized, implying that Hsc70 is involved in the folding of cyclin D1 prior to its assembly into complexes with CDK4. It has also been suggested that the necessity for coexpression of Hsc70 along with cyclin

D1 insinuates that Hsc70 may be a limiting factor when cyclin D1 is over-expressed (Diehl *et al.*, 2003).

Cdc2-kinase has been shown to interact with Hsp70-2 gene (expressed only in spermatogenic cells) in mouse testis cells, it was concluded that Hsp70-2 acts as a molecular chaperone for cdc2-kinase, and is required for its formation (Zhu *et al.*, 1997). Another key molecule of the cell cycle control system is the retinoblastoma protein (pRB), which acts as a suppressor molecule by suppressing transcription in its nonphosphorylated or hypophosphorylated state, while bound to the E2F (eukaryotic) family of transcription factors. G1-Cdk is required to phosphorylate pRB and in this way activates E2F-dependent transcription of S-phase genes subsequently allowing for DNA synthesis (Inoue *et al.*, 1995). Hsc70 has been shown to bind selectively to nonphosphorylated pRB, thereby rendering it unsusceptible to *in vitro* phosphorylation (Helmbrecht *et al.*, 2000).

Various co-chaperones modulate the ATPase activity of Hsp70 and thus influence the affinity of the chaperone for polypeptide substrates (Hartl, 1996). In eukaryotes, the Hsp70 co-chaperone, Hsp40, stimulates the hydrolysis of ATP thereby stimulating the ATPase activity of Hsp70. Nucleotide exchange factors such as BAG1 a (Bcl2-associated anthanogene) promote nucleotide exchange thereby enhancing the ATPase activity of Hsp70 (reviewed by Hohfeld, 1998; Hennessy *et al.*, 2005; Bracher and Brodsky, 2006). In *E. coli*, however, this process is regulated by the ATPase-activating protein DnaJ (bacterial homolog of Hsp40) and a nucleotide exchange factor GrpE. Only in the presence of both proteins, is DnaK (bacterial homologue of Hsp70) able to undergo efficient cycles of ATP-binding and hydrolysis. Hip (Hsp70 interacting protein) is a 50-kDa cytosolic protein that stimulates the assembly of the Hsp70-Hsp40-substrate complex. Hip has been found to interact with the ATPase domain of Hsc70 and is capable of stabilizing its ADP-bound conformation such that the unfolded polypeptide has more time to attain its proper conformation before being released from the chaperone complex (reviewed in Hennessy *et al.*, 2005; Rosser and Cyr, 2006; Bracher and Brodsky, 2006).

Once it is released, the polypeptide either folds to its native state, or is passed on to other molecular chaperones, which includes the Hsp90 chaperone machinery.

### 1.1.10 Hsp90

The Hsp90 family of proteins is one of the most abundant cytosolic protein families in all eukaryotic cells (~ 2% of cytosolic proteins) and is essential for viability, in contrast to its eubacterial homolog HtpG, which is dispensable (Frydman, 2001). The Hsp90 chaperone family includes Hsp90 (90 kDa heat shock protein) of the eukaryotic cytosol, termed Hsp90α and β in humans (major and minor isoforms respectively), Hsp86 and Hsp84 in mice, Hsp83 in *Drosophilia*, Hsc82 and Hsp82 in yeast, and as mentioned above, HtpG in bacterial cytosol (Young *et al.*, 2001). Hsp90 is associated with the folding of signal-transducing proteins such as steroid hormone receptors and protein kinases, and is required for the maintenance of most proteins *in vivo*. It is a homodimer with both the N-terminus and C-terminus being implicated in the binding of substrate polypeptides (reviewed in Pearl and Prodromou, 2006).

There are two ATP binding sites within the N- and C- terminal domains of Hsp90, and ATP hydrolysis is crucial to the functioning of Hsp90 *in vivo* (Csermely and Kahn, 1991; Csermely *et al.*, 1993; Panaretou *et al.*, 1998; Young and Hartl, 2000; Söti *et al.*, 2002; Johnson *et al.*, 2007). The ATPase activity of human Hsp90 is very weak but binding of Hsp90 to certain client proteins like GR has been shown to increase the ATPase activity of Hsp90 up to 200 times (McLaughlin *et al.*, 2002). Within the eukaryotic cytosol, Hsp90 is known to interact with a variety of co-chaperone proteins that assemble into a multichaperone complex, and these co-chaperones may or may not modulate Hsp90 activities. The Hch1/Aha1 proteins have been identified as Hsp90 co-chaperones, accelerating the ATPase activity of yeast Hsp90 to 12 times its basal level (Panaretou *et al.*, 2002). Cdc37 (p50) is a co-chaperone and an inhibitor of the Hsp90 ATPase activity, and this suppression is restored to normal levels when Cdc37/p50 is displaced by Cpr6 (Siligardi *et al.*, 2002). The immunophilin, FKBP59, showed little effect on the basal ATPase activity rate of Hsp90, but increased the client protein-stimulated rate

considerably. This was in contrast to p23, another Hsp90 co-chaperone involved in stabilizing the Hsp90-GR complexes. Both the basal and the client protein-stimulated ATPase activity of Hsp90 was inhibited by binding of p23, and it was further proposed that p23 may play an important role in arresting Hsp90 in a high-affinity state for client proteins (McLaughlin *et al.*, 2002; McLaughlin *et al.*, 2006).

Crystallographic as well as biochemical studies of Hsp90 and its interactions with co-chaperones have contributed greatly to the understanding of how its ATP hydrolysis contributes to its interactions with co-chaperones and substrates (Prodromou *et al.*, 1997; Stebbins *et al.*, 1997; Meyer *et al.*, 2003; Harris *et al.*, 2004; Ali *et al.*, 2006; Johnson *et al.*, 2007). The ADP-bound form of Hsp90 is described as 'relaxed' and hence ideal for client protein loading, whereas the ATP-bound form of Hsp90 is described as a 'closed' conformation because it is capable of tightly retaining the substrate. The efficient release of the substrate from Hsp90 is thus carried out by the conversion of the ATP to ADP state, and this regulation of the ATPase activity of Hsp90 by various co-chaperones allows for optimal binding and releasing of the substrate (Young and Hartl, 2000; McLaughlin *et al.*, 2002; Siligardi *et al.*, 2002; McLaughlin *et al.*, 2004). Note that this is in contrast to the ATP regulated substrate-binding cycle of Hsp70 described in section 1.1.9. The benzoquinone ansamycin antibiotic geldanamycin blocks this cycle by maintaining Hsp90 in an ADP-bound state, thereby acting as a specific inhibitor of Hsp90 (Panaretou *et al.*, 1998).

Most co-chaperones bind to Hsp90 through a modular domain containing three 34 amino acid, helix-turn-helix tetratricopeptide repeat (TPR) motifs (Young *et al.*, 2001). TPRs are protein-protein interaction modules found in varying numbers of tandem repeats and present in a number of proteins that are functionally unrelated (Blatch and Lässle, 1999). TPR motifs are associated mostly with multiprotein complexes, and have been shown to be vital for the functioning of chaperone, cell cycle and protein transport complexes (Blatch and Lässle, 1999). The specific recruitment of TPR-domain co-chaperones, which compete with each other for a binding site at the C-terminus of Hsp90, has been detailed

by crystallographic and biochemical studies of the various interactions (Young *et al.*, 1998; Scheufler *et al.*, 2000).

Although both Hsp70 and Hsp90 protein folding systems act independently of each other and on different substrates, some protein substrates are processed by Hsp70 and then transferred to Hsp90. This association between the two major chaperone machineries, Hsp70 and Hsp90 is coordinated by a number of co-chaperones, in particular, Hop - the Hsp70/Hsp90 Organizing Protein (reviewed by Odunuga *et al.*, 2004). Much interest has been generated regarding the role of the Hsp90-Hsp70-co-chaperone heterocomplex in regulating various steroid receptors (SR) (reviewed in Cheung and Smith, 2000; Smith, 2000; Pratt *et al.*, 2004b). Different members of the SR family reside within the cytosol, and in the absence of their particular steroid hormone, exist in an inactive or non-transformed state. Once the appropriate hormone diffuses into the cell, it binds to its receptor and results in the transformation of that receptor into an active transcription factor, which is capable of activating or repressing the expression of the steroid response genes. Binding of the SR to Hsp90 is believed to stabilize the receptor in an optimal conformational state that allows efficient binding of SR to the appropriate hormone (Picard *et al.*, 1990; Kosano *et al.*, 1998; McLaughlin and Jackson, 2002).

The inactive forms of many SRs exist as relatively large complexes, whereas the active forms are homodimers with their steroid ligands tightly bound. Analysis of the purified inactive form of various receptors revealed the presence of the steroid-binding component, typically a 50-100-kDa polypeptide, a number of polypeptides between 50-70 kDa, and Hsp 90 (Catelli *et al.*, 1985). It is now known that a minimal system of five purified proteins, Hsp90, Hsp70, Hop, Hsp40 and p23, are essential for the assembly of the glucocorticoid receptor (GR)-Hsp 90 heterocomplex, which causes the simultaneous opening of the steroid binding cleft to access by the steroid (Kanelakis *et al.*, 2002). The first step in this assembly is the ATP-dependent and Hsp40-dependent binding of Hsp70 to the GR (stabilized by Hip), which primes the receptor for subsequent ATP-dependent activation by Hsp90, Hop and p23. This is followed by rapid binding of the primed GR-

Hsp70 complex with Hsp90 and the rate-limiting step appears to be the ATP-dependent opening of the steroid binding cleft after Hsp90 binding (Kanelakis *et al.*, 2002). p23 is an acidic 23 kDa protein which binds to, and stabilizes, preformed GR-Hsp90 heterocomplexes in an ATP-independent manner. It has been postulated that p23 is not essential for GR folding to the hormone-binding site, but rather it stabilizes the GR-Hsp90 heterocomplex once the ATP-dependent conformation of Hsp90 has been achieved (Yoshihiro *et al.*, 1999). Other investigations by Kanelakis *et al*. (2002) suggest however that there is no difference between the ATP-bound, ADP-bound, and the unbound state of Hsp90 in its ability to bind to the primed GR-Hsp70 complex.

According to the model of GR-Hsp90 heterocomplex assembly proposed by Pratt *et al*. (2001), the Hsp90/Hsp70 based chaperone complex (also known as a foldosome) converts the GR ligand-binding domain from a folded conformation (where the hydrophobic steroid binding cleft is closed and inaccessible to the hormone) to a partially unfolded conformation (in which the cleft is opened to access by steroid). Binding of p23 stabilizes the GR-Hsp90 complex. The adaptor protein, Hop, then dissociates leaving the TPR acceptor site on Hsp90 open (Pratt *et al.*, 2001).

The presence of high molecular weight mammalian immunophilins (FKBP52, FKBP51 and CyP-40) have been discovered in SR-Hsp90 heterocomplexes (Pratt and Toft, 1997). The major immunophilin in the GR-Hsp90 heterocomplex, FKBP52, is shown to bind to the free TPR acceptor site on Hsp90, after Hop dissociates from the GR-Hsp90 heterocomplex (Pratt *et al.*, 2001). In the final GR-Hsp90 heterocomplex, Hsp70 is usually absent or otherwise present at substoichiometric levels with respect to the receptor (Pratt *et al.*, 2001).

In unstressed cells, the localization of Hsp90 is predominantly in the cytoplasm, although some Hsp90 is present in the nucleus too (reviewed in Pratt and Toft, 1997; Pratt *et al.*, 1999; Pratt and Toft, 2003). Under stressful conditions Hsp90 translocates from the cytoplasm into the nucleus, a redistribution seen in some cell types but not in all (Pratt

and Toft, 1997; Langer *et al.*, 2003). As mentioned in section 1.1.5, binding of Hsp90 to SR is known to sequester SR to the cytosol. Molybdate, which binds to Hsp90 and stabilizes SR-Hsp90 complexes *in vivo*, has been shown to trap the SRs in the cytoplasm of cells suggesting that in the presence of molybdate, the receptors cannot be imported into the nuclei (Yang and DeFranco, 1996; Pratt and Toft, 1997). On the basis of this experiment, Yang and DeFranco (1996) proposed that SR-Hsp90 complex formation was a dynamic process in which the components were constantly dissociating and being reformed under physiological conditions in the cell. This would be necessary to permit the association of SRs with the macromolecular components that participate in the delivery of receptors to their nuclear sites of action. Thus the stabilization of the complex by molybdate hinders this dynamic process, anchoring the Hsp90-SR complex to the cytosol and thereby suggesting a role for Hsp90 in protein movement mechanism.

A second postulation regarding the role of Hsp90 in SR subcellular trafficking was made soon after, by Czar *et al.* (1997), based on experiments conducted with geldanamycin, which disrupts the function of Hsp90 and obstructs the steroid-dependent movement of GR from the cytoplasm to the nucleus. Thus it was also suggested that Hsp90 may itself be involved in the nuclear trafficking of SR as part of a transportosome, or it may be associated with the attachment of the SR to a trafficking machinery within the cell (Czar *et al.*, 1997; Pratt *et al.*, 2004a). In normal cells, the retrograde movement of particles toward the nucleus is known to occur along microtubules in a process that requires the molecular motor protein cytoplasmic dynein (Pratt, 1993). It is believed that the immunophilin, FKBP52, which attaches to the SR-Hsp90 heterocomplex, plays an active role in the transportosome function by linking the SR to cytoplasmic dynein, thereby generating retrograde movement toward the nucleus along microtubular tracks (Pratt *et al.*, 2001). The Hsp90-chaperoned transcription factor, p53, is transported to the nucleus by cytoplasmic dynein. It was shown that Hsp90 binding immunophilins were responsible for linking p53-Hsp90 complexes to dynein. The nuclear translocation of p53 was shown to be inhibited either when p53-Hsp90 binding was inhibited, or when immunophilin binding to dynein was inhibited (Galigniana *et al.*, 2004)

Hsp90 is known to be heavily phosphorylated in animal cells, and *in vitro* studies have shown that the purified protein acts as a substrate for double-stranded DNA-activated kinase (Welch *et al.*, 1983; Garnier *et al.*, 2001). The phosphorylation of Hsp90 has been linked to its chaperoning activity with its phosphorylation appearing to be coupled with the release of Hsp90 from its client protein (Zhao *et al.*, 2001). Ppt1 (a protein phosphatase found in the yeast system, and belonging to the PPP family of serine/threonine phosphatases) specifically dephosphorylates Hsp90 by directly interacting through its TPR domain. Deletion of the *ppt1* gene results in the hyperphosphorylation of Hsp90 *in vivo* and consequently a decrease in the efficiency of its chaperone activity (Wandinger *et al.*, 2006).

A number of investigators have reported interactions between Hsp90 and various protein kinases. Studies conducted by Miyata & Yahara (1992) reported that Hsp90 co-purified with CKII *in vitro* and enhanced the activity of CKII. Munoz and Jimenez (1999) demonstrated the possibility of an interaction between Hsp90 and cdc2 kinase in the fission yeast *Schizosaccharomyces pombe*, through the regulation of Wee1 by *swo1*, the gene coding for Hsp90. Wee1 encodes a tyrosine kinase that inhibits entry into mitosis by phosphorylation of cdc2 kinase, and *swo1* acts as a suppressor of the over-expression of Wee1 (Munoz and Jimenez, 1999). Translocation of Hsp90α to the cell surface under high glucose conditions has been observed, and this has been postulated to be associated with phosphorylation of Hsp90α by the cAMP-dependent protein kinase A (Lei *et al.*, 2007).

### 1.1.11 Hop (Hsp70-Hsp90-Organizing Protein)

The 60-kDa scaffolding protein Hop, was first identified in the yeast system by Nicolet and Craig during a genetic screen for proteins that were involved in the heat shock response (Nicolet and Craig, 1989). The most well known function of Hop is its interaction with Hsp70 and Hsp90 within intermediate steroid receptor complexes and in this context, Hop was shown to be essential for the *in vitro* assembly of steroid receptors with Hsp90 (Smith *et al.*, 1993; Dittmar *et al.*, 1996). Homologues of Hop have also been

identified in humans (Honoré *et al.*, 1992), mice (Blatch *et al.*, 1997), rats (Demand *et al.*, 1998), insects (Adams *et al.*, 2000), plants (Zhang *et al.*, 2003), parasites (Webb *et al.*, 1997) and viruses (Cheng *et al.*, 2002), and are classified as belonging to the stress-inducible protein 1 (STI1) family (Nicolet and Craig, 1989). For the purposes of this study, the term 'Hop' will refer to the protein of mammalian origin. However, any reference to a specific species of the protein will be specified as such, for example, yeast Hop and mouse Hop.

The various homologues of Hop are structurally characterized by the presence of nine TPR motifs; the TPR motifs are grouped into three domains, each comprising three TPRs. The N terminal TPR domain of Hop (TPR1) is required for Hsp70 binding (van der Spuy *et al.*, 2000) and a central TPR motif-containing region is essential for Hsp90 binding (Chen *et al.*, 1996b; Odunuga *et al.*, 2003). In yeast Hop, it has been shown, however, that both TPR1 and TPR2B are required for Hsp70 interaction *in vivo* and that although TPR2A was sufficient for yeast Hop-Hsp90 interactions *in vivo*, an isolated TPR2A domain was not sufficient for Hsp90 binding unless it was combined with TPR2B (Flom *et al.*, 2007). The TPR acceptor site on Hsp90 is comprised of five C-terminal residues MEEVD and Hsp70 is bound to TPR1 of Hop through the last eight residues of Hsp70 (GPTIEEVD) (Scheufler *et al.*, 2000; Brinker *et al.*, 2002; Odunuga *et al.*, 2003). A single mutation in TPR2A, R341E, was shown to disrupt the stable yeast Hop-Hsp90 interactions (Carrigan *et al.*, 2004; Flom *et al.*, 2006). Furthermore, the deletion of an amino acid in TPR2A, A304 as well as one in TPR2B, A438, disrupted yeast Hop-Hsp90 interaction and had a deleterious effect on yeast Hop activity *in vivo* (Flom *et al.*, 2006). It is now accepted that there may be networks of interactions between Hop and the chaperones Hsp70 and Hsp90, apart from those mediated by the TPR domains, which allow for its functionality as a scaffolding protein (Odunuga *et al.*, 2003; Carrigan *et al.*, 2005; Flom *et al.*, 2007).

For example, Hop also contains two smaller domains with characteristic DP repeat motifs comprising of four amino acid sequences, reflected in an arrangement that corresponds to

TPR1-DP1-TPR2A-TPR2B-DP2 (Prapapanich *et al.*, 1998; Carrigan *et al.*, 2005). *Drosophila melanogaster* Hop which lacks DP1 (dHop) can still bind to both Hsp70 and Hsp90 and even complement for and thereby rescue any growth defects in yeast that arise from a deficiency of yeast Hop, but interestingly, it cannot support GR function in yeast (Carrigan *et al.*, 2005). Moreover, the disruption of DP2 was shown to abrogate binding to Hsp70, suggesting that DP2 may interact with TPR 1 (Carrigan *et al.*, 2005).

Initial studies of Hop focused on its interaction with Hsp70 and Hsp90, mostly in the context of the assembly of this multichaperone complex in SR regulation. Hop appears to be regulated between a monomeric and dimeric state, interacting with the dimeric Hsp90 as a dimer while associating with Hsp70 as a monomer (Hernandez *et al.*, 2002). In yeast Hop, TPR2A was found to be necessary and sufficient for its dimerization properties *in vitro* (Flom *et al.*, 2007). The assembly of the progesterone receptor (PR) and the glucocorticoid receptor (GR) requires the participation of Hsp70, which brings the substrate protein into contact with Hsp90 via the scaffolding function of Hop, as detailed in section 1.1.7. In yeast Hop, it was shown that both TPR1 and TPR2 domains had to be present on the same polypeptide, in order to maintain regulation of SR activation by Hsp70 and Hsp90 (Song and Masison, 2005).

It has been suggested that yeast Hop may not be essential to mediate associations between Hsp70, Hsp90 and target proteins (Chang *et al.*, 1997). Although comparisons between the yeast and mammalian Hsp90 chaperone complexes have shown conservation of many of the basic elements (Chang and Lindquist, 1994) this was in contrast to previous reports maintaining that mammalian Hop was necessary for efficient assembly of steroid receptor-Hsp90 complexes *in vitro* (Smith *et al.*, 1993; Chen *et al.*, 1996b; Dittmar *et al.*, 1996). It was also shown that Hop was essential in integrating Hsp70-Hsp90 interactions (Chen and Smith, 1998; Song and Masison, 2005). Moreover, purified Hsp90 and Hsp70 had not been shown to associate in a complex unless Hop was present (Chen *et al.*, 1996b).

A conflicting report by Morishima *et al.* (2000), however, showed that Hop was not necessarily essential for GR folding by the Hsp90 chaperone machinery, but rather was capable of enhancing the rate of this phenomenon. Moreover, the authors showed that some GR activation was achievable with purified Hsp70 and Hsp90 in the absence of Hop. This suggested that both Hsps may interact directly with each other, but that Hop, being an adaptor protein, was able to bring Hsp70 and Hsp90 into better proximity with each other, thereby facilitating this interaction and ensuring an efficient folding machinery for substrate proteins (Morishima *et al.*, 2000). This is also consistent with the latest published report on yeast Hop showing that certain mutations in yeast Hop caused a reduced recovery of Hsp70 in Hsp90 complexes *in vivo* (Flom *et al.*, 2007).

Taking into consideration the fact that dHop lacking DP1 cannot support GR activity in yeast, though it is still capable of binding to Hsp70 and Hsp90, it was interesting to note that the substitution of DP2 of human Hop by DP2 from dHop also failed to support GR activity. However, a substitution of DP2 from dHop with DP2 from human Hop was shown to regain the ability to enhance GR activity in yeast (Carrigan *et al.*, 2005). It is possible therefore, that the DP2 domains may be responsible for Hop's ability to enhance GR activity, besides its Hsp70 binding capabilities. Carrigan *et al.* (2005) have thus proposed a novel role for Hop in GR maturation *in vivo*, which is independent of Hsp70/90 binding and showed using chimeric studies, that DP2 is critical for this "new" role of Hop.

### 1.1.12 Hop Modulates Hsp70 and Hsp90 Chaperone Pathways

Despite its designated role as an 'adaptor' protein, Hop has been shown to actively modulate the functions of both Hsp70 and Hsp90 during its interactions with these major heat shock proteins. The impairment of an Hsp70-dependent and Hsp90-dependent chaperone pathway upon deletion of the respective TPR1 and TPR2 domain of yeast Hop was clearly demonstrated (Song and Masison, 2005). Deletion of TPR1 did not affect Hsp90 dependent client protein activity, and deletion of TPR2 also had no adverse effect on Hsp70 dependent client protein activity. These deletions, however, impaired client

protein folding pathways that involved both Hsp70 and Hsp90 (Song and Masison, 2005). This implied Hop was a not only a concurrent but also an independent regulator of Hsp70 and Hsp90 chaperone pathways.

A number of possible modifications of Hop on the Hsp90 chaperone pathway have been reported. The protein levels of Hop were seen to be increased in GR-Hsp90 complexes in the presence of Hsp90 inhibitor, geldanamycin, compared to GR-Hsp90 complexes in the absence of geldanamycin (Morishima *et al.*, 2000). This may be due to the fact that geldanamycin-inhibited Hsp90 is in an ADP-bound conformation, which has higher affinity for Hop, than the ATP-conformation (Sullivan *et al.*, 1997; Morishima *et al.*, 2000). GR incubated with geldanamycin in the absence of Hop displayed little association with Hsp90, whereas a more stable GR-Hsp90 association was detected in the presence of Hop (Morishima *et al.*, 2000). The effect of Hop on GR-Hsp90 interactions in the presence of geldanamycin could either be due to the stable retention of Hsp90 by Hop, or due to an influence that Hop may be exerting on the geldanamycin-Hsp90 conformation such that its affinity for GR is increased (Morishima *et al.*, 2000).

Furthermore, the exclusion of Hop has shown reduced activity, but not accumulation, of two structurally and functionally unrelated Hsp90 client proteins, the steroid receptor GR and the oncogenic tyrosine kinase v-Src (Chang *et al.*, 1997). The exclusion of Hop did not, however, have an effect on the activity of c-Src which is a protein closely related to v-Src but less dependent on Hsp90. This suggests that Hop is an important factor in specifically promoting the maturation of Hsp90 client proteins (Chang *et al.*, 1997) and could facilitate the transfer of certain substrates from Hsp70 to Hsp90 with greater efficiency. This is also consistent with suggestions made by Carrigan *et al.* (2005) regarding a novel role for Hop in enhancing GR maturation.

It has been suggested that Hop may change its conformation during the assembly of the Hsp70-Hop-Hsp90 chaperone heterocomplex, due to the fact that the affinity and stoichiometry of Hsp70-Hop binding is dramatically affected by subsequent binding of

Hsp90. Although Hsp70 binds to Hop with a relatively lower affinity than Hsp90, this affinity is increased five fold in the presence of Hsp90 (Hernandez *et al.*, 2002). Hsp90 may thus be altering the conformation of Hop to one that better accommodates interactions of Hop with Hsp70. Another possibility is that Hop binding to Hsp90 may open up a new conformation of Hsp90 that provides contact sites for Hsp70 binding (Murphy *et al.*, 2001; Hernandez *et al.*, 2002).

As part of the Hsp70-Hop-Hsp90 multichaperone machinery, Hop is also involved in a process called "chaperone-mediated autophagy", one that targets cytosolic proteins to the lysosomes for degradation in response to stress conditions such as prolonged starvation or serum withdrawal (Agarraberes and Dice, 2001). Protein substrates have to become unfolded in order to be transported into the lysosomal lumen. Hop is speculated to be part of the strategy employed to stabilize the lysosomal Hsp70-substrate complex on the lysosomal surface in such a way that it allows for the complete unfolding of the substrate protein before import into the lysosome (Agarraberes and Dice, 2001).

Apart from modulating their chaperoning pathways, Hop has also been reported to individually modulate both Hsp70 and Hsp90. Yeast Hop stimulates ATP hydrolysis of Hsp70, enhancing its ATPase activity by a factor of 200 and is a non-competitive inhibitor of Hsp90's ATPase activity (Richter *et al.*, 2003; Wegele *et al.*, 2003). Studies conducted by Wegele *et al.* (2003) showed that yeast Hop was capable of accelerating ATP hydrolysis of Hsp70 to a greater extent than any other stimulation factor including yeast Hsp40. Even when yeast Hop was added to a pre-formed Hsp70-Hsp40 complex, it was still able to activate the ATPase activity of Hsp70 and moreover, yeast Hsp40 was shown to be unable to replace yeast Hop in a preformed Hsp70-Hop complex. Binding of yeast Hop to Hsp90 and Hsp70 allowed the activation of Hsp70 ATPase and inhibition of Hsp90 ATPase at the same time (Wegele *et al.*, 2003). In the human system, Hop has not shown any effect on Hsp70's ATPase activity, alone or in combination with Hsp90 (Chen *et al.*, 1996b). Although human Hop does not affect Hsp90's ATPase cycle, it has shown

to be capable of inhibiting the client protein-stimulated ATPase activity of Hsp90 (McLaughlin *et al.*, 2002).

The ATPase inhibition of Hsp90 by yeast Hop is achieved by bringing about a conformational change in Hsp90, the restriction of its N-terminal dimerization, which is required for ATP hydrolysis. This was confirmed by studies demonstrating a Hop binding site in the N-terminal region of Hsp90, in addition to the already characterized C-terminal peptide region that interacts with the TPR2A domain of Hop (Richter *et al.*, 2003). This also suggests that through the suppression of ATP-turnover by Hsp90, Hop plays a role in preparing Hsp90 for fresh "loading" of substrate protein (Prodromou *et al.*, 1999; Siligardi *et al.*, 2002). Interestingly, studies on yeast Hop have also suggested that the DP2 domain is important for the capacity of yeast Hop to modulate Hsp90's functions (Flom *et al.*, 2006).

### 1.1.13 Hop's Interactions Beyond Hsp70 and Hsp90

A number of reports on various protein-protein interactions involving Hop, and which may or may not involve Hsp70 and/or Hsp90, have been published; a summary of the network of interactions involving Hop is schematically illustrated in figure 1.3. TPR-mediated protein interactions of Hop are not exclusive to the Hsp70/Hsp90 multichaperone complex. Studies done with *Saccharomyces cerevisiae* have shown that in the presence of non-fermentable carbon sources like ethanol and glycerol, yeast Hop, in addition to other Hsp90 co-chaperones Cpr7 and Cns1, interacts with Hsp104 through its N-terminal TPR1 domain independently of Hsp90 (Abbas-Terki *et al.*, 2001). Hsp104 is a stress tolerance factor, which acts in concert with Hsp40 and Hsp70 to reactivate denatured proteins (Glover and Lindquist, 1998).

Yeast Hop has also demonstrated direct interactions with Cdc37, a co-chaperone of Hsp90 (Abbas-Terki *et al.*, 2002). Yeast Hop is not essential for growth of yeast cells at $30^{o}$C but growth impairment can occur at higher and lower temperatures or in the presence of minimal media (Nicolet and Craig, 1989; Smith *et al.*, 1993). Under normal

conditions however, a combination of Cdc37 and yeast Hop mutations has shown to be synthetically lethal to yeast implying that their interaction may contribute to the vital functioning of yeast (Abbas-Terki *et al.*, 2002). Cdc37 is a molecular chaperone as well as co-chaperone of Hsp90 involved in the prevention of aggregation of polypeptides and folding of protein kinases. Thus it is possible that the interaction of yeast Hop with Cdc37 is a crucial step in the initiation of Cdc37 into the chaperone dependent-folding pathway (Lee *et al.*, 2004). The interaction between yeast Hop and Cdc37 is speculated to occur via both TPR1 and TPR2 domains of Hop but possibly not on the same binding sites as those involved in binding of Hop to both Hsp70 and Hsp90 (Abbas-Terki *et al.*, 2002). These findings were consistent with other reports showing the interaction of Hop with the mammalian homologue of Cdc37, p50, and the authors suggested the presence of a complex comprising of Hsp90, Hop and p50 in which one of the Hsp90 co-factors acted as the central component (Harst *et al.*, 2005).

Hop was shown to stimulate the nucleotide exchange of the eukaryotic chaperonin-containing TCP1 (CCT), also known as the TCP-1 ring complex (TriC), which is involved in the proper folding of actins and tubulins (Gebauer *et al.*, 1998). This interaction led to the interference of CCT's substrate-associative capabilities. CCT cooperates with Hsp70 in refolding of luciferase *in vitro*, and this phenomenon is proposed to occur *in vivo* for certain substrates after translation or after stress-induced damage. The interaction of Hop with CCT was mediated through its C-terminal domain, in contrast to its interaction with Hsp70, which is mainly through its N-terminal domain, and this is consistent with the observation that the presence of Hsp70 did not affect Hop-CCT interactions (Gebauer *et al.*, 1998).

A novel role of mouse Hop, in neuroprotection, has been proposed by (Zanata *et al.*, 2002; Coitinho *et al.*, 2007). Recombinant mouse Hop was found to bind to $Prp^{c}$ (a protein whose expression is crucial to the propagation of neurological disease, in particular, Prion disease) both *in vitro* and *in vivo*. The interaction of $Prp^{c}$ with mouse Hop was found to transduce neuroprotective signals. Using behavioral studies in rats, it

was also shown that the interaction of mouse Hop with $Prp^c$ enhanced short term and long term memory formation, and the mouse Hop peptide 230-245 which was reported to interact with $Prp^c$ (Zanata *et al.*, 2002) had a potent enhancing effect on memory performance (Coitinho *et al.*, 2007). A number of other molecules have shown *in vitro* association with $Prp^c$ such as Hsp60, BiP, Bcl-2 and a 37/67-kDa laminin receptor (Martins *et al.*, 2001), but physiological relevance in the form of neuroprotection has only been attributed to the $Prp^c$-laminin complex. The laminin receptor-binding site on the $Prp^c$ molecule maps to a region of amino acids that is significantly distinct from that of the mouse Hop-$Prp^c$ binding domain. It is suspected that mouse Hop may therefore participate within a $Prp^c$-laminin complex wherein association of $Prp^c$ with both molecules may supply an additive effect (Zanata *et al.*, 2002). Interestingly, the amino acids 230-245 of mouse Hop that contain the $Prp^c$ –binding site, overlaps with TPR2A domain of Hop, and are known to contain crucial residues required for Hop-Hsp90 interaction.

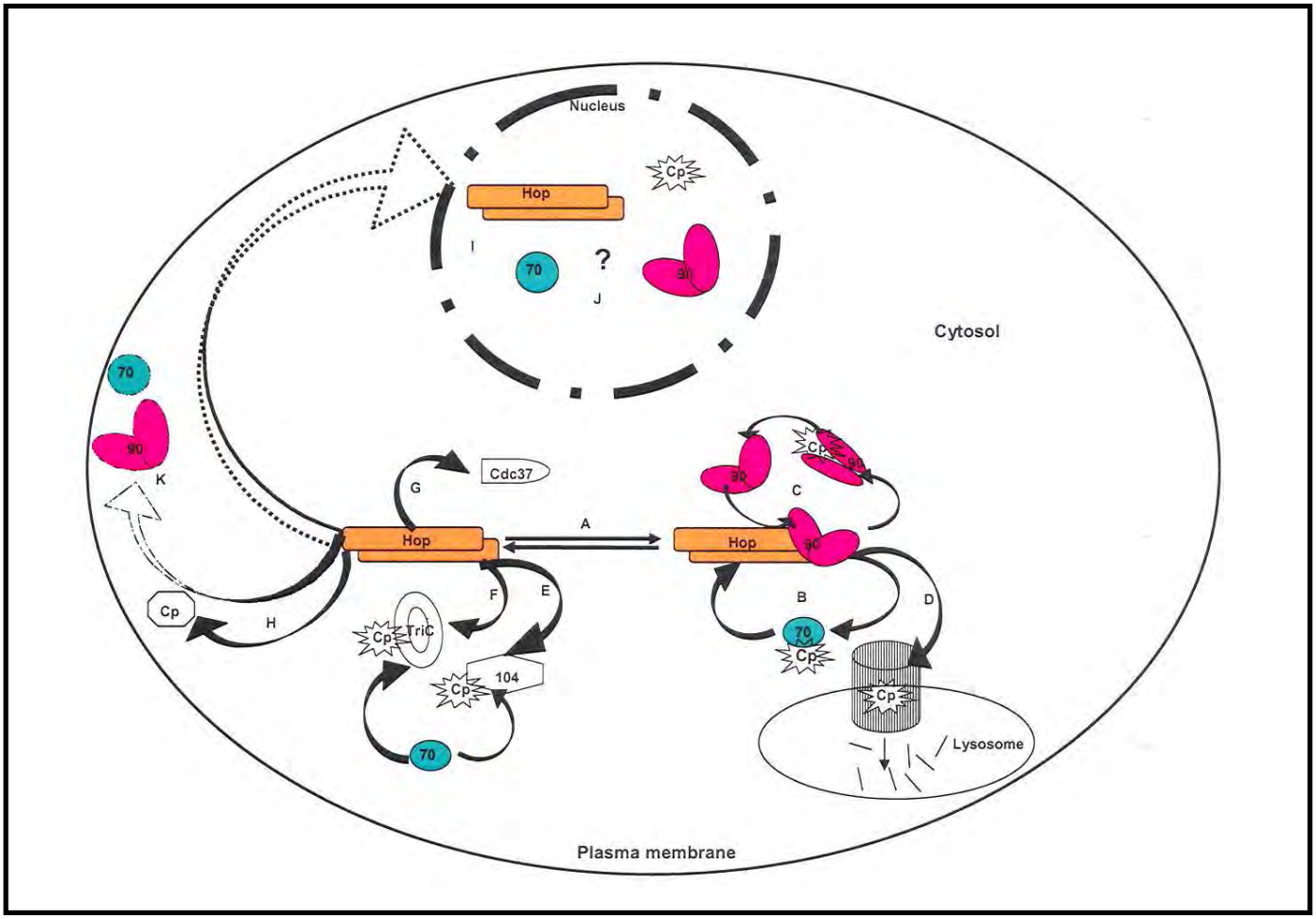


**Figure 1.3: Functions of Hop *in vivo* (updated and adapted from Daniel *et al.*, 2006).** Although free Hop exists within the cell, most of Hop is bound to Hsp90 (A). The most well known function of Hop is as the Hsp70-Hsp90 co-chaperone, facilitating the transfer of the client protein from Hsp70 to Hsp90 (B). Transfer of the client protein from Hsp70 onto Hsp90 is followed by the dissociation of both Hop and Hsp70 from the multichaperone complex. The client protein is refolded by Hsp90 and then released, thereby freeing Hsp90 (C). The Hsp70-Hop-Hsp90 multichaperone machinery is involved in chaperone-mediated autophagy, facilitating the degradation of unfolded polypeptides (D). Free Hop interacts directly with Hsp104 which may involve Hsp40 (E). Hop also interacts directly with TriC (F). Hop has also been shown to interact with Cdc37, an Hsp90 co-chaperone, independently of Hsp90 (G). Mouse Hop interacts with client proteins like the $Prp^{c}$, and this interaction is believed to be localized to the plasma membrane (H). Hop has been captured in the nucleus under G1/S arrest of the cell cycle. It is believed to translocate to the nucleus (shown in dotted lines) through a potential bipartite NLS (I). The major chaperone partners of Hop, Hsp70 and Hsp90, have also been shown to translocate to the nucleus under specific conditions. It is thus speculated that Hop may be involved as a scaffolding protein within the nucleus facilitating the assembly of the Hsp70-Hsp90 chaperone heterocomplex. Hop may also have multiple nuclear functions, some of which may be independent of Hsp70 and Hsp90 (J). We further speculate that Hop may be interacting with Hsp70 and Hsp90 at the plasma membrane (K). Although Hop has been shown as a dimer in this figure, the stoichiometry of Hop in many of these interactions is unknown. Heat shock proteins are identified by their molecular weight stated as numbers. CP stands for client protein.

## 1.2 Motivation for this Study and Problem Statements Associated Therewith

Subcellular localization studies done on mammalian cells showed that mouse Hop was localized predominantly to the cytosol with a small amount of the protein also being found in the nucleus (Lässle *et al.*, 1997; Longshaw *et al.*, 2004). A greater nuclear translocation of mouse Hop was seen only under conditions of G1/S arrest or when nuclear export of the protein was inhibited, suggesting that mouse Hop was dynamically shuttling between the cytosol and the nucleus and that nuclear translocation of Hop was cell cycle regulated (Longshaw, 2002; Longshaw *et al.*, 2004). Some reports have also shown the detection of about 6% of mouse Hop to be localized to the membranes (Zanata *et al.*, 2002; Coitinho *et al.*, 2007).

Two NLS sequences were identified in the central region of mouse Hop, of which the bipartite NLS at K222-K239 was predicted to be functional (Blatch *et al.*, 1997); this putative NLS, when fused to EGFP, was shown to be capable of translocating EGFP to the nucleus (Longshaw, 2002; Longshaw *et al.*, 2004). However, the functionality of the NLS has not yet been established within the context of the Hop protein and critical residues within this NLS have not yet been mapped out. Human Hop has been found in the golgi apparatus and small vesicles in normal cells, and nucleolar localization of human Hop has only thus far been described in SV40-transformed cells (Honoré *et al.*, 1992). The chaperone partners of Hop, Hsp90 and Hsp70, although generally cytosolic, have both been detected in the nucleus under certain stressful conditions (Pratt and Toft, 1997; Nollen *et al.*, 2001; Langer *et al.*, 2003). Since the Hsp70/Hsp90 chaperone heterocomplex has thus far been shown to be cytosolic, understanding the subcellular localization patterns of Hop is critical to understanding the nature of its biological interactions, both in the context of its co-chaperone capacity, as well as within complexes and roles that extend beyond Hsp70 and Hsp90.

Hop has previously been proposed to be a phosphoprotein due to various reports showing the elevation of acidic isoforms of human Hop after viral transformation (Honoré *et al.*, 1992) and mouse Hop after heat shock (Lässle *et al.*, 1997). *In vitro* experiments done on mouse Hop showed that it contained two phosphorylation sites for CKII and cdc2-kinase at S189 and T198 respectively (Longshaw *et al.*, 2000). However, Hop has thus far not been shown to be phosphorylated *in vivo*. Interestingly, both *in vitro* phosphorylation sites are located upstream of the predicted bipartite NLS thus constituting a postulated CcN motif (Longshaw *et al.*, 2000; Longshaw, 2002). Therefore, similar to the regulation of subcellular localization patterns of SV40 large T-ag (Jans and Hubner, 1996), previous studies using phosphorylation mimic-derivatives of mouse Hop suggested that phosphorylation by CKII and cdc2-kinase may promote the nuclear import or cytosolic retention of mouse Hop respectively (Longshaw *et al.*, 2004). Thus it is postulated that phosphorylation of mouse Hop is a key factor in regulating the assembly of the Hsp70/Hsp90 chaperone heterocomplex based on its possible regulation of the subcellular localization of mouse Hop.

Hop is generally found complexed to Hsp90 and is known to interact with Hsp70 within this complex (Smith *et al.*, 1993; Chang *et al.*, 1997; Hernandez *et al.*, 2002). The Hop-Hsp90 complex may thus be a prerequisite for many of its biological functions within the cell. It is therefore, especially interesting to note that the proposed phosphorylation sites (S189 and T198) are immediately upstream of Hsp90 binding TPR2A domain of Hop, and that the proposed bipartite NLS site (K222-K239) overlaps with TPR2A. Figure 1.4 shows the amino acid sequence of the TPR2A domain with a flanking C-terminal helix. The overlapping residues of the putative bipartite NLS with the TPR2A domain are shown in grey. This implies that the interaction of Hop with Hsp90 as a co-chaperone may be regulated by phosphorylation at one or both of these sites and that Hop-Hsp90 complex may regulate, or may be regulated by, the subcellular localization of Hop under stressed or unstressed conditions.

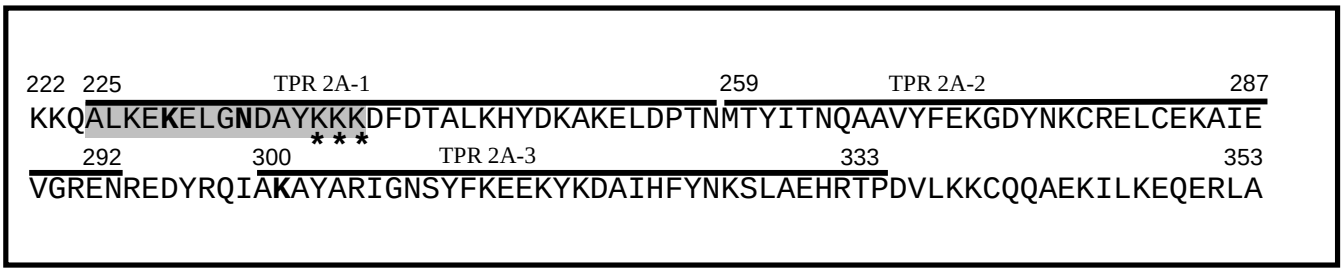


**Figure 1.4: Partial amino acid sequence of Hop showing the predicted bipartite NLS, the TPR2A domain and a flanking C-terminal helix (Adapted from Daniel *et al.*, 2006)** TPR2A comprises of three TPR motifs (residues are shown by a thick black overline) denoted as TPR2A-1, TPR2A-2 and TPR2A-3 (Scheufler *et al.*, 2000). The proposed NLS extends from K222-K239 (Longshaw *et al.*, 2000; 2004). The residues against a gray background are those which form part of the putative NLS and which overlap with TPR2A-1 motif. The major arm of the bipartite NLS is denoted by an asterisk under each residue. The residues shown in bold, K229, N233 and K301 form part of the carboxylate clamp and have been shown to be important for Hsp90 binding (Odunuga *et al.*, 2003).

Based on the literature that has been published thus far on Hop, a number of questions have arisen regarding the factors regulating Hop's involvement as a co-chaperone in the Hsp70/Hsp90 chaperone heterocomplex, such as its subcellular localization and its phosphorylation status. How does the subcellular localization of Hop affect its functions, particularly as a scaffolding protein and with regards to its Hsp partners? Is the postulated bipartite NLS functional within mouse Hop and what conditions prompt the nuclear translocation of Hop? Is Hop phosphorylated *in vivo*? How does stress affect both the phosphorylation status of Hop and its subcellular localization? How does phosphorylation of Hop and its subcellular localization affect its interaction with Hsp90?

## 1.3 Primary Hypothesis

The co-chaperone Hop is phosphorylated by cell cycle kinases *in vivo*, and its phosphorylation status regulates both its subcellular localization, as well as its fundamental function of assembling the Hsp70/Hsp90 multichaperone heterocomplex.

## 1.4 Secondary Hypotheses

(i) Hop is phosphorylated *in vivo* under normal and heat shock conditions.

(ii) Hop co-localizes with Hsp70 and Hsp90 under heat shock conditions and this co-localization is different to that observable under normal conditions.

(iii) Hop contains a functional bipartite NLS *in vivo* and functionality of this NLS affects Hop-Hsp90 interactions.

(iv) Phosphorylation of Hop affects its interaction with Hsp90, and this in turn regulates the subcellular localization of Hop.

# CHAPTER 2

# THE PHOSPHORYLATION STATUS OF HOP

*"The most exciting phrase to hear in science, the one that heralds new discoveries, is not 'Eureka!' ('I've found it!') but rather 'hmm… that's funny' "*
*- Isaac Asimov*

## 2.1 INTRODUCTION

Post-translational phosphorylation of proteins catalyzed by protein kinases often plays a critical role in cell signaling and therefore acts as an important 'molecular switch' within the cellular environment. Previous reports have put forward suggestive evidence that Hop belongs to a phosphoprotein family (Nicolet and Craig, 1989; Honoré *et al.*, 1992; Lässle *et al.*, 1997; Longshaw *et al.*, 2000) implying that phosphorylation of Hop may act as a signal for some of its biological functions *in vivo*. An acidic isoform of the yeast homolog of Hop, STI1, was reported which suggested that this protein was post-translationally phosphorylated (Nicolet and Craig, 1989). Shifts in the isoform composition of human Hop to more acidic isoforms after viral transformation (Honoré *et al.*, 1992) and similar changes in isoform composition of mouse Hop after heat shock for 10 minutes at 42$^{o}$C (Lässle *et al.*, 1997), implied that phosphorylation of a sub-population of Hop may be stress-induced or stress-regulated. The co-chaperone, Hop, was shown to be phosphorylated *in vitro* by cell cycle kinases, CKII and cdc2-kinase, at positions S189 and T198, respectively (Longshaw *et al.*, 2000). Both these phosphorylation sites were located upstream of a potential bipartite NLS and mimicking phosphorylation at either site was found to have an effect on the subcellular localization of Hop *in vivo* (Longshaw *et al.*, 2004).

The main aim of this study was to derive conclusive evidence as to the phosphorylation status of Hop *in vivo* and to determine whether an acute heat shock response could modify its phosphorylation status, in NIH 3T3 mouse fibroblast cells.

The specific objectives of this study were to:

1. Successfully detect an acute heat shock response in NIH 3T3 mouse fibroblast cells using inducible Hsp70 as a marker.
2. Determine the phosphorylated status of Hop *in vivo* using 2D gel electrophoresis and Western analysis as tools.
3. Compare the phosphorylated status of Hop *in vivo* under normal and heat shock conditions.

## 2.2 EXPERIMENTAL PROCEDURES

All general laboratory materials and specialized reagents used are as listed in the Appendix, Section A1. The generation of recombinant antibodies against the C-terminus of Hop is described in Appendix Section B1. All the cells used in the studies described in this chapter as well as subsequent chapters were obtained from cell lines, and were either NIH 3T3 mouse fibroblast cells or Baby Hamster Kidney (BHK) – 21 cells.

### 2.2.1 Tissue Culture and Heat Shock of NIH 3T3 Mouse Fibroblast Cells

NIH 3T3 mouse fibroblast cells were maintained in Dulbecco's modified Eagle's medium (DMEM) supplemented with 10% heat inactivated fetal calf serum, penicillin (100 U $mL^{-1}$) and streptomycin (100 U $mL^{-1}$) in a humidified atmosphere, at 37°C with 5% $CO_2$. An acute heat shock response was obtained by treating the cells at 80% growth confluence to pre-warmed DMEM and then incubating for 10 to 30 minutes at 42$^{o}$C (Kuhl and Rensing, 2000).

### 2.2.2 Harvesting Cells for One-Dimensional (1D) and Two-Dimensional (2D) Gel Electrophoresis

Cells were harvested at 80% confluency for 1D gel electrophoresis by trypsinization followed by three washes with phosphate buffered saline (PBS) pH 7.4. The harvested cells were resuspended in minimum volume of lysis buffer (50 mM Tris-HCl, 150 mM NaCl, 0.02% sodium azide, 100 μg $mL^{-1}$ Phenyl methyl sulphonyl fluoride (PMSF), 1 μg $mL^{-1}$ aprotinin and 1% Triton X-100) and incubated at 4$^{o}$C for 10 minutes to allow lysis to occur. The lysate was centrifuged at 12000 g for 30 minutes at 4$^{o}$C to remove insoluble cell debris, and the supernatant used immediately for 1D sodium dodecyl suphate polyacrylamide gel electrophoresis (SDS-PAGE). This was carried out by treating the lysate with SDS sample denaturing and reducing buffer (62.5 mM Tris-HCl, pH 6.8, 10% v/v glycerol, 2% w/v SDS, 5% v/v β-mercaptoethanol, 0.05% w/v bromophenol blue) and boiling for 5 minutes (Laemmli, 1970).

For 2D gel electrophoresis, NIH 3T3 fibroblast cells growing at 80% confluency were harvested by scraping in ice cold PBS. The cell pellets obtained were resuspended into

2D lysis buffer (40 mM Tris-HCL, 8 M Urea, 4% Triton X-100, 1 μg $mL^{-1}$ aprotinin and 100 μg $mL^{-1}$ PMSF) and lysed on ice for one hour. The lysate was centrifuged at 13000 rpm for 30 minutes on a benchtop microfuge to remove insoluble cell debris. Protein concentration was determined using the 2D-Quant kit as described in section 2.2.4.1 and the protein samples were further processed for 2D gel electrophoresis using the 2D clean-up kit that is described in section 2.2.4.2.

### 2.2.3 SDS-PAGE

Discontinous SDS-PAGE analysis was carried out according to Laemmli (1970). A (0.1%)-SDS-(4%)-PAGE stacking gel was pre-cast on top of a (0.1%)-SDS-(12%)-PAGE resolving gel in a Bio-Rad Protean III electrophoresis system. Protein samples were added to the SDS-PAGE sample denaturing buffer described in section 2.2.2 and heated to 95$^{o}$C for 5 minutes. The protein samples were loaded onto the gel and resolved at 200 V for 45 minutes in SDS-PAGE running buffer (0.025 M Tris, 0.0192 M glycine, 1% (w/v) SDS). The gel was removed and incubated with shaking for 1 hour in coomassie blue stain (0.1% (w/v) coomassie brilliant blue R-250, 40% (v/v) methanol, 10% (v/v) glacial acetic acid) and 3 hours in destain solution (40% (v/v) methanol, 10% (v/v) glacial acetic acid).

### 2.2.4 2D Gel Electrophoresis

#### 2.2.4.1 Protein Quantitation

Due to the presence of reducing agents like DTT, and other 2D-specific reagents, which can interfere with standard protein assays such as the Bradford assay, a specific 2D-Quant kit (Amersham Biosciences, USA) was employed to quantitatively precipitate sample protein from the cell lysate, while leaving behind interfering contaminants in the solution. The standard procedure as detailed in the manufacturer's instructions was strictly adhered to for the protein quantitation analysis using this kit. The procedure involved the pelleting of the protein by centrifugation steps and its resuspension into an alkaline solution of cupric ions that bound to the polypeptide backbones of all protein present. The assay then made use of a colorimetric agent which, when added to the reaction, bound to any unreacted cupric ions. The color density was thus inversely

proportional to the concentration of protein in the sample. Protein concentration was estimated by comparison to a standard curve generated using a standard BSA solution (2 mg/mL) provided in the kit.

#### 2.2.4.2 Protein Clean-Up

Protein precipitation using the 2D Clean-Up kit (Amersham Biosciences, USA) was employed to selectively separate proteins in the cell lysate from contaminating substances such as detergents, salts, lipids, phenolics and nucleic acids that can interfere with effective IEF. Manufacturer's instructions were followed for this procedure, using 'procedure A' for sample volumes of 1-100 μL containing 100 μg of protein per sample. The precipitated proteins obtained were resuspended in sample rehydration buffer (9 M Urea, 2% Triton X-100, 2% Ampholytes, 0.002% bromophenol blue, 100 mM DTT) to a final concentration of 1 μg/μL, and was ready to be processed by isoelectric focusing.

#### 2.2.4.3 Isoelectric Focusing (IEF)

Total protein obtained after the protein clean-up procedure (120 μg) was applied onto an immobilized pH gradient (IPG) strip within the chambers of a Zoom® IPGRunner™ Cassette and rehydrated overnight as per manufacturer's instructions. Rehydrated IPG strips were focused by performing IEF in triple distilled water. The applied electric potential (V) was increased in a step-wise fashion as follows: 200 V (20 minutes), 450 V (15 minutes), 750 V (15 minutes) and 1000 V (120 minutes), with a total power of 0.1 W $strip^{-1}$ and current, 0.05 mA $strip^{-1}$.

After IEF, the IPG strips were removed from the Zoom® IPGRunner™ cassette and equilibrated in SDS-Equilibration buffer (1.5 M Tris-HCL, pH 8.8, 6 M Urea, 30% Glycerol, 2% SDS, 0.1% w/v bromophenol blue, 10 μg/μL) for 1 hour at room temperature with shaking. A 0.5% agarose gel containing a molecular weight marker well and a well for the IPG strip, was pre-cast on top of a (0.1%)-SDS-(12%)-PAGE resolving gel in a Bio-Rad Protean III electrophoresis system. The equilibrated IPG strip containing the protein samples was then carefully loaded onto the agarose gel, and SDS-PAGE analysis was conducted as described in section 2.2.3. This was followed by Western

analysis, which is described in section 2.2.5. When IPG strips with a linear pI range were used, the approximate pI's of the spots resolved by 2D gel electrophoresis were estimated by calculating the distance migrated by the spot as a percentage of gel length and reading off the pI from a graph of 'spot position' vs pH generated by Amersham (www.amershambiosciences.com; refer to Appendix A2).

### 2.2.5 Western Analysis

#### 2.2.5.1 Protein Transfer/Blotting onto Nitrocellulose

Western analysis was carried out on the resolved proteins according to Towbin *et al*. (1979). Following electrophoresis, the gel was equilibrated in ice-cold transfer buffer (25 mM Tris, 192 mM glycine, 20% (w/v) methanol) along with a nitrocellulose membrane and 3MM Whatman filter paper. The pre-equilibrated SDS-PAGE gel was placed against the nitrocellulose membrane, sandwiched between pieces of equilibrated 3MM Whatman filter paper, and the proteins transferred from the gel to the membrane in a small scale Bio-Rad Western transfer set (Bio-Rad, UK), in chilled transfer buffer at 100 V for 1 hour. The transfer was kept chilled by the insertion of a cooling unit containing ice and continuous stirring on a magnetic stirrer. To determine whether the transfer was successful, the nitrocellulose membrane was stained with Ponsceau stain (0.5% (w/v) Ponceau S, 1% (v/v) glacial acetic acid) for 1 minute. The stain was removed by rinsing with distilled water.

#### 2.2.5.2 Chemiluminescence-Based Immunodetection

After Western transfer of proteins onto a nitrocellulose membrane, the membrane was washed twice in TBS-Tween (50 mM Tris-HCl, pH 7.5, 150 mM NaCl and 0.2% v/v Tween-20) and blocked overnight in blocking solution (5% w/v non-fat milk powder in TBS-Tween) at 4$^{o}$C. Proteins were then specifically detected by incubating the membrane with primary antibody diluted into blocking solution for 2 hours at room temperature with shaking. This was followed by four washes with TBS-Tween for 15 minutes each at room temperature with shaking.

The membrane was incubated with horseradish peroxidase (HRP)-conjugated secondary antibody for 1 hour at room temperature with shaking, followed by four washes with TBS-Tween for 15 minutes each as before. The membrane was then incubated with luminol based detection reagents (ECL Advance Western blot detection kit) for five minutes, and visualized using the Bio-Rad's VersaDoc$^{TM}$ Model 4000 imaging system.

#### 2.2.5.3 Primary and Secondary Antibody Dilutions

Monoclonal mouse anti-human Hsp70 (inducible) was used at a dilution of 1:5000; Recombinant Anti-Hop at a dilution of 3:1000; HRP-conjugated sheep anti-mouse secondary antibody at a dilution of 1:5000; and HRP-conjugated anti-human F(ab')$_2$ secondary antibody at a dilution of 1:50000 in blocking solution.

### 2.2.6 Analysis of the Phosphorylated State of Hop *In Vivo*

In order to satisfactorily determine the phosphorylation status of Hop *in vivo*, NIH 3T3 cells were either treated with phosphatase inhibitors (PI), to limit or eliminate any dephosphorylation of Hop, or treated with shrimp alkaline phosphatase (SAP), which dephosphorylated any phosphorylated isoforms of Hop. Cell lysate obtained from the cells treated under each of the conditions specified, were comparatively analyzed using 2D gel electrophoresis followed by Western analysis using antibodies generated against Hop (final concentration 2 μg/mL)

For the treatment of cells with phosphatase inhibitors, NIH 3T3 cells were incubated with serine/threonine phosphatase inhibitor, okadeic acid, (diluted to 30 nM in DMEM) at 37$^{o}$C for 30 minutes (Bianchini *et al.*, 1991; Zennadi *et al.*, 2004) prior to heat shock or further lysis preparation for 2D gel analysis. Tyrosine phosphatase inhibitor, sodium vanadate (Huyer *et al.*, 1996) was added into the lysis buffer to a final concentration of 2 mM and the cells were then lysed as described in section 2.2.2, in preparation of 2D gel electrophoresis.

SAP treatment was carried out by incubating cells that were not treated with any phosphatase inhibitors, with 10 U SAP in lysis buffer at 4$^{o}$C for 1 hour followed by

centrifugation at 12000 g to remove insoluble cell debris (section 2.2.2). Protein samples obtained from both treatments described above were submitted to 2D gel electrophoresis and Western analysis, and the spots corresponding to possible isoforms of Hop were comparatively analyzed by estimating the pI's as described in section 2.2.4.3.

## 2.3 RESULTS

### 2.3.1 Heat Shock Response was Induced at 42°C But Hop Protein Levels Did Not Change

Acute heat shock conditions to temperatures between 40 and 45.5°C for less than one hour applied to mammalian cells are described as short-term heat shock exposure (Kuhl and Rensing, 2000). Hsp72 was used as a marker of the heat shock response as this protein is induced under heat stress (Tavaria *et al.*, 1996; Takayama *et al.*, 1997). Mouse NIH 3T3 cells were subjected to heat shock at 42°C for 10, 20 and 30 minutes and equivalent amounts of protein were subjected to SDS-PAGE and Western analysis for the detection of Hsp72 (inducible Hsp70) and for Hop. Levels of Hsp72 were shown to be markedly increased with an increase in the duration of heat shock, as seen in figure 2.1, panel B (compare lanes 2-5). Panel C of figure 2.1, lanes 2-5 showed that the levels of Hop did not change significantly upon heat shock for 0, 10, 20 and 30 minutes of heat shock. These results are representative of three independently conducted experiments.

### 2.3.2 Acidic Isoforms of Hop Emerged After Heat Shock

Figure 2.2 shows the comparative 2D profile of Hop after Western analysis from cells that were grown normally at 37°C and those that were subjected to heat shock at 42°C. The isoforms of Hop were resolved on a non-linear pI strip range 3-10 and all isoforms were seen between pI's of approximately 6 and 6.4. Under normal conditions, a major (figure 2.2, 0 min; Bold large asterisk) and a minor isoform (figure 2.2, 0 min; Medium asterisk) were detected. After heat shock, there was a reduction in the amount of the major isoform and an increase in the minor isoform (figure 2.2, 30 mins). Moreover, there was an emergence of at least two more relatively acidic isoforms (figure 2.2, 30 min; smaller asterisks). The presence of a negatively charged phosphate group after phosphorylation of a protein allowed the inference of relatively acidic isoforms to be associated with phosphorylation. The non-linear nature of resolution of the strip used for IEF made it difficult to assign individual pI's to each spot. The results obtained are representative of three independently conducted experiments.

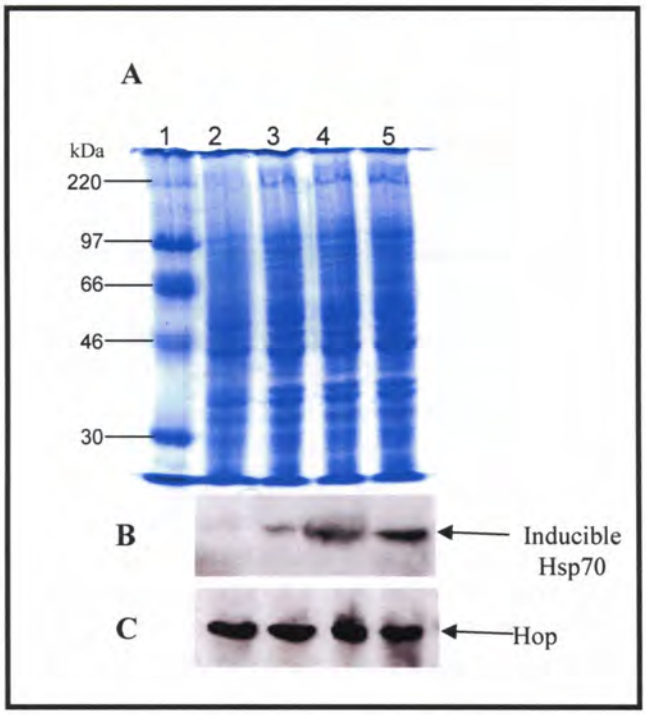


**Figure 2.1: Heat shock response was induced at 42°C but the protein levels of Hop were not changed by the heat shock response. A:** Mouse NIH 3T3 cells were subjected to varying durations of heat shock at 42°C and total protein was subsequently harvested and quantified. A: Total protein lysates (30 μg) were resolved by SDS-PAGE and stained with Coomassie Blue (Lane 1: molecular mass markers; Lane 2: 0 min heat shock; Lane 3: 10 mins heat shock; Lane 4: 20 mins heat shock; Lane 5: 30 mins heat shock). **B:** Western analysis was performed using antibodies generated toward the inducible Hsp70 to detect increasing levels of inducible Hsp70 with heat shock. **C:** Antibodies generated toward the C-terminus of Hop were used to detect whether there was any change in the steady state levels of Hop during the duration of the heat shock treatment. The protein levels of Hop did not change signficantly between the various durations of heat shock applied. This figure represents the results obtained from three experiments conducted independently.

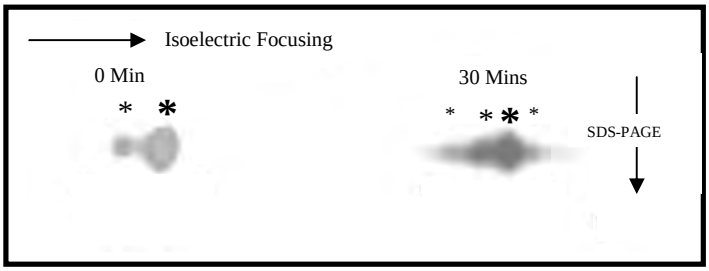


**Figure 2.2: Acidic isoforms of Hop emerged after heat shock.** Mouse NIH 3T3 cells were subjected to 0 and 30 minutes of heat shock at 42$^{o}$C and total protein was subsequently harvested. Total protein (120 μg) was resolved by 2D gel electrophoresis (isoelectric focussing and SDS-PAGE steps indicated) using a non-linear pI strip range of 3-10 followed by Western blot analysis for the detection of Hop. The major isoform obtained under normal conditions is indicated by the bold asterisk and the minor isoform, by a medium asterisk. Two other isoforms representing relatively acidic isoforms, which emerged after heat shock treatment are also indicated by smaller asterisks. All isoforms were identified within a pI range of 6-6.4, however individual pI's were not assigned to any one isoform due to difficulties arising from the non-linear nature of the pI strip used. This figure represents the results obtained from three independent experiments.

### 2.3.3 Hop was Phosphorylated *In Vivo* at 37°C

An analysis of the phosphorylated state of Hop *in vivo* was conducted by a more rigorous determination of the isoform profile of Hop in the presence of PI and after SAP treatment. Furthermore, the isoforms of Hop were separated with greater resolution on a linear pI strip range of 4-7 (figure 2.3). For lysates treated with PI and no SAP added, Hop was found to exist not only as a major and minor isoform, but also as three more relatively acidic isoforms (figure 2.3; upper panel). The major isoform with a calculated pI of approximately 6.1 was labeled '0' and the minor isoform found at pI of approximately 6.0 was labeled '+1'. A third isoform, approaching a pI of 6.0 and merging with isoform +1 was labeled '+2'. The two other relatively more acidic isoforms at pIs less than 5.9 were designated by asterisks and were not assigned approximate pI's. Treatment of the cell lysate with SAP caused a considerable reduction in isoforms +1 and +2 (figure 2.3; lower panel) suggesting that they were dephosphorylated by SAP treatment. These results provided evidence of *in vivo* phosphorylation of at least two subpopulations of Hop under normal conditions. The most acidic isoform obtained under normal conditions (designated by an asterisk) disappeared after SAP treatment, indicating that this isoform may correspond to a minor phosphorylated isoform of Hop. A prominent isoform, designated '+3' was detected after SAP treatment at an approximate pI of 5.9, and this isoform was not prominent in lysate obtained from normally grown cells that were treated with PI (figure 2.3; upper panel). The results are representative of at least two independent experiments.

### 2.3.4 Hop was Phosphorylated Differently *In Vivo* at 42°C Versus 37°C

The isoform composition of Hop after 30 minutes of heat shock (figure 2.4; upper panel) differed from that of normal conditions in that there was a reduction in the amount of the major isoform 0. There was also an increase of a number of minor acidic isoforms, the most prominent of which had an approximate pI of 5.9 and was designated '+3'. This isoform was also seen in the SAP treated normal lysate (figure 2.3, lower panel). All the other minor isoforms that increased after heat shock were not designated approximated pI's, and were indicated by asterisks. However, it was noted that these isoforms were found at pI's of 5.9 or lower. Treatment of the heat shocked cell lysate with SAP yielded

an isoform profile for Hop (Figure 2.4; lower panel) which included a slight increase of the previously major isoform 0, and the complete absence of isoform +2. Isoform +3 showed a considerable reduction after treatment with SAP. The results obtained are representative of at least two independent experiments.

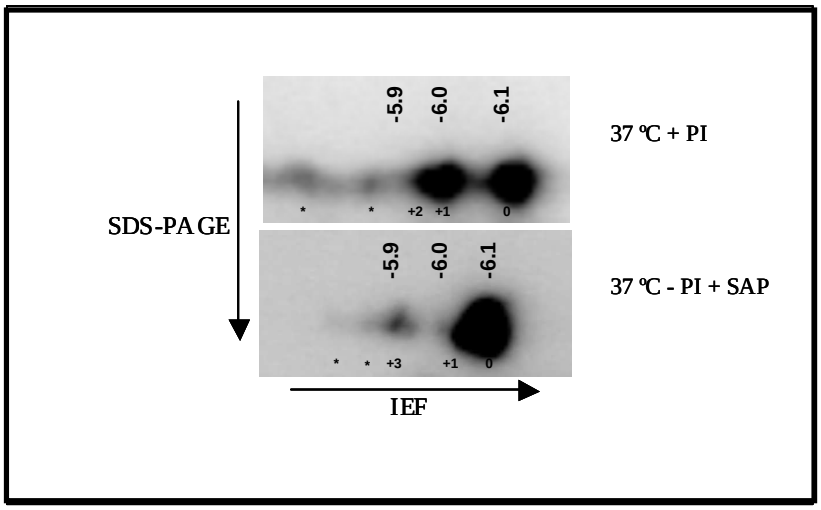


**Figure 2.3: Hop was phosphorylated *in vivo* at 37°C:** Mouse NIH 3T3 total protein lysate (120 μg) was resolved by 2D-gel electrophoresis, followed by Western analysis for the detection of Hop. The isoelectric focusing (IEF) and SDS-PAGE steps are shown. The upper panel shows the Western of lysates prepared from cells that were grown under 37°C and treated with phosphatase inhibitors (37°C + PI); the lower panel shows the Westerns of lysates prepared from cells that were also grown at 37°C and treated with shrimp alkaline phosphatase (SAP) but not treated with PI (37°C – PI + SAP). Approximate pI's for the prominent isoforms were estimated and are indicated at the top of each panel. The position of the isoforms with assigned pI's did not always coincide due to technical discrepancies such as slight changes in gel size. The major isoform under normal conditions, with an approximate pI of 6.1 was arbitrarily given the label '0'. Any isoform that was found to be more acidic than '0' was labeled with increasing positive numbers. Additional isoforms which were not assigned a pI value were labeled with an asterisk. The figure presented represents the results obtained from at least two independently conducted experiments.

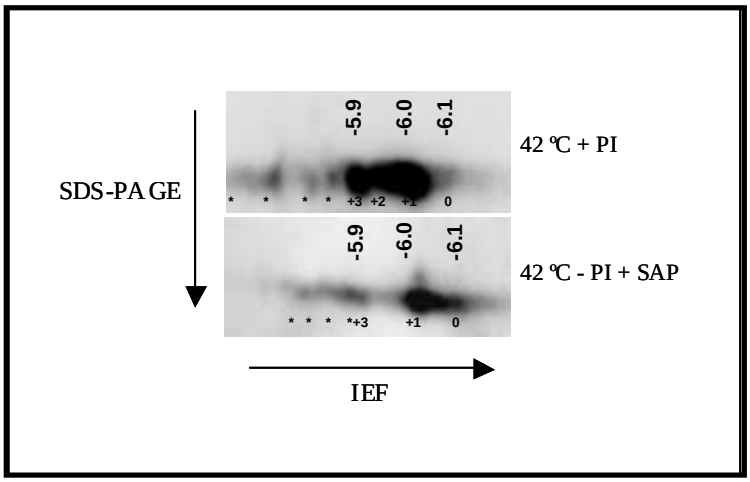


**Figure 2.4: Hop was phosphorylated differently *in vivo* at 42°C versus 37°C:** Mouse NIH 3T3 total protein lysate (120 μg) obtained from cells that were heat shocked at 42°C for 30 minutes were resolved by 2D-gel electrophoresis, followed by Western analysis for the detection of Hop. The isoelectric focusing (IEF) and SDS-PAGE steps are shown. The upper panel shows the Western of lysates prepared from cells that were grown under 42°C and treated with phosphatase inhibitors (42°C + PI); the lower panel shows the Westerns of lysates prepared from cells that were also grown at 42°C and treated with shrimp alkaline phosphatase (SAP) but not treated with PI (42°C – PI + SAP). Approximate pI's for the prominent isoforms were estimated and are indicated at the top of each panel. The position of the isoforms with assigned pI's did not always coincide due to technical discrepancies such as slight changes in gel size. The major isoform under normal conditions, with an approximate pI of 6.1 was arbitrarily given the label '0'. Any isoform that was found to be more acidic than '0' was labeled with increasing positive numbers. Additional isoforms which were not assigned a pI value were labeled with an asterisk. The figure presented represents the results obtained from at least two independently conducted experiments.

## 2.4 DISCUSSION

The separation of the isoforms of mouse Hop on a non-linear pI strip of 3-10 (figure 2.4) showed the presence of two isoforms under normal conditions, with an increase in acidic isoforms after heat shock for 30 minutes. These results were comparable to other studies that showed that mouse Hop migrated as a major and minor, relatively more acidic, isoform (Lässle *et al.*, 1997; Zanata *et al.*, 2002). Upon heat shock for ten minutes, there was a significant decrease in the major isoform and an increase in both the numbers of acidic isoforms and their amount (Lässle *et al.*, 1997).

Earlier studies on mouse Hop (Lässle *et al.*, 1997) were conducted using a cell lysate that was treated with a tyrosine phosphatase inhibitor (sodium vanadate). The initial isoform analysis reported by the present study (figure 2.2) was, however, conducted on a cell lysate that was not treated with any phosphatase inhibitors, and was nevertheless comparable with results published by Lässle *et al.* (1997). Therefore, in light of the present study, the findings of Lässle *et al.* (1997) can be re-interpreted as suggestive of phosphorylation of Hop at sites other than tyrosine. This is consistent with later findings that suggested phosphorylation at serine and threonines (Longshaw *et al.*, 2000; Longshaw *et al.*, 2004). However, on the basis of these results, further strategies were employed to directly test the presence of phosphorylated isoforms of Hop. Mouse fibroblast cells were either treated with phosphatase inhibitors, which included the tyrosine phosphatase inhibitor, sodium vanadate, as well as the serine/threonine phosphatase inhibitor, okadeic acid, or the cells were treated with SAP, a protein phosphatase. Lysates obtained from each treatment were resolved by 2D gel electrophoresis, using a pI strip of 4-7 for better resolution, followed by Western analysis for the detection of Hop.

The results obtained showed that under normal conditions, not only did Hop exist as a major (0) and minor isoform (+1), but also as three more relatively acidic isoforms (figure 2.3; upper panel). Treatment of the cell lysate with SAP in the absence of PI (figure 2.3; lower panel), showed a considerable decrease in isoform +1 and +2. These

results provided, for the first time, evidence of *in vivo* phosphorylation of at least two subpopulations of Hop under normal conditions.

Heat shock is also known to exert both inhibitory and activating effects on various kinases and phosphatases, thus influencing the phosphorylation status of certain proteins (Duncan and Hershey, 1989; Bagi and Hidvegi, 1990; Somero, 1995). Since Hop was shown to be phosphorylated under normal conditions, it was of interest to analyze the phosphorylated status of Hop when the cell was heat shocked. Analysis by 2D showed that the isoform composition of Hop under acute heat shock conditions (figure 2.6; upper panel) differed from that of normal conditions in that there was a reduction in the amount of the major isoform '0'. This was consistent with data published by Lässle *et al.* (1997). Moreover, a number of minor acidic isoforms were observed to be present after heat shock, of which +3 at pI 5.9 was the most distinctive. Treatment of heat shocked cell lysate with SAP yielded an isoform profile for Hop (figure 2.4; lower panel) which included a slight increase in the levels of the previously major isoform 0, and the complete disappearance of isoform +2. Interestingly, isoform +3 showed a considerable decrease after treatment with SAP. It was debatable as to whether all the minor isoforms appearing after heat shock and designated by asterisks were generated by phosphorylation, since some of them were still observable when normal cell lysate was treated with SAP. Therefore, although heat shock may lead to a number of modifications of Hop in mammalian cells, the data presented here implies that differential phosphorylation of Hop as one of these modifications.

The phosphorylation of Hop as a result of heat shock may differ within the mammalian and yeast system. Early studies carried out on yeast Hop (Nicolet and Craig, 1989) reported two major and two minor isoforms of the protein with pI's ranging from 5.75 to 6.05, implying differential phosphorylation of yeast Hop *in vivo*. However, there was no apparent change in the isoform composition of yeast Hop after heat stress (Nicolet and Craig, 1989), suggesting that the heat shock conditions used did not change the phosphorylation state of Hop in the yeast system. The present study has shown that

mouse Hop is indeed phosphorylated *in vivo* under normal conditions, and differentially phosphorylated under acute heat stress (42$^{o}$C for 30 minutes).

It is likely, based on the presence of okadeic acid in the experimental conditions, that under normal conditions, phosphorylation of Hop may be attributable to phosphorylation at the serine or threonine residues. Hop contains six possible sites within its amino acid sequence, which may be phosphorylated by CK II and two possible sites which may be phosphorylated by cdc2-kinase (Blatch *et al.*, 1997). It has been established that Hop is indeed phosphorylated *in vitro* by CKII at Serine 189, as well as by cdc2-kinase at Threonine 198 (Longshaw *et al.*, 2000).

Heat shock is known to induce the activation of mitogen-activated protein (MAP) kinases (Rouse *et al.*, 1994; Chen *et al.*, 1995). The possibility that Hop may be phosphorylated by stress-related kinases has been previously investigated and Hop was found to have a potential phosphorylation site for MAPKAP kinase 2 and two potential sites for S6 kinases within its amino acid sequence (Lässle *et al.*, 1997). Although *in vitro* analysis showed that none of the GST-Hop fusion proteins examined were phosphorylated by any of these kinases, when possible folding artifacts of the fusion proteins are taken into consideration, these results do not completely rule out the possibility that Hop may also be phosphorylated by a stress kinase pathway *in vivo* (Lässle *et al.*, 1997).

Another major signaling event that the heat shock response induces is the transcriptional induction of heat shock proteins (Duncan and Hershey, 1989; Lee *et al.*, 2005). However, after submitting mouse fibroblast cells to heat shock at 42$^{o}$C for 30 minutes, no increase of Hop was observed at the protein level (figure 2.3). Other reports have shown that heat shock as well as viral transformation in mammalian cells, caused an increase in mRNA levels of mouse and human Hop respectively, and although human Hop was upregulated after viral transformation (Honoré *et al.*, 1992), there was no change in the expression levels of Hop in mouse cells after heat shock (Lässle *et al.*, 1997). In contrast to the mouse homolog, the parasitic (*Leishmania major*) and the plant homolog of Hop have

been shown to be stress-inducible both at the genetic level, as well as at the protein level (Webb *et al.*, 1997; Zhang *et al.*, 2003).

Hop's differential phosphorylation under normal and stress conditions could have various implications with regards to its function, particularly in terms of its scaffolding properties within the Hsp70-Hsp90 chaperone heterocomplex. Previous studies on the *in vitro* phosphorylation of Hop by cell cycle kinases suggested that the phosphorylation of Hop may play a part in regulating its subcellular localization (Longshaw *et al.*, 2000; Longshaw *et al.*, 2004). It is thus likely that the differential phosphorylation patterns exhibited by Hop may be better understood within the context of the subcellular localization patterns that it presents, and that a functional significance of Hop's phosphorylation may lie in the regulation of its subcellular localization.

# CHAPTER 3

# THE SUBCELLULAR LOCALIZATION OF HOP

*"It is a good morning exercise for a research scientist to*

*discard a pet hypothesis every day before breakfast."*

*- Konrad Lorenz (Pioneer of Ethology)*

## 3.1 INTRODUCTION

The various functions of Hop, within as well as outside the realm of an Hsp70-Hsp90 co-chaperone, are largely dependent on its subcellular localization. Early studies reported the occurrence of human Hop in the Golgi apparatus and small vesicles in normal cells, whereas a nucleolar localization of Hop was seen in SV40-transformed cells (Honoré *et al.*, 1992). In mouse fibroblast cells grown under normal conditions, the localization of Hop was reported to be predominantly cytoplasmic, with a low incidence of Hop being identified in the nucleus (Lässle *et al.*, 1997; Longshaw *et al.*, 2004). However, when these cells were arrested in the G1/S phase, or treated with Leptomycin B, a *Streptomyces* metabolite which inhibits the CRM1 dependent nuclear export of proteins (Kudo *et al.*, 1999), a predominantly nuclear accumulation of Hop was reported (Longshaw *et al.*, 2004).

This implied that Hop was constantly shuttling between the nucleus and cytosol, but the export of Hop from the nucleus was occurring at a faster rate than its import (Longshaw *et al.*, 2004). A bipartite NLS was proposed (Longshaw, 2002), which when fused to EGFP (enhanced green fluorescent protein) resulted in the localization of EGFP to the nucleus (Longshaw *et al.*, 2004), suggesting that this NLS was indeed functional. Other studies using immunoprecipitation techniques with membrane fractions from mouse brain tissue have shown that at least a portion of the Hop population is localized at the cell surface, where it interacts with $Prp^c$ (a protein whose expression is crucial to the propagation of neurological disease, in particular, Prion disease) both *in vitro* and *in vivo* (Zanata *et al.*, 2002).

Previous work reported that the nuclear translocation of Hop was cell cycle regulated since arresting the cells in G1/S phase showed increased nuclear translocation (Longshaw *et al.*, 2004). Stress conditions like heat stress are known to cause arrest of the cell in the G1/S phase of the cell cycle (Kuhl and Rensing, 2000). Thus, one of the main objectives of this study was to compare the subcellular localization patterns of Hop under normal growth conditions ($37^oC$), acute heat shock conditions ($42^oC$ for 30 minutes) and hydroxyurea treatment which arrests the cells in the G1/S phase (Longshaw *et al.*, 2004).

A second objective was to study the functionality of the previously proposed bipartite NLS ($K^{222}$ - $K^{239}$) *in vivo.* Other studies on bipartite NLSs have shown that usually the major arm of a bipartite NLS is critical for functionality *in vivo* due to its ability to bind to the major binding site on importin-α (Conti *et al.*, 1998; Conti and Kuriyan, 2000; Fontes *et al.*, 2000; Friedrich *et al.*, 2006). Moreover, when the major binding site on importin-α is not involved in interactions with NLSs, the IBB domain is found to occupy this binding site thereby inhibiting nuclear transport of any importin-α complex (Catimel *et al.*, 2001). Based on this, the residues of the major arm of the proposed NLS were predicted to be critical for functionality of the NLS activity *in vivo*. It was thus of interest to mutate the residues within the putative NLS that were predicted to be important for NLS functionality, and test the functionality of this NLS by studying the subcellular localization patterns of the NLS-mutant proteins under normal conditions, heat shock and hydroxyurea treatment. In light of the partnership of Hop with Hsp70 and Hsp90, an investigation into the subcellular localization of both these major heat shock proteins was also warranted in order to understand the broader context of the subcellular localization of Hop. Thus it was also of interest to compare the subcellular localization of Hop with that of Hsp70 and Hsp90 under normal and heat shocked conditions.

The specific objectives of this study were to:

1. Successfully generate Hop-EGFP and its mutational constructs, Hop-K239A-EGFP and Hop-K237/238/239A-EGFP.
2. Transiently transfect mammalian cells with Hop-EGFP and its derivative constructs, Hop-K239A-EGFP and Hop-K237/238/239A-EGFP, and study the subcellular localization patterns of these constructs under normal conditions, acute heat shock conditions (42$^{o}$C for 30 minutes) and after treatment of the cells with 10 mM hydroxyurea to induce G1/S arrest of cells.
3. Biochemically fractionate mammalian cells into its various subcellular compartments, and perform Western analysis detection of Hop, Hsp70, Hsp90 and β-actin (a cytosolic marker protein).

## 3.2 EXPERIMENTAL PROCEDURES

### 3.2.1 The Subcellular Localization of Hop-EGFP and Derivatives of the Putative NLS Under Normal Conditions, Heat Shock and G1/S Arrest, Using Confocal Fluorescence Microscopy

#### 3.2.1.1 Generation and Analysis of Plasmid Constructs Encoding Hop-EGFP and its Mutant Derivatives

The Hop-EGFP plasmid construct and its mutants Hop-K239A-EGFP and Hop-K237/238/239A-EGFP were generated from pSK-mSTI1-EGFP. pSK-mSTI1-EGFP contains cDNA encoding the full-length protein mSTI1 (mouse homolog of Hop) fused at its C-terminal with EGFP (Longshaw, 2002; Longshaw *et al.*, 2004). All mutations were carried out by site-directed mutagenesis using a double-stranded whole plasmid linear amplification procedure (Appendix A8). For screening purposes, silent mutations were engineered to create restriction sites except where the desired codon change(s) automatically generated restriction sites. The specific mutagenic primers are listed in Section C of the Appendix.

After mutagenesis, 1 μL of the mutated DNA was used to transform *E.coli* XLI blue cells. Modified plasmids were isolated from *E.coli* harboring them using the Qiagen miniprep kit. All plasmid constructs and their mutations were confirmed both by restriction enzyme analysis (Appendix A9) and by DNA sequencing (Appendix A11) according to plasmid maps generated by Vector NTI Advance ™ 10 (Invitrogen Corporation, USA). The large size of pB-mSTI1-EGFP (17.39 kbp) made it difficult to manipulate. Hence all mutations within Hop were conducted on the pSK-mSTI1-EGFP plasmid and then the mSTI1-EGFP encoding fragment from pSK-mSTI1-EGFP, both mutated and wild type, was further subcloned into pBCMGSNeo (Karasuyama and Melchers, 1988) *Xho*I/*Not*I sites to produce pB-mSTI1-EGFP as previously described (Longshaw, 2002; Longshaw *et al.*, 2004). Plasmid DNA restriction analyses were visualized by 0.8% agarose gel electrophoresis as described in Appendix A10. Unfortunately the pBCMGSNeo plasmid as supplied was not fully sequenced by Karasuyama and Melchers (1988), and therefore all cloning work was carried out with

reference to an approximated restriction map (figure 3.3 A). The inserts of the plasmids used in this study were, however, confirmed as correct by sequencing as described in Appendix A11. All plasmid constructs listed retain their original cloning nomenclature, which refers to mSTI1 (mouse homolog of Hop). However to avoid confusion, the proteins they encode have been labeled mouse Hop.

#### 3.2.1.2 The Subcellular Localization of Hop-EGFP and Its Mutant Derivatives Under Various Treatments by Confocal Laser Scanning Fluorescence Microscopy

##### 3.2.1.2.1 Tissue Culture and Heat Shock of BHK-21 Cells

BHK-21 cells were used for all subcellular localization studies due to the ease of transient transfections of relatively large plasmids, as compared to NIH 3T3 mouse fibroblast cells. The BHK-21 cells were maintained in DMEM supplemented with 10% heat inactivated fetal calf serum, penicillin (100 U $mL^{-1}$) and streptomycin (100 U $mL^{-1}$) in a humidified atmosphere, at 37°C with 5% $CO_2$. An acute heat shock response was obtained by treating the cells at 80% growth confluence to pre-warmed DMEM and then incubating for 30 minutes at 42$^{o}$C (Kuhl and Rensing, 2000).

##### 3.2.1.2.2 Transient Transfection of BHK-21 Cells and Preparation of Cells For Confocal Microscopy

BHK-21 cells were transiently transfected with pB-mSTI1-EGFP and its mutant derivatives. Transient transfections were carried out using IBAfect, a polycationic transfection reagent based on liposome technology, in combination with MA Lipofection Enhancer (IBA, Germany). The MA Lipofection Enhancer is based on a technique that associates plasmid DNA to magnetic nanoparticles. Exploiting magnetic force with the help of a magnet plate allows for the rapid and efficient delivery of the full nucleic acid dose into the target cells.

BHK-21 cells were grown to 60% confluency on 13 mm cover slips in 24 well plates. Plasmid DNA (1 μg) was incubated with IBAfect (3 μL) in serum-free DMEM at room temperature for 20 minutes. This was followed by the addition of MA Lipofection

Enhancer (1 μL), mixed well by pipetting up and down, and incubated at room temperature for 15 minutes. The DNA-IBAfect-MA Lipofection Enhancer mixture was added to the cells and mixed well by pipetting. The 24 well plate was placed on a 24 well plate-magnet for 15 minutes at room temperature. The cells were then incubated at 37$^{o}$C for 48 hours, before further treatments. Acute heat shock conditions were achieved for 30 minutes as described in section 3.2.1.2.1. Arrest of cells in the G1/S phase was achieved by treating transfected cells with 10 mM hydroxyurea (Longshaw *et al.*, 2004). Cells were fixed in 4% paraformaldehyde for 10 minutes and nuclei stained with 2 mg mL$^{-1}$ 4', 6-diamidino-2-phenylindole (DAPI; Sigma) in PBS.

#### 3.2.1.2.3 Confocal Laser Scanning Fluorescence Microscopy

Slides were mounted in fluorescent mounting solution (DAKO). Cells expressing Hop-EGFP or its derivative EGFP-conjugated proteins were viewed and captured using the Zeiss LSM 510 Meta confocal microscope (40 x oil immersion objective) and LSM 510 software (Zeiss). A FITC/EGFP filter with an excitation wavelength of 488 nm and an emission wavelength within the range of 505-550 nm was used to visualize the EGFP fluorescence (green) and in a separate channel, a DAPI filter with an excitation wavelength of 405 nm and an emission wavelength within the range of 420-480 nm was used to visualize DAPI-stained nuclei (blue). For quantification purposes, cells were divided into three categories: cells showing (i) predominantly cytoplasmic fluorescence, (ii) cytoplasmic and nuclear fluorescence and (iii) predominantly nuclear fluorescence. Average values were taken from six different fields and the error bars represent standard deviations.

### 3.2.2 The Subcellular Localization of Hop, Hsp70 and Hsp90 Under Normal and Heat Shock Conditions Using Biochemical Fractionation

Whole BHK-21 cells were fractionated into cytoplasmic, nuclear, membrane and cytoskeletal fractions using the ProteoExtract® Subcellular Proteome Extraction Kit (S-PEK, Calbiochem) (Sabio *et al.*, 2005). This method takes advantage of different solubility of the various subcellular compartments in four specific buffers resulting in the

sequential extraction of subcellular proteomes, which are in the native and functional state.

BHK-21 cells were grown to 80% confluence as described in 3.2.1.2.1 in T 75 cm tissue culture flasks and either directly subjected to biochemical fractionation, or heat shocked before being biochemically fractionated by S-PEK according to the supplier's specifications. Each appropriate extraction reagent for the extraction of a specific subcellular proteome (in the order of decreasing complexity, i.e. cytosolic, membranous, nuclear and cytoskeletal), along with a protease inhibitor cocktail, as provided in the kit, was added directly into the tissue culture flask, without the need for cell removal, and incubated with agitation under the conditions described. In the case of nuclear extraction of proteins, Benzonase ® (DNase/RNase) provided by the kit was also added into the extraction buffer.

Proteins obtained from each fraction were resolved using SDS-PAGE and then subjected to Western analysis, probing for β-actin (monoclonal anti-mouse β-actin at a final dilution of 1:4000), Hsp72/73 (monoclonal mouse anti-human Hsp72/73 which detects both the inducible and the constitutive Hsp70; final dilution: 1:5000), Hsp90 (monoclonal rat anti-human Hsp90; final dilution: 1:5000) and Hop (dilution: 3:1000). The secondary antibodies used were HRP-conjugated sheep anti-mouse and HRP-conjugated goat anti-rat IgM at final dilutions of 1:5000. The analysis was conducted on total protein obtained from equivalent number of cells.

## 3.3 RESULTS

### 3.3.1 pB-mSTI1-EGFP and its Derivative Constructs Were Successfully Generated

The pSK-mSTI1-EGFP plasmid shown in figure 3.1 A (Longshaw, 2002; Longshaw *et al.*, 2004) was screened by restriction endonucleases digestion and the resultant DNA fragments were resolved by 0.8% agarose gel electrophoresis as shown in figure 3.1 B. Lane 2 shows the uncut parent plasmid, which resolved into a higher mobility fragment that corresponds to the supercoiled DNA and a lower mobility fragment which is the nicked DNA. Digestion of pSK-mSTI1-EGFP with *Not* I and *Xho* I separately linearized the plasmid and produced an expected fragment of 5296 bp (lanes 3 and 4 respectively) compared to the double digestion of pSK-mSTI1-EGFP with *Not* I and *Xho* I together, which produced the two expected 2918 and 2378 bp fragments (lane 5).

Site-directed mutagenesis was carried out on pSK-mSTI1-EGFP to produce pSK-mSTI1-K239A-EGFP (figure 3.2 A) and pSK-mSTI1-K237/238/239A-EGFP (figure 3.2 B). An *Nsi* I digestion site was engineered onto the plasmid along with the above-mentioned mutations, in order to facilitate restriction endonuclease digestion. Figure 3.2 C shows the digestion of the various pSK-mSTI1-EGFP constructs with *Nsi* I. Lane 2 corresponds to uncut parental plasmid, which has resolved into the expected supercoiled DNA fragment of higher mobility and the nicked DNA fragment of lower mobility. Treatment of the parental plasmid with *Nsi* I did not digest the plasmid and produced the fragments comparable to the uncut plasmid (lane 3). The pSK-mSTI1-K239A-EGFP plasmid was linearized by *Nsi* I into the expected 5296 bp band (lane 5), which can be compared to the uncut plasmid (lane 4). The presence of a higher mobility band and a lower mobility band in lane 5 corresponds to the presence of supercoiled and nicked DNA respectively and shows that the plasmid was partially digested. Similarly, digestion of pSK-mSTI1-K237/238/239-EGFP with *Nsi*I resulted in an expected fragment of 5296 bp (lane 7) when compared to the uncut plasmid (lane 6). The presence of supercoiled and nicked DNA was also detected after digestion of the plasmid with *Nsi* I (lane 7) indicating partial digestion. All mutations were furthermore confirmed by sequencing.

Following successful mutagenesis and confirmation of the mutagenic constructs obtained, the mSTI1-EGFP encoding fragment from pSK-mSTI1-EGFP, both mutated and wild type, were subcloned into pBCMGSNeo (Karasuyama and Melchers, 1988) *Xho*I/*Not*I sites to produce pB-mSTI1-EGFP as described previously (Longshaw *et al.*, 2004) and shown in figure 3.3 A. The successful ligation reactions were tested by restriction endonuclease digestion using Hind III as shown in figure 3.3 B. Lanes 2, 4 and 6 show the resolution of uncut plasmids (pB-mSTI1-EGFP, pB-mSTI1-K239A-EGFP and pB-mSTI1-K237/238/239A-EGFP) into supercoiled and nicked DNA. The digestion of all three plasmids resulted in the expected fragments of approximate sizes 7700, 5000, 3790 and 902 bp (lanes 3, 5 and 7) indicating that the coding regions for mSTI1-EGFP, mSTI1-K239A-EGFP and mSTI1-K237/238/239A-EGFP were successfully ligated into the pB vector. The mutations were confirmed by sequencing.

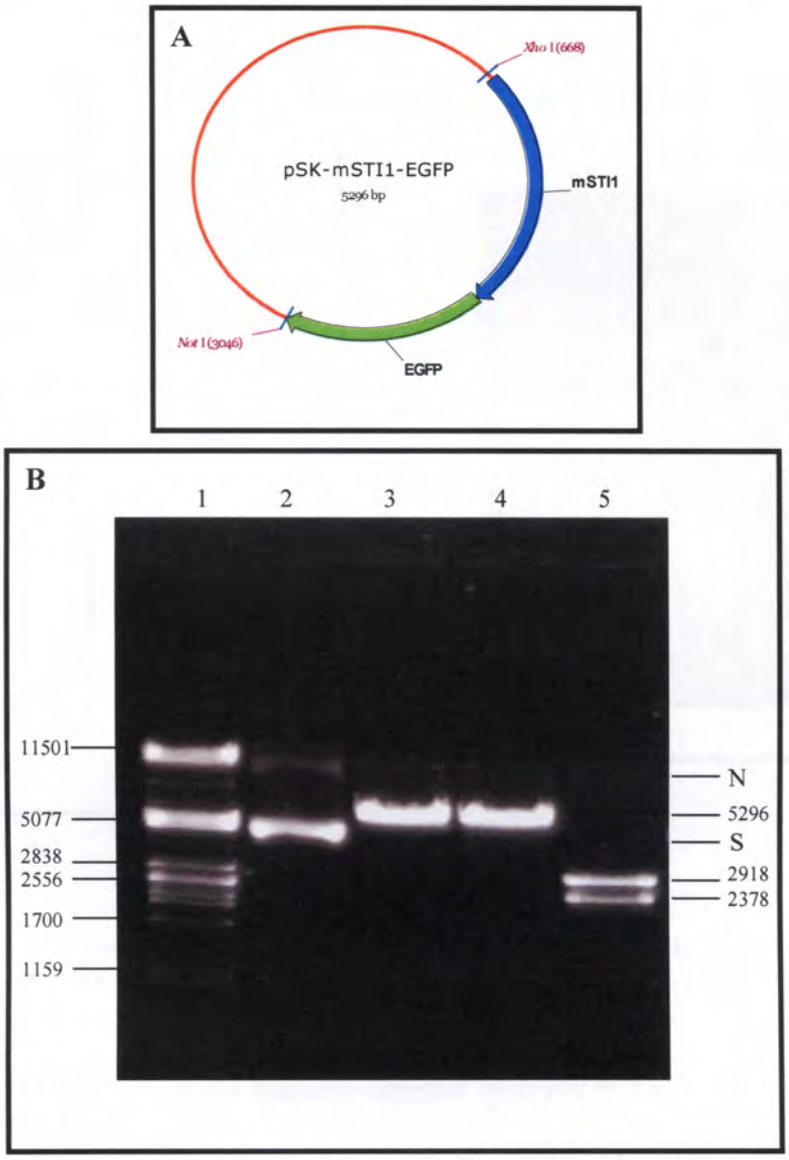


**Figure 3.1: The identity of pSK-mSTI1-EGFP was restriction analyzed with *Not* I and *Xho* I.** pSK-mSTI1-EGFP **(A)** was digested with restriction endonucleases and the digested fragments were further resolved on a 0.8% agarose gel **(B)**. B: Lane 1: Lambda markers digested with *Pst* I; Lane 2: Undigested pSK-mSTI1-EGFP; Lane 3: pSK-mSTI1-EGFP linearized by *Not* I; Lane 4: pSK-mSTI1-EGFP linearized by *Xho* I; Lane 5: pSK-mSTI1-EGFP doubly digested with *Not* I and *Xho* I to release two expected fragments at 2918 and 2378 bp. Sizes of each DNA marker in fragment in basepairs (bp) are annotated on the left and expected sizes of the fragments obtained after each digest are annotated on the right (bp). Nicked (N) and supercoiled (S) DNA fragments are also indicated on the right hand side of the gel.

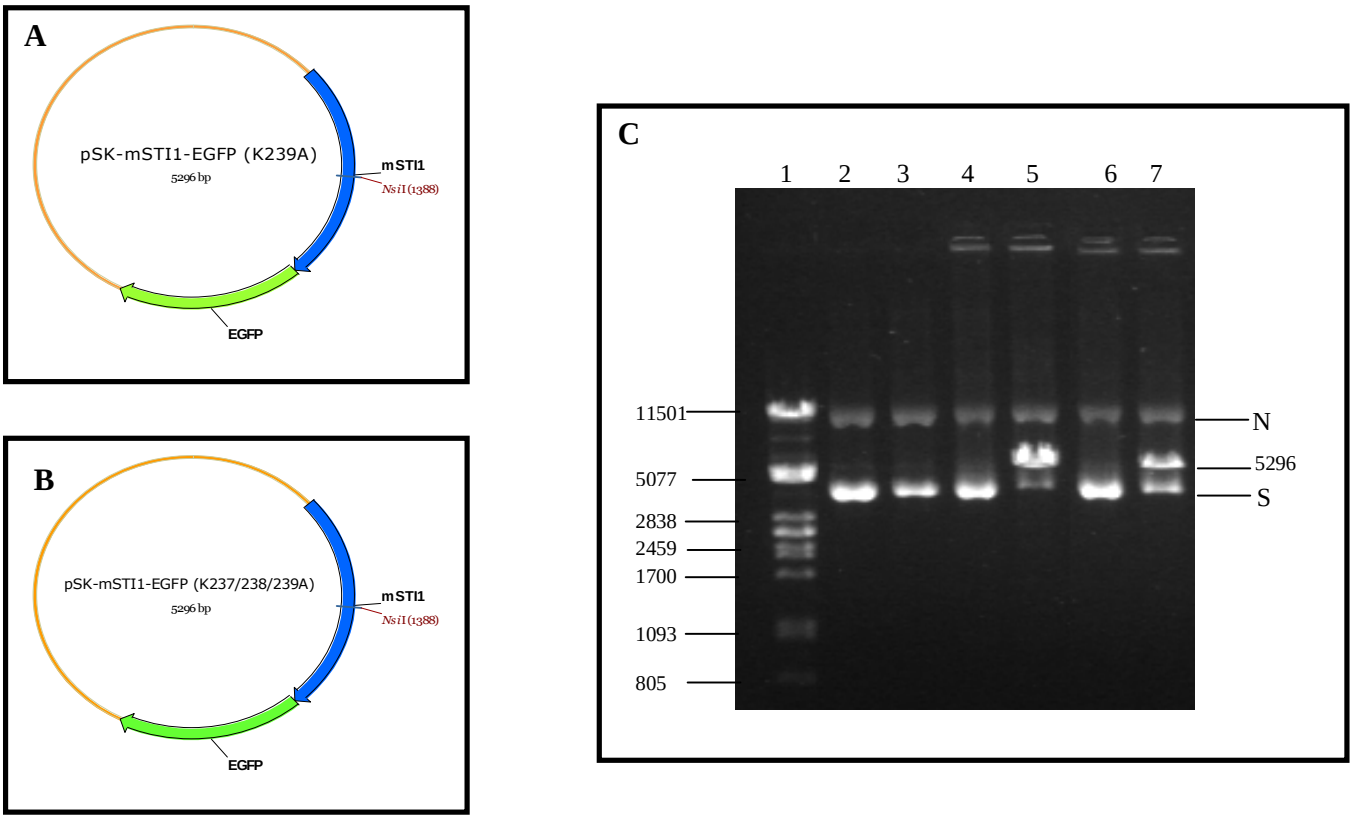


**Figure 3.2 Codon changes for the K239A and K237/238/239A substitutions were successfully engineered in pSK-mSTI1-EGFP.** Successful mutations engineered in pSK-mSTI1-EGFP to produce the constructs pSK-mSTI1-EGFP (K239A) **(A)** and pSK-mSTI1-EGFP (K237/238/239A) **(B)** were analyzed by restriction enzyme digest, followed by resolution of all digested fragments on a 0.8% agarose gel **(C)**. (C) Lane 1: Lambda markers digested with *Pst* I; Lane 2: Undigested pSK-mSTI1-EGFP; Lane 3: pSK-mSTI1-EGFP treated with *Nsi* I but undigested; Lane 4: pSK-mSTI1-K239A-EGFP uncut; Lane 5: pSK-mSTI1-K239A-EGFP linearized by *Nsi* I. Lane 6: pSK-mSTI1-K237/238/239A-EGFP uncut; Lane 7: pSK-mSTI1-K237/238/239A-EGFP linearized by *Nsi* I. Sizes of each DNA marker fragment in basepairs (bp) are annotated on the left and expected sizes of the fragments obtained after each digest (bp) are annotated on the right. The linearized fragment was seen at the expected size of 5296 bp for all mutated constructs digested with *Nsi* I. Nicked (N) and supercoiled (S) DNA fragments are annotated on the right hand side of the gel.

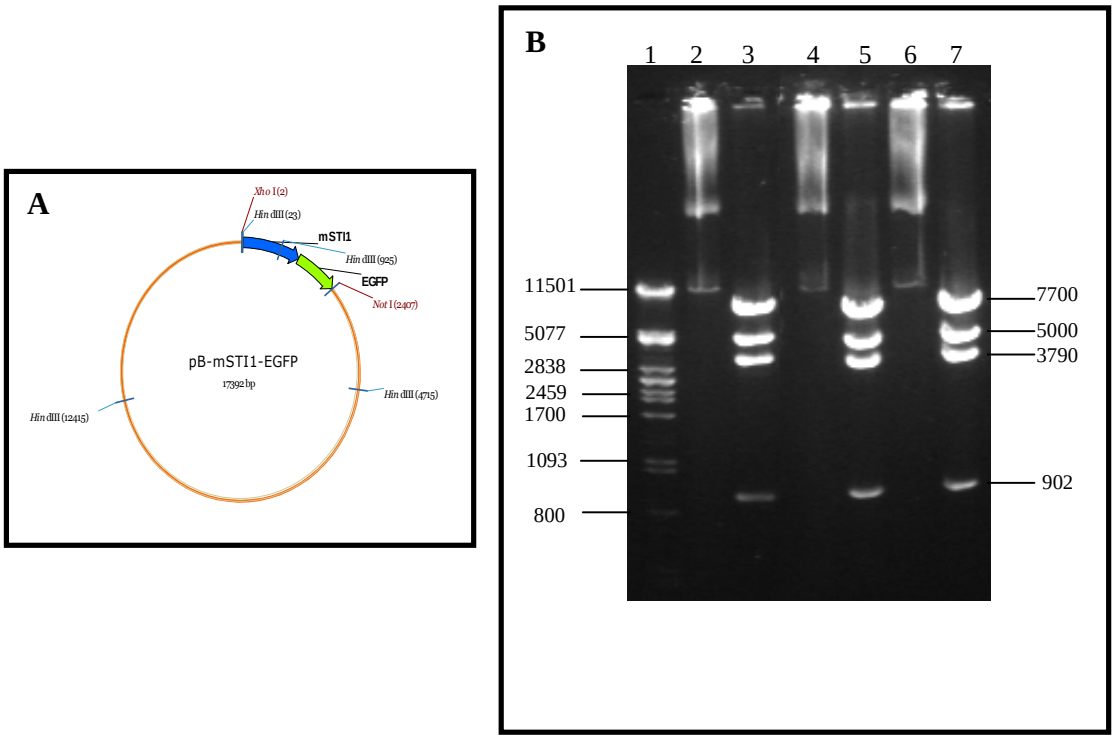


**Figure 3.3: The coding regions for mSTI1-EGFP, mSTI1-K239A-EGFP and mSTI1-K237/238/239A-EGFP were successfully ligated into the pBCMGSneo (pB) vector.** After mutagenesis in pSK-mSTI1-EGFP was conducted and confirmed using restriction endonuclease analysis and sequencing, both mutated and unmutated mSTI1-EGFP fragments were released from the pSK vector and ligated into the pB vector using the *Xho*I/*Not*I restriction sites **(A)**. The pB vector and the ligated products were digested with *Hind* III and all digested fragments were analyzed on 0.8% agarose gel **(B)**. B: Lane 1: Lambda markers digested by *Pst* I; Lane 2: pB-mSTI1-EGFP uncut; Lane 3: pB-mSTI1-EGFP digested by *Hind* III; Lane 4: pB-mSTI1-K239A-EGFP uncut; Lane 5: pB-mSTI1-K239A-EGFP digested by *Hind* III Lane 6: pB-mSTI1-K237/238/239A-EGFP uncut; Lane 7: pB-mSTI1-K237/238/239A-EGFP digested by *Hind* III. Sizes of each DNA marker fragment in basepairs (bp) are annotated on the left and expected sizes of the fragments obtained after each digest (bp) are annotated on the right. *Hind* III digested all successfully ligated constructs into four fragments of expected sizes, 7700, 5000, 3790 and 902 bp.

### 3.3.2 Hop-EGFP and its Derivative Constructs were Predominantly Localized to the Cytosol Under Normal Conditions.

The subcellular distribution pattern of exogenous mouse Hop in BHK-21 cells using a Hop-EGFP fusion protein showed that under normal conditions Hop-EGFP localized predominantly to the cytosol of most cells with very little nuclear localization (figure 3.4, top panel). Quantitative analysis of the cells showed that Hop was predominantly localized to the cytosol in more than 90% of the cells and that Hop localized equivalently to both the cytosol and the nucleus in less than 10% of the cells (figure 3.5). The cells were transfected with pB-EGFP alone as a control (data not shown), and EGFP was seen to be distributed evenly throughout the nuclear and cytosolic compartments in all the cells and under all the conditions tested (Longshaw, 2002; Longshaw *et al.*, 2004).

Both NLS mutants, Hop-K239A-EGFP and Hop-K237/238/239A-EGFP also showed a predominantly cytosolic localization under normal conditions (figure 3.4, middle and bottom panels). However, quantitative analysis of the cells displayed a decrease in the total percentages of cells that showed mutated Hop localizing predominantly to the cytosol when compared to unmodified Hop (figure 3.5). Furthermore, Hop-K239A-EGFP and Hop-K237/238/239A-EGFP showed increased incidences of localization to both the cytosol and nucleus (> 20% and > 40% respectively) compared to unmodified Hop-EGFP (figure 3.5).

### Hop-EGFP and its Derivative Proteins Localized to the Nucleus Under Heat Shock

When the cells were subjected to heat shock at 42$^{o}$C for 30 minutes, Hop-EGFP showed increased nuclear, but not nucleolar, localization (figure 3.6, top panel) compared to normal conditions. More than 70% of the cells displayed both cytosolic and nuclear localization, with around 10% percentage of the cells showing a predominantly nuclear localization of Hop (figure 3.6).

Hop-K239A-EGFP and Hop-K237/238/239A-EGFP also showed increased incidences of nuclear localization under heat shock conditions, with a similar number of cells showing

both cytosolic and nuclear localization of the mutants (figure 3.5). Both Hop-EGFP mutant derivatives showed a slightly greater incidence of predominantly nuclear localization compared to unmodified Hop-EGFP after heat shock. Interestingly, Hop-K237/238/239A-EGFP did not display any incidences of predominantly cytosolic localization, whereas Hop-K239A-EGFP and Hop-EGFP showed < 20 % incidence of this localization pattern after heat shock. Like Hop-EGFP, both Hop-NLS mutants did not show any nucleolar localization.

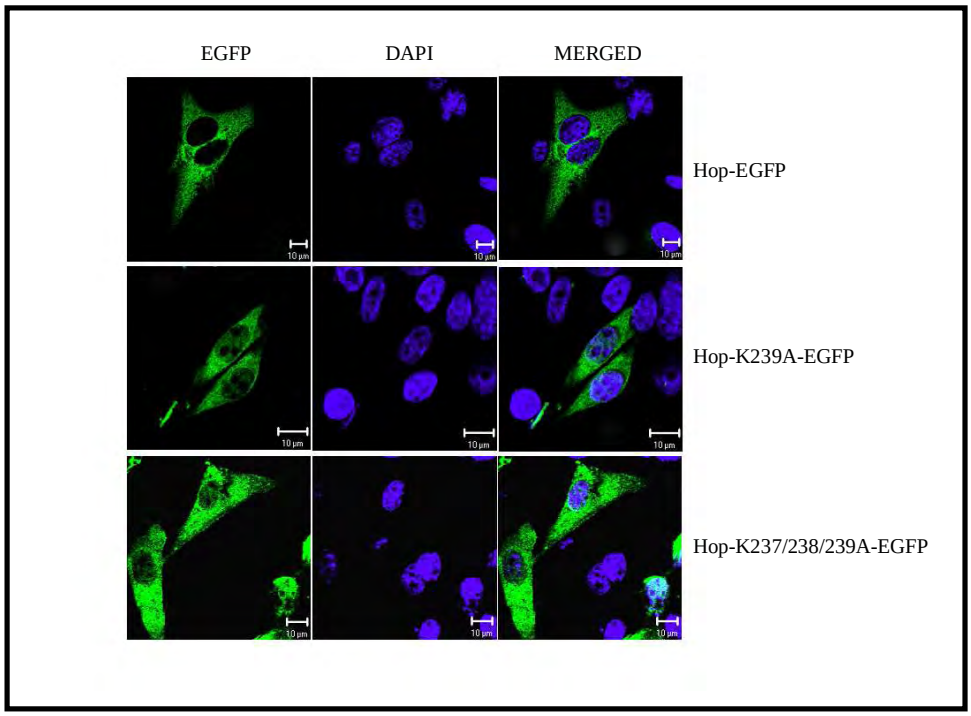


**Figure 3.4: Hop-EGFP and its NLS mutants localized predominantly to the cytosol under normal conditions**. BHK-21 cells were transiently transfected with plasmids expressing Hop-EGFP and its NLS mutant derivatives (Hop-K239A-EGFP and Hop-K237/238/239A-EGFP). Scale bars, 10 μM were automatically calculated and inserted into the figures using the LSM 510 software (Zeiss). The EGFP (green) and DAPI-stained nuclei (blue) were visualized with two separate channels using a FITC/EGFP and DAPI filter respectively.

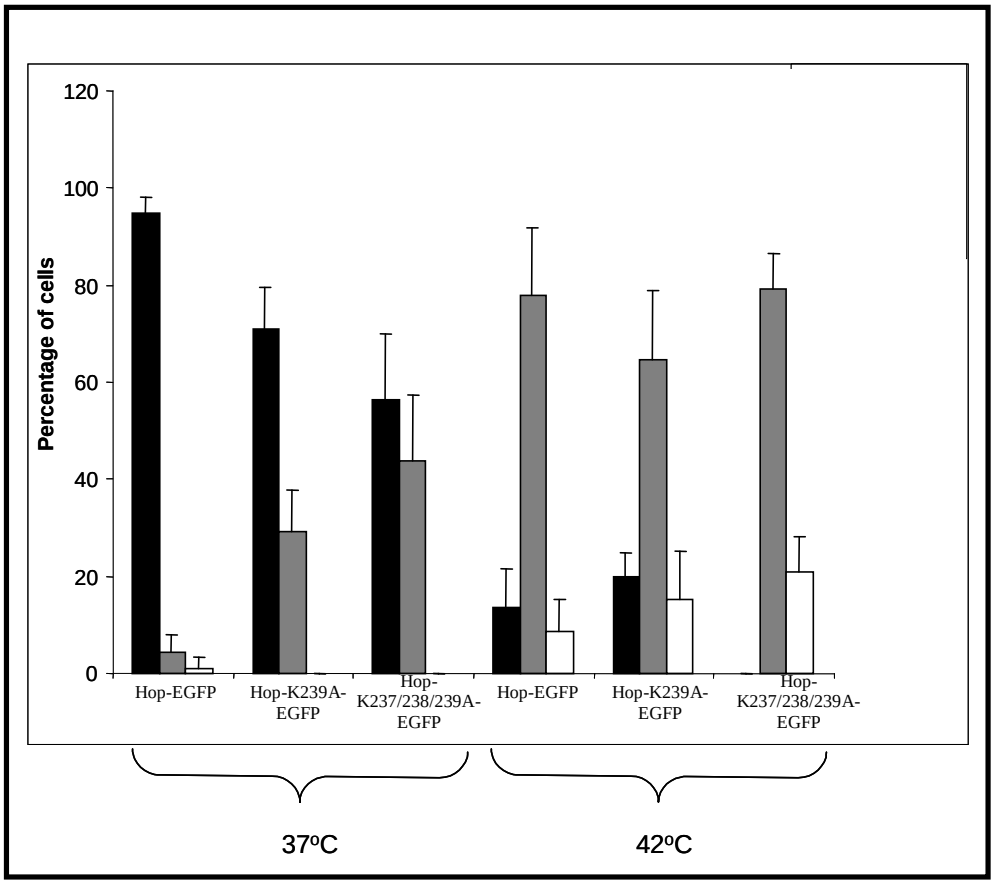


**Figure 3.5: Hop-EGFP and its derivatives were predominantly cytosolic under normal conditions but translocated to the nucleus under heat shock conditions**. BHK-21 cells were transiently transfected with plasmids expressing Hop-EGFP, Hop-K239A-EGFP and Hop-K237/238/239A-EGFP and then treated normally (37$^{o}$C) or heat shocked for 30 minutes (42$^{o}$C). Cells showing predominantly cytosolic fluorescence (black bars), cytosolic and nuclear fluorescence (grey bars) and predominantly nuclear fluorescence (white bars) were quantitated. Average values were taken six different fields (30-40 transfected cells per field); these results are representative of three independent transfections for each plasmid construct and for each treatment. The error bars represent standard deviations.

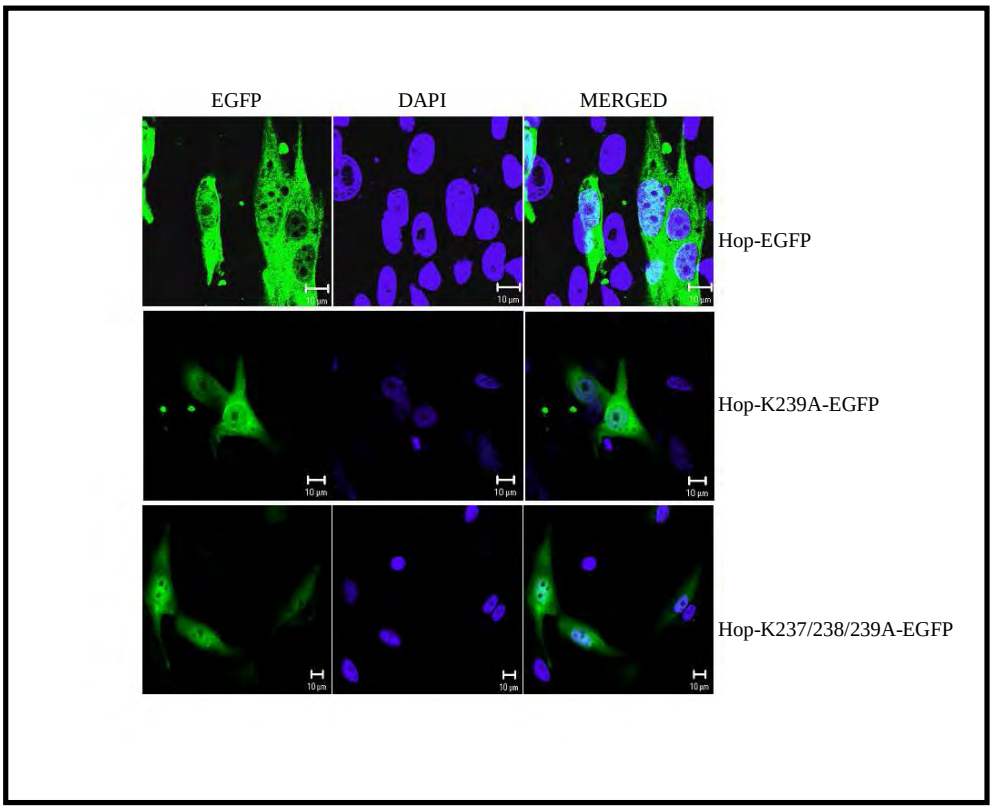


**Figure 3.6: Hop-EGFP and its NLS derivatives localized to the nucleus during heat shock**. BHK-21 cells were transiently transfected with plasmids expressing Hop-EGFP and its NLS mutant derivatives (Hop-K239A-EGFP and Hop-K237/238/239A-EGFP), and then subjected to heat shock at 42$^{o}$C for 30 minutes. Scale bars, 10 μM were automatically calculated and inserted into the figures using the LSM 510 software (Zeiss). The EGFP (green) and DAPI-stained nuclei (blue) were visualized with two separate channels using a FITC/EGFP and DAPI filter respectively.

### 3.3.4 Hop-EGFP and its NLS Mutants Showed Increased Incidence of Nuclear Localization Under Conditions of G1/S Arrest

As shown in figure 3.7, Hop-EGFP showed an increased incidence of nuclear but not nucleolar localization when the cells were treated with hydroxyurea, which arrested the cells in the G1/S phase. This finding was consistent with previous studies (Longshaw, 2002; Longshaw *et al.*, 2004). However, mutating the major arm of the putative NLS of Hop did not affect its localization patterns. Both Hop-K239A-EGFP and Hop-K237/238/239A-EGFP showed a similar localization pattern to unmodified Hop-EGFP when the cell was arrested in the G1/S phase of the cell cycle.

### 3.3.5 β-actin Localizes Predominantly to the Cytosol Under Normal and Heat Shock Conditions

Biochemical fractionation of BHK-21 cells that were grown at 37$^{o}$C (normal conditions) and that were heat shocked at 42$^{o}$C for 30 minutes were analyzed by SDS-PAGE and Western detection for β-actin (figure 3.8). β-actin is a protein found predominantly in the cytosol, membranous and cytoskeletal fractions of the cell. It is not found in the nucleus under normal conditions (Wada *et al.*, 1998). This protein was thus used as a marker of the various fractions obtained biochemically, particularly to distinguish between nuclear and non-nuclear fractions. As expected, β-actin was found predominantly in the cytosolic and membranous fractions under normal and heat shock conditions. A small fraction of β-actin was detected in the cytoskeletal fractions particularly after heat shock. β-actin was not found in the nuclear extracts of normally treated cells (figure 3.8, first panel) as was expected, suggesting that the nuclear fractions obtained by biochemical fractionation techniques employed was relatively free of contamination by cytosolic proteins. However, a slight increase of β-actin was seen in heat shocked nuclear extracts, but this was not unexpected as β-actin has been reported to translocate to the nucleus during heat shock (Iida *et al.*, 1992; Wada *et al.*, 1998). This result, therefore, also confirmed that the nuclear fractions were indeed obtained from heat-shocked cells.

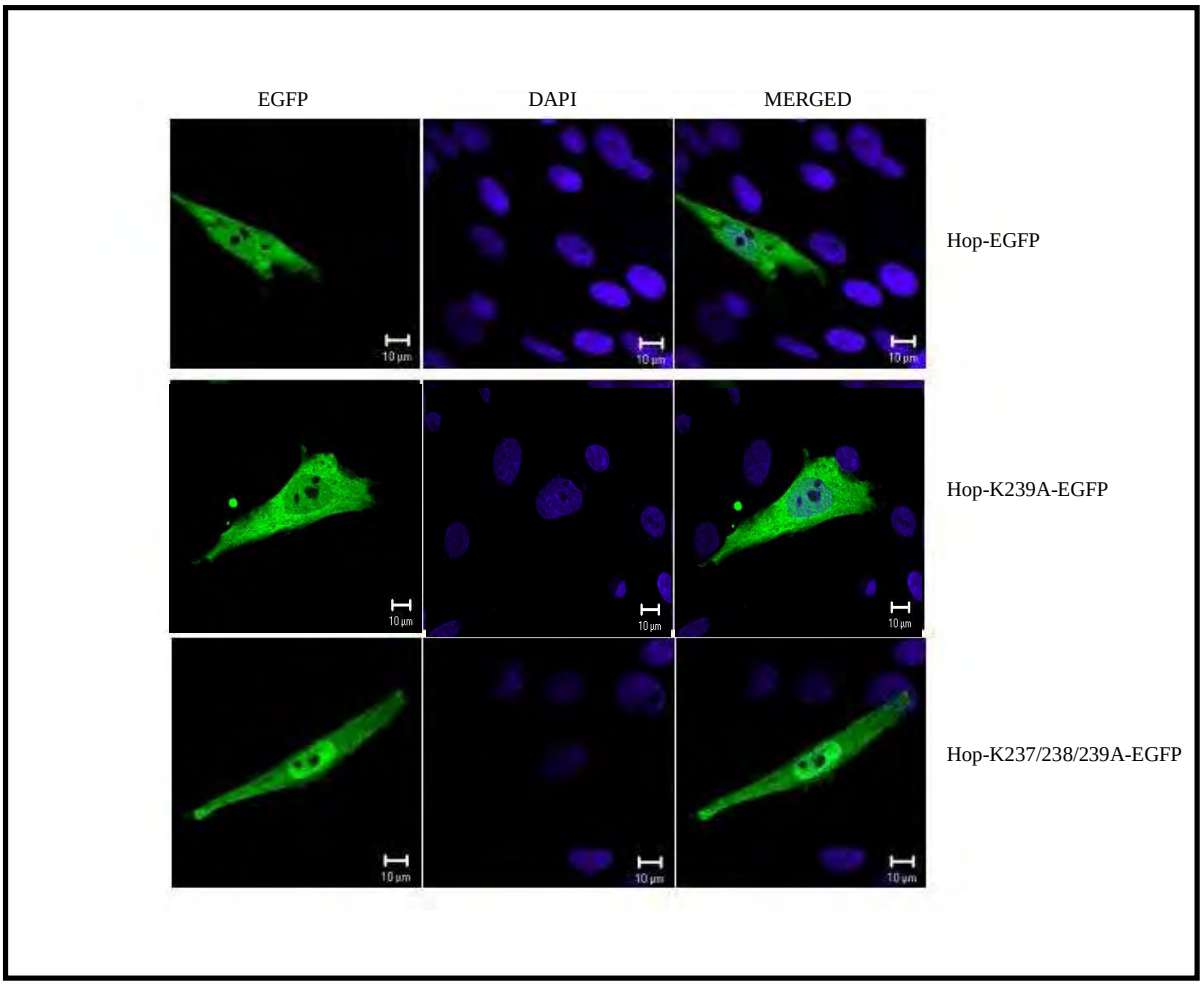


**Figure 3.7: Hop-EGFP and its NLS mutants localize to the nucleus when the cells are treated with hydroxyurea**. BHK-21 cells were transiently transfected with plasmids expressing Hop-EGFP and its NLS mutant derivatives (Hop-K239A-EGFP and Hop-K237/238/239A-EGFP), and treated with hydroxyurea (10 mM) for 5 hours. Scale bars, 10 µM were automatically calculated and inserted into the figures using the LSM 510 software (Zeiss). The EGFP (green) and DAPI-stained nuclei (blue) were visualized with two separate channels using a FITC/EGFP and DAPI filter respectively.

### 3.3.6 Hsp70 Translocated to the Nucleus After Heat Shock

Hsp70 is a predominantly cytosolic protein that has been found to translocate to the nucleus after heat shock (Chu *et al.*, 2001; Nollen *et al.*, 2001; Diehl *et al.*, 2003). Using Western analysis to detect Hsp70 in the biochemically isolated fractions of BHK-21 cells grown normally, as well as heat shocked, it was shown that Hsp70 was predominantly localized to the cytosol with a fraction of Hsp70 localizing to the membranes (figure 3.2, second panel). After heat shock, there was a distinct presence of Hsp70 in the nuclear fractions when compared to the nuclear fraction obtained from cells that were not heat shocked. This validated the presence of a nuclear extract having been successfully isolated by biochemical fractionation. Hsp70 was also detected in the cytoskeletal fraction after heat shock but not in the cytoskeletal fraction obtained from non-heat shocked cells (figure 3.8, second panel).

### 3.3.7 Endogenous Hop Co-fractionated With Hsp70 and Hsp90 to the Cytosol, Membranes and Cytoskeletal Fractions Under Normal Conditions and After Heat Shock

Biochemical fractionation of the cells followed by Western analysis of Hsp70, Hsp90 and Hop showed that all three proteins co-fractionated to the cytosolic fractions under normal and heat shocked conditions (figure 3.8, panels 2, 3 and 4). The predominant presence of endogenous Hop (as opposed to exogenous Hop, see section 3.3.2) in the cytosol was confirmatory of the confocal microscopic data described in section 3.3.2. There was an induction in the amount of Hsp70 found in all heat-shocked fractions compared to normal, attributable to the presence of inducible Hsp70 (Hsp72).

Figure 3.8 (panel 4) showed that Hop also localized to the membranes under normal conditions, and there was an increased amount of Hop in the membrane fraction after heat shock. Furthermore, Hsp70 and Hsp90 were localized to the membrane fraction under normal conditions, with an increased translocation of these proteins to the membranes after heat shock (figure 3.8, panels 2 and 3).

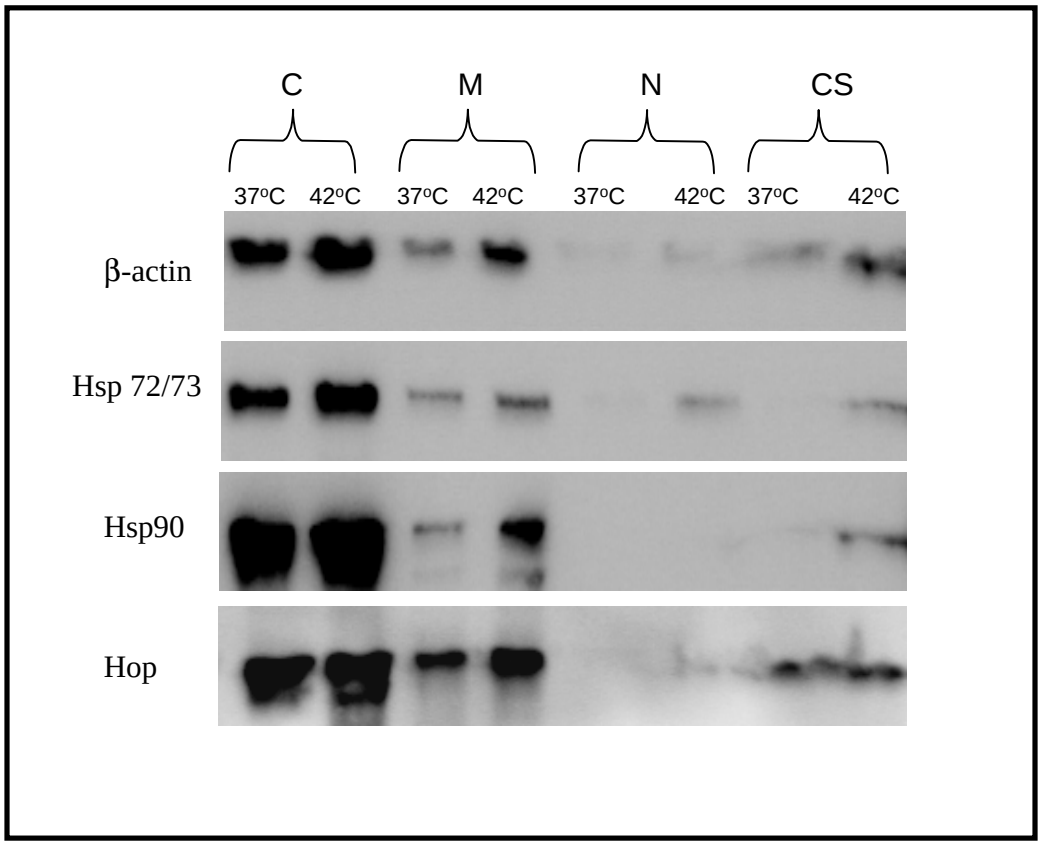


**Figure 3.8: Biochemical fractionation analysis of Hop, Hsp70 and Hsp90 under normal conditions and heat shock conditions.** Western blot analysis using antibodies for the detection of β-actin (cytoplasmic and membrane marker), Hsp72/73, Hsp90 and Hop, after the biochemical fractionation of BHK-21 whole cell lysates obtained from cells grown at 37°C (normal conditions) and cells incubated for 30 minutes at 42°C (heat shock). C: cytosolic fraction, M: membranous fraction, N: nuclear fraction, CS: cytoskeletal fraction. Subcellular fractions were prepared from whole cell lysates using equivalent number of cells for each treatment. The results presented are representative of three independent experiments.

Hop was detected in the cytoskeletal fractions of cells obtained from normally grown cells as well as cells that were heat shocked (figure 3.8, panel 4). Hsp70 and Hsp90, though absent in the normal cytoskeletal fractions, co-fractionated along with Hop in the heat shocked cytoskeletal fractions (figure 3.8, panels 2 and 3).

### 3.3.8 Endogenous Hop Co-fractionated With Hsp70 But Not Hsp90 in Heat Shocked Nuclear Fractions

A slight presence of endogenous Hop was detected in the nuclear fraction of heat shocked cell lysate, but this was absent in the lysate obtained from cells that were not heat-shocked (figure 3.8, panel 4). Hop was seen to co-fractionate with Hsp70, but not Hsp90 in heat shocked nuclear fractions (figure 3.8, panels 2 and 3).

## 3.4 DISCUSSION

Previous investigations into the subcellular localization of mouse Hop showed a generally cytosolic accumulation of the protein, with a small proportion of Hop in the nucleus (Lässle *et al.*, 1997; Longshaw *et al.*, 2004). The results of this study performed with BHK-21 cells grown under normal conditions agree with the above mentioned reports that the majority of cells showed a predominantly cytosolic localization of exogenous mouse Hop with a small percentage of nuclear Hop also being detected (figure 3.3, panel 1 and 3.5). Furthermore, detection of endogenous Hop in BHK-21 cells after biochemical fractionation predominantly in the cytosolic fraction, confirmed this finding (figure 3.2, panel 4).

Endogenous Hop was also detected in the membranous fraction of BHK-21 cells grown under normal conditions (figure 3.8, fourth panel). In the fractionation experiments conducted for this study, the membrane fraction would have contained membranes from various cellular compartments, i.e. both inter and intra-cellular membranes. Although it is likely that membraneous Hop may correspond to Hop localizing at the cell surface, based on the previous reports of Hop-$Prp^c$ interaction (Zanata *et al*., 2002), we cannot exclude the possibility of Hop localizing to other membraneous structures such as lysosomal membranes (Agarraberes et al., 2001) within the cell. The mechanism of Hop's translocation to the membrane is unknown as no transmembrane domain or signal peptide for membrane transport has been identified within the amino acid sequence of Hop (Lässle *et al.*, 1997; Zanata *et al.*, 2002). It was proposed by Zanata *et al*. (2002), however, that Hop may participate in a protein complex that is taken into the cell membrane or that it may be secreted by a pathway that is distinct from the classical route through the ER and Golgi apparatus as described by Muesch *et al*. (1990). Although mouse Hop has not yet been shown to localize to the Golgi apparatus, human Hop has been detected in the Golgi apparatus and small vesicles (Honoré *et al.*, 1992).

Short-term heat shock in mammalian cells can cause the transient arrest of the cell cycle at the G1/S phase by suppressing the hyperphosphorylation of retinoblastoma protein (pRb) which is required to release transcription factor E2F in order for the cell to enter

into the S phase (Khandijan, 1995). The arrest of mouse fibroblast cells in the G1/S phase has previously shown to cause an increased nuclear localization of Hop (Longshaw *et al.*, 2004). As for mouse cells, this study showed the nuclear localization of Hop under G1/S arrest in hamster cells. Furthermore, this study showed for the first time in a mammalian system, that a significantly higher nuclear (but not nucleolar) localization of Hop occurred under heat shock (figures 3.4 and 3.5). This suggests that the heat shock conditions used in this study promoted G1/S arrest of the cells and thus, that Hop localization and function is probably stress regulated on a primary level and cell cycle regulated on a secondary level.

Although the confocal microscopic data (figure 3.4 and 3.5) showed a higher incidence of nuclear localization of Hop under heat shocked conditions, the detection of endogenous Hop in the nuclear fractions of heat shocked BHK-21 cells was very slight (figure 3.2, fourth panel). This may be attributed to the invasive nature of the biochemical fractionation procedure, which rendered it more difficult to capture Hop in the nucleus under heat shock. It may also be indicative of the dynamic nature of Hop's nuclear translocation, which is consistent with the observations published by Longshaw *et al*. (2004). In presenting this data, it is acknowledged that although Hsp70 localizing to heat shocked nucleus provided evidence of a nuclear fraction being successfully isolated from heat shocked cells, this is not sufficient to prove the presence of nuclear proteins under normal conditions.

The SDS-PAGE profile of the biochemically fractionated cells showed the presence of lower molecular weight proteins in both nuclear fractions (data not shown), which may correspond to the presence of histones. However, detection by Western analysis of the presence of a nuclear marker control such as histone, which is localized in the nucleus of cells under normal conditions, would have been essential in confirming the presence of nuclear proteins. It is therefore arguable that the low levels of Hop and Hsp70, and the absence of Hsp90 in heat-shocked fractions may be due to the sub-optimal recovery of nuclear proteins. Had a histone marker been successfully employed, the comparison of

nuclear histone levels to histones in total lysate would have allowed the efficiency of nuclear protein recovery to be assessed.

Residues within the major arm of the proposed NLS in mouse Hop were mutated and functionality of the NLS *in vivo* was analyzed by studying the subcellular localization patterns of the derivative mutant proteins, Hop-K239A-EGFP and Hop-K237/238/239A-EGFP. Both Hop mutants displayed a predominantly cytosolic localization under normal conditions (figure 3.3 middle and lower panels), but showed significantly higher incidences of nuclear localization than unmutated Hop-EGFP (figure 3.5). Under heat-shocked conditions, both mutants showed a higher incidence of nuclear localization, similar to unmutated Hop; interestingly however, a greater percentage of cells showed 'predominantly nuclear' localization of Hop-K237/238/239A-EGFP than that of Hop-EGFP after heat shock (figure 3.5).

Since mutation of the major arm of the proposed NLS did not obstruct nuclear localization of Hop, it was concluded that unlike previously reported classical bipartite NLSs, residues of the major arm of the proposed NLS of Hop were not directly involved in translocation of Hop into the nucleus. However, since these residues are part of the major arm of a bipartite NLS which has been shown to be capable of translocating EGFP to the nucleus on its own (Longshaw *et al.*, 2004) one cannot exclude an indirect effect of these proposed residues on nuclear translocation of Hop. Moreover, such an indirect effect on NLS functionality would be consistent when considering the increased nuclear translocation of the Hop-NLS mutants versus unmodified Hop under heat shock and G1/S arrest.

Hsp70 and Hsp90 were both shown to co-fractionate with Hop in the cytosolic fractions (figure 3.2, panels 2, 3 and 4) as was expected. Previous reports have described the interactions of Hop with Hsp70 and Hsp90 to form the multichaperone heterocomplex within the cytosol (Chen and Smith, 1998; Pratt and Toft, 2003; Pratt *et al.*, 2004b). It was also expected that both Hsp70 and Hsp90 would co-fractionate with Hop in the nucleus after heat shock, since it is already established that both these major heat shock

proteins translocate to the nucleus under heat stress (Biggiogera *et al.*, 1996; Bharadwaj *et al.*, 1999; Chu *et al.*, 2001; Nollen *et al.*, 2001; Langer *et al.*, 2003). Moreover, previous work done in a haploid amphibious system (*Xenopus* oocytes) showed that invertebrate Hop co-localized with Hsp70 and Hsp90 in the nucleus before and after heat shock for 1 hour (Bharadwaj *et al.*, 1999). The present study however, using biochemical fractionation as a tool, showed that only Hsp70 co-fractionated with Hop and not Hsp90. The movement of Hsp90 into the nucleus may be of a similar nature to that of Hop since very little Hop was captured in the heat shocked nuclear fractions obtained by biochemical fractionation. Thus the absence of Hsp90 in the heat shocked nuclear fractions of the cells may be due to the inefficiency of this procedure to reflect such a dynamic transition, rather than a true reflection of the localization patterns of Hsp90 under heat shock. The significance of Hop moving into the nucleus may lie in the likely participation of Hop in complexes with nuclear Hsp70 and Hsp90. Hop was proposed to be involved in the Hsp70-Hsp90 heterocomplex required for the folding of the heat shock transcription factor 1 (HSF1) which is an entirely nuclear protein (Bharadwaj *et al.*, 1999). Hop may also be recruited to the nucleus for functions that are completely independent of Hsp70 and/or Hsp90.

Under the heat shock conditions used, there was a significant increase in the amount of Hop in the membrane fraction (figure 3.8) indicating that the heat shock response may increase the recruitment of Hop to membranous structures. Hsp70 and Hsp90 were both found to co-fractionate with Hop in the membrane fractions, and as in the case of Hop, the heat shock response also increased the recruitment of Hsp90 to the membranes. This implied that Hop might be involved in client protein transfer from Hsp70 to Hsp90 even within membranes. In both the mammalian and the yeast system, it is known that the majority of Hop is found bound to Hsp90 (Smith *et al.*, 1993; Chang *et al.*, 1997; Prodromou *et al.*, 1999). Thus the co-increase in amounts of Hsp90 and Hop in the membrane fraction may be further indication of Hop-Hsp90 complexes within the membrane, and these may or may not be independent of Hsp70 functions. However, the possibility of membrane-associated Hop and Hsp90 occurring in separate membrane complexes cannot be excluded.

Endogenous Hop was also detected in the membranous fraction of BHK-21 cells grown under normal conditions (figure 3.8, fourth panel), a finding which is consistent with reports of the interaction of Hop with $Prp^{c}$ at the cell membrane (Zanata *et al.*, 2002). T

A further sub-population of Hop was identified in the cytoskeletal fraction of cell lysate under normal and heat shock conditions with no comparative difference in levels detected (figure 3.8). No specific cytoskeletal role for Hop has yet been elucidated, apart from its proposed interactions with eukaryotic chaperonin-containing TCP1 (CCT), also known as the TCP-1 ring complex (TriC), which may be involved in the proper folding of actins and tubulins (Gebauer *et al.*, 1998). Although neither Hsp70 nor Hsp90 were detected in the cytoskeletal fractions under normal conditions, there was a definite presence of both these chaperones in the cytoskeletal fractions after heat shock. Hsp70 is also known to interact with CCT during the refolding of luciferease *in vitro*, and this phenomenon is proposed to occur *in vivo* for certain substrates after translation or after stress-induced damage (Gebauer *et al.*, 1998). Early reports showed the co-localization of Hsp90 immunofluorescence with the cytoskeleton (Fostinis *et al.*, 1992; Czar *et al.*, 1996) and possible association with tubulins (Sanchez *et al.*, 1988). It is thus possible that Hsp70, Hsp90 and Hop are together involved in the chaperoning assembly of various cytoskeletal structures.

The co-fractionation of Hop with Hsp90 in the cytosol, membranes, cytoskeleton and possibly nucleus under various conditions was particularly interesting due to previous reports on the majority of cellular Hop being found in complexes with Hsp90 (Smith *et al.*, 1993; Chang *et al.*, 1997; Prodromou *et al.*, 1999). Moreover, the residues of the proposed NLS of mouse Hop were seen to overlap with residues which have already been shown to be critical for Hop-Hsp90 interaction (Scheufler *et al.*, 2000; Odunuga *et al.*, 2003; Longshaw *et al.*, 2004). Other studies showed that phosphorylation sites on mouse Hop at the serine and threonine residues (S189 and T198 respectively) may play a part in regulating the subcellular localization of Hop (Longshaw *et al.*, 2000; Longshaw *et al.*, 2004). It is possible thus, that the differentially phosphorylated isoforms of Hop may be

localized to different subcellular compartments of the cell. Taking the results from the previous and the present chapter together, it is proposed that phosphorylation of Hop and Hop-Hsp90 interactions may be mechanistically involved in regulating the subcellular localization of Hop.

# CHAPTER 4

# ROLE OF THE PUTATIVE NLS AND *IN VITRO* PHOSPHORYLATION SITES OF HOP IN HOP-HSP90 BINDING

*"Insanity: doing the same thing over and over again and expecting different results."*

*- Albert Einstein*

## 4.1 INTRODUCTION

The majority of cellular Hop is found in a stable complex with Hsp90 in both yeast and mammalian systems, as shown by *in vitro* and *in vivo* experimentation (Smith *et al.*, 1993; Chang *et al.*, 1997; Prodromou *et al.*, 1999). Hop exists as a dimer in solution (Prodromou et al., 1999; van der Spuy et al., 2001) and associates with Hsp90 in a dimer-dimer interaction (Prodromou *et al.*, 1999; Hernandez *et al.*, 2002). It has been established that it is the central TPR2A domain of Hop which is involved in mediating interactions with the TPR acceptor site on Hsp90, found in the C-terminal region and comprising of an EEVD motif (Chen *et al.*, 1996b; Brinker *et al.*, 2002; Odunuga *et al.*, 2003). However it is also proposed that there may be networks of interactions between Hop and Hsp90 besides those mediated by the TPR domains of Hop, which allow for its functionality as a scaffolding protein (Odunuga *et al.*, 2003; Flom *et al.*, 2006; Flom *et al.*, 2007).

A direct interaction between Hop and the ATP-binding site in the N-terminal domain of Hsp90 has been suggested based on studies that showed a weakened binding of Hop to Hsp90 when part of the N-terminal ATP-binding domain of Hsp90 was deleted (Chen *et al.*, 1998). In addition, yeast Hop was shown to inhibit the ATPase activity of Hsp90 *in vitro*, as well as displace geldanamycin, which binds to the ATP-binding site of Hsp90 in the N-terminus (Prodromou *et al.*, 1999). Based on *in vitro* biochemical studies, a change in the conformation of Hop and/or Hsp90 during its interaction has been speculated (Prodromou *et al.*, 1999). Changes in the structural conformation of Hop when bound to Hsp90 are not unexpected, since it is known that binding of Hop to Hsp90 reduces the number of Hsp70 binding sites on the Hop dimer from two sites to one site, but at the same time, increases the affinity of Hsp70-Hop binding five fold (Hernandez *et al.*, 2002). Hsp90 may alter the conformation of Hop to one that better accommodates Hsp70, or Hop-Hsp90 binding may open up a new conformation of Hsp90 which provides contact sites for Hsp70 binding (Murphy *et al.*, 2001; Hernandez *et al.*, 2002).

Although a bipartite NLS was proposed in mouse Hop, which on its own has been shown to be functional (Longshaw *et al.*, 2004), results of the previous chapter showed that

predicted residues within the major arm of this putative NLS were not directly involved in translocation of Hop into the nucleus. These residues of the major arm of the putative bipartite NLS of Hop overlap with the TPR2A domain which modulates interactions between Hop and the 'EEVD' motif of Hsp90 (as shown in figure 1.4). Residues within the spacer region of the NLS (N233, K229 and K301), which also overlap with TPR2A, have already been shown to be crucial for Hop-Hsp90 interactions (Scheufler *et al.*, 2000; Odunuga *et al.*, 2003). It was thus speculated that the residues, which formed part of the major arm of the putative NLS, were involved in Hop-Hsp90 interaction, and in this way, the nuclear localization of Hop was affected by Hop-Hsp90 interaction.

The results obtained from chapter 2 showed that Hop was phosphorylated *in vivo*. Previous work has detailed two *in vitro* phosphorylation sites for CKII and cdc2 kinase on mouse Hop, which were identified at S189 and T198, respectively. These were found upstream of the putative NLS and evidence was presented that suggested that phosphorylation at either of these sites could affect the subcellular localization of Hop (Longshaw *et al.*, 2000; Longshaw *et al.*, 2004). S189 and T198 are found immediately upstream of the TPR2A domain of mouse Hop. The main objective of this study was to test the hypothesis that phosphorylation of Hop might play a significant role in the binding of Hop to Hsp90, and Hop-Hsp90 binding may be mechanistically involved in regulating the subcellular localization of Hop.

The specific objectives of this study were to:

1. Generate GST-Hop and its mutational constructs, GST-Hop-K239A, GST-Hop-K237/238/239A, GST-Hop-S189E and GST-Hop-T198E.
2. Purify GST-Hop and its derivative proteins for SPR and co-precipitation studies.
3. Determine any possible interactions of the major arm of the proposed NLS with Hsp90.
4. Determine whether phosphorylation of Hop at the S189 or T198 position affects its interactions with Hsp90.

## 4.2 EXPERIMENTAL PROCEDURES

### 4.2.1 Generation and Analysis of Plasmid Constructs Encoding GST-Hop and its Derivative Proteins

The GST-Hop protein and its various derivatives were generated from the plasmid pGEX3X2000, which contains the cDNA encoding the full-length protein mSTI1 fused to the C-terminus of glutatione-S-transferase (GST-Hop). All mutations were carried out by site-directed mutagenesis using a double-stranded whole plasmid linear amplification procedure (Appendix A8). For screening purposes, silent mutations were engineered to create restriction sites except where the desired codon change(s) automatically generated restriction sites. The specific mutagenic primers are listed in Section C of the Appendix. All plasmid constructs and their mutations were confirmed both by restriction enzyme analysis (Appendix A9) and by DNA sequencing (Appendix A11).

### 4.2.2 Expression and Purification of GST-Tagged Proteins

pGEX3X2000-derived plasmid constructs were transformed into *E.coli* XL1 Blue cells (Appendix A4) and expressed and purified using the protocol detailed in Appendix Section A6.

### 4.2.3 Surface Plasmon Resonance Spectroscopy (SPR) Analysis

Surface plasmon resonance (SPR) studies were performed using a Biacore X apparatus (BIACORE, Sweden) to measure the interactions of GST-Hop and its various mutant derivatives with Hsp90 in real-time. SPR refers to the angle with which an incident beam of light strikes a metal surface. Interactions between biomolecules on this metal surface cause corresponding changes in the angle and intensity of the reflected light, and this is used to detect any such molecular interaction that occurs on the metal surface. The running buffer for SPR (10 mM Hepes containing 140 mM KCl and 0.001% Tween) analysis was filter-sterilized and degassed before use. The Biacore X apparatus was primed with the running buffer using the standard priming protocol, which involved the washing and equilibration of the Biacore chip (Sensor chip CM5) and valves within the instrument with running buffer at room temperature. A mixture of N-hydroxy-succinimide and 1-ethyl-3 –[3-dimethylaminopropyl] carbodiimide (NHS/EDC) was

injected into the first flow cell to activate the surface of the chip by modification of the carboxymethyl groups to N-hydroxysuccinimide esters.

Purified Hsp90 (40 μL of 60 μg/mL stock solution) was immobilized onto the activated carboxymethylated dextran surface of the chip by amine coupling (the N-hydroxysuccinimide esters reacted spontaneously with the amines on the Hsp90 to form covalent links) by injection into the first flow cell only. The second flow cell was used as a control for non-specific binding to the chip, and therefore no Hsp90 was immobilized on it. Approximately 9165 response units (RU) of Hsp90 were immobilized onto the first flow cell of the chip. Any unreacted N-hydroxysuccinimide esters and unbound Hsp90 was deactivated and washed out by injecting ethanolamine hydrochloride (40 μL) into both flow cells.

The purified GST-Hop proteins were dialyzed to exchange the elution buffer containing Tris-HCL for the SPR running buffer before conducting the SPR analysis. Increasing concentrations (0.2 μM, 1 μM and 5 μM) of various GST-Hop constructs were passed over the immobilized Hsp90 at a continuous flow rate of 10 μL minute$^{-1}$ and the associated kinetics were recorded. GST (0.2 μM, 1 μM and 5 μM) was also passed through both cells and any non-specific binding to Hsp90 and/or the chip was monitored. Regeneration of the chip in between each consecutive protein concentration or protein construct was achieved by passing 10 mM HCl on the chip at a flow rate of 10 μL minute$^{-1}$. All experiments were performed at room temperature.

The data was analyzed using the BIAevaluation software version 3.0. Binding curves were generated by plotting response units (RU) versus time (seconds) and then fitted onto the Langmuir binding model. This was used to determine the apparent dissociation constants ($K_D$ values), which were taken as apparent affinities of binding.

### 4.2.4 GST-Co-Precipitation Assays

In separate 1 mL reactions, GST-Hop fusion proteins (GST alone was used as a negative control, and GST-C334 which contained the C-terminal TPR domains essential for Hop-

Hsp90 binding was used as the positive control) were coupled to glutathione-agarose beads to a final concentration of 0.3 μM (note that a final volume of 1 mL was sufficient to dilute out the presence of reduced glutathione). Binding to the beads was allowed to occur for 1 hour at 4°C, after which unbound fusion protein was removed by washing three times in ice-cold PBS. Hsp90 binding assays were carried out using purified Hsp90 (Söti *et al.*, 1998), which was added to a final concentration of 0.2 μM. After incubation for 3 hours at 4°C, the beads were collected and washed extensively in ice-cold PBS to remove nonspecifically bound extract proteins.

The bound proteins were solubilized in SDS sample buffer (70 μL) and resolved using SDS-PAGE. Chemiluminescence-based Western analysis (see section 2.2.5 and 2.2.6) was used to detect the co-precipitation of Hsp90 (monoclonal rat anti-human Hsp90 at a final dilution of 1:5000 was used as the primary antibody, and an HRP-conjugated goat anti-rat IgM was used as the secondary antibody at a final dilution of 1:5000) with the various GST-Hop fusion proteins.

## 4.3 RESULTS

### 4.3.1 pGEX3X2000 and its Derivatives Were Successfully Generated

Site-directed mutagenesis was used to generate the following modified plasmids: pGEX3X2000(K239A), pGEX3X2000(K237/238/239A) as shown in figure 4.1 A and B respectively. Treatment of the parent plasmid pGEX3X2000 (figure 4.1 C) with Hind III produced a linearized fragment of approximately 7017 as was expected (figure 4.1 D, lane 2 and E, lane 4). Partial digestion of the DNA was seen in figure 4.1 D, lane 4. An *Nsi* I restriction endonuclease site was engineered into the codon changes associated with the K239A and K237/238/239A substitutions, such that treatment of pGEX3X2000 (unmodified plasmid) with *Nsi* I did not fragment the plasmid, as shown in lane 3 of both figure 4.1 D and E. However, treatment of pGEX3X2000 (K239A) and pGEX3X2000 (K237/238/239A) with *Nsi* I yielded linearized fragments of expected size 7017 bp in figure 4.1 D lane 5 and figure 4.1 E lane 6 respectively. Controls showing undigested pGEX3X2000 (K239A) and pGEX3X2000 (K237/238/239A) were shown in lanes 4 of figure 4.1 D and 5 of figure 4.1 E respectively.

Phosphorylation mimics were also constructed by generating the following plasmids: pGEX3X2000(S189E) (figure 4.2 A) and pGEX3X2000(T198E) (figure 4.2 B), which were analyzed by restriction endonuclease digestion as shown in figure 4.2 D and E. Treatment of the parent plasmid pGEX3X2000 (figure 4.2 C) with *Hind* III produced a linearized fragment of approximately 7017 as was expected (figure 4.2 D, lane 4). The codon change for the S189E substitution was engineered onto the parent plasmid with an *Acc* I restriction site that was not present on the parent plasmid. Hence pGEX3X2000 treated with *Acc* I did not produce any digested fragments (figure 4.2 D, lane 3). However, treatment of pGEX3X2000 (S189E) with *Acc* I linearized the plasmid into the expected sized fragment of 7017 bp (figure 4.2 D, lane 6). Uncut controls of pGEX3X2000 and pGEX3X2000 (S189E) are shown in lanes 2 and 5 of figure 4.2 D. The T198E substitution was engineered on the parent plasmid such that an additional *Eag* I site was included after modification. Thus pGEX3X2000 was linearized by treatment with *Eag* I (figure 4.2 E, lane 3) whereas pGEX3X2000 (T198E) treated with *Eag* I was digested into two fragments of expected sizes, 5564 and 1453 bp (figure 4.2 E, lane 6).

The uncut controls of both parent and modified plasmids are shown in lanes 2 and 4 of figure 4.2 E). All plasmids were further confirmed by sequencing analysis.

### 4.3.2 GST-Hop and its Derivative Proteins Were Successfully Expressed and Purified

GST-Hop and its derivative proteins were heterologously over-produced in *E. coli* XLI Blue cells carrying the respective pGEX3X2000 plasmid or its derived constructs, as shown in figure 4.3. The proteins were then purified by S-hexyl glutathione agarose affinity chromatography after optimally expressing them by 5 hours of IPTG induction. The majority of the protein was recovered in the soluble fractions after clarification of the cell extracts. Aliquots of the purified proteins were resolved by SDS-PAGE to confirm the enrichment of the eluent with GST-Hop or its derivative proteins according to van der Spuy *et al*. (2000).

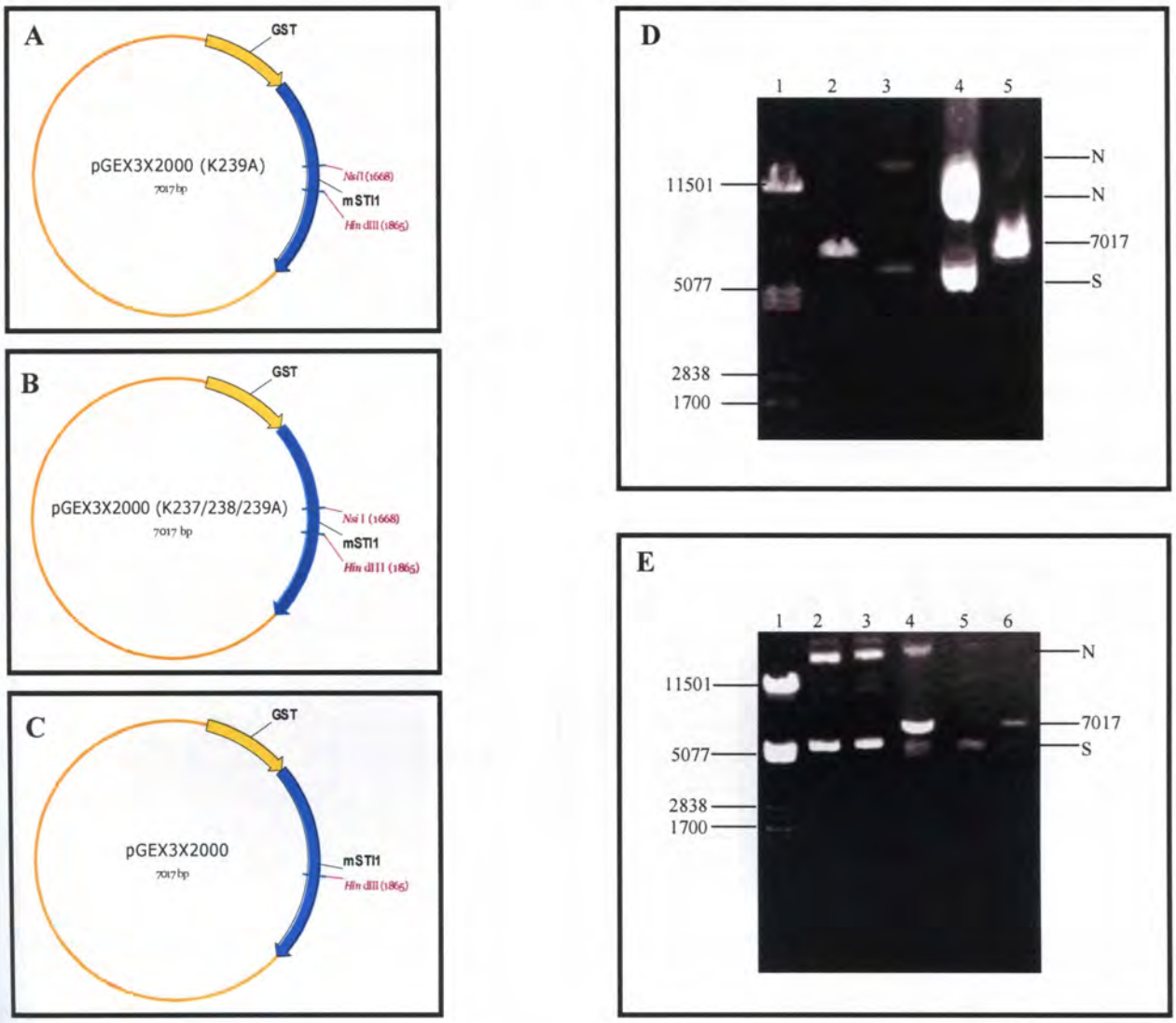


**Figure 4.1 pGEX3X2000 and its NLS-mutated derivatives were successfully generated.** Site-directed mutagenesis was used to generate the following modified plasmids: **(A)** pGEX3X2000(K239A), **(B)** pGEX3X2000(K237/238/239A) from the parent plasmid **(C)** pGEX3X2000. The mutations were analyzed by restriction endonucleases and the resultant fragments were resolved on a 0.8% agarose gel (**D** and **E**). Sizes of each DNA marker fragment in basepairs (bp) are annotated on the left and expected sizes of the fragments obtained after each digest (bp) are annotated on the right. Nicked (N) and supercoiled (S) DNA fragments are annotated on the right hand side of the gel. **(D)** pGEX3X2000 (K239A) was analyzed by digestion with *Nsi* I. Lane 1: Lambda markers digested with *Pst* I; Lane 2: pGEX3X2000 linearized with *Hind* III; Lane 3: pGEX3X2000 treated with *Nsi* I but uncut; Lane 4: pGEX3X2000 (K239A) undigested; Lane 5: pGEX3X2000 (K239A) linearized with *Nsi* I. **(E)** pGEX3X2000 (K237/238/239A) was analyzed with *Nsi* I. Lane 1: Lambda markers digested with *Pst* I; Lane 2: Uncut pGEX3X2000; Lane 3: pGEX3X2000 treated with *Nsi* I but uncut; Lane 4: pGEX3X2000 linearized with *Hind* III; Lane 5: pGEX3X2000 (K237/238/239A) undigested; Lane 6: pGEX3X2000 (K237/238/239A) linearized with *Nsi* I.

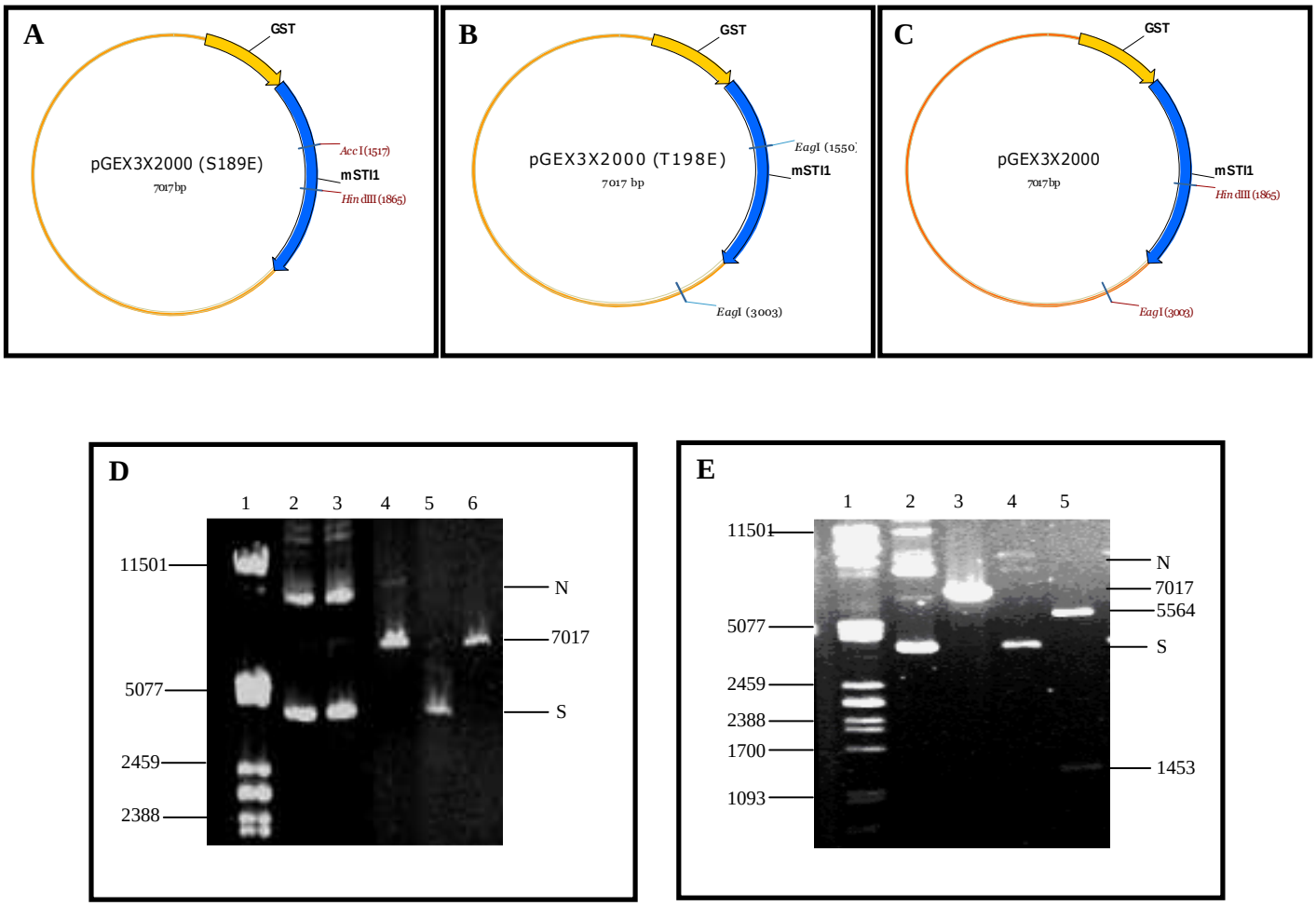


**Figure 4.2: Phosphorylation mimic constructs pGEX3X2000 (S189E) and pGEX3X2000 (T198E) were successfully generated and confirmed using restriction endonuclease analysis.** Site-directed mutagenesis was used to generate the following modified plasmids: **(A)** pGEX3X2000(S189E), **(B)** pGEX3X2000(T198E) from the parent plasmid, **(C)** pGEX3X2000. The mutations were analyzed by restriction endonucleases and the resultant fragments were resolved on a 0.8 % agarose gel. Sizes of each DNA marker fragment in basepairs (bp) are annotated on the left and expected sizes of the fragments obtained after each digest (bp) are annotated on the right. Nicked (N) and supercoiled (S) DNA fragments are annotated on the right hand side of the gel **(D)** pGEX3X2000 (S189E) was analyzed by digestion with *Acc* I. Lane 1: Lambda markers digested with *Pst* I; Lane 2: pGEX3X2000 uncut; Lane 3: pGEX3X2000 treated with *Acc* I but uncut; Lane 4: pGEX3X2000 linearized with *Hind* III at the expected fragment size of 7017 bp; 5: pGEX3X2000 (S189E) uncut; 6: pGEX3X2000 (S189E) linearized with *Acc* I (7017 bp). **(E)** pGEX3X2000 (T198E) was analyzed with *Eag* I. Lane 1: Lambda markers digested with *Pst* I; Lane 2: Uncut pGEX3X2000; Lane 3: pGEX3X2000 linearized with *Eag* I (7017 bp); Lane 4: pGEX3X2000 (T198E) undigested; Lane 6: pGEX3X2000 (T198E) fragmented with *Eag* I into two bands of expected sizes, 5564 and 1453 bp.

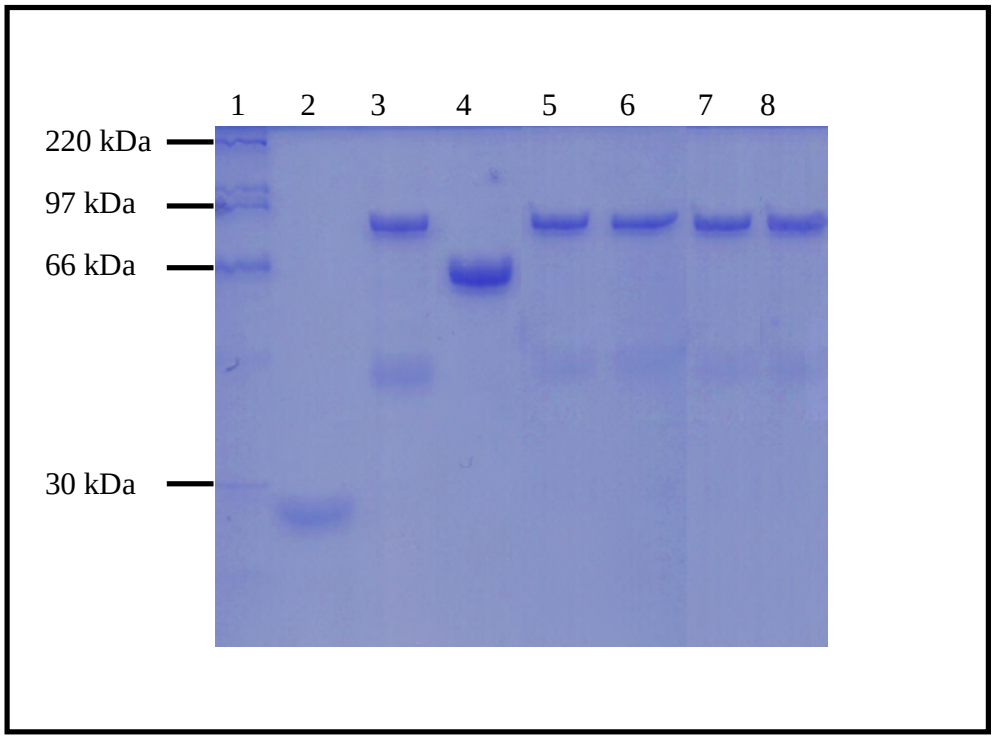


**Figure 4.3 GST-Hop and its derivative proteins were successfully expressed and purified.** All GST-Hop proteins were heterologously over-produced in *E. coli* XLI Blue cells carrying the respective pGEX3X2000 plasmid or its derived constructs and further analyzed by SDS-PAGE. Lane 1: Molecular mass markers; Lane 2: GST; Lane 3: GST-Hop; Lane 4: GST-C334; Lane 5: GST-Hop-K239A; Lane 6: GST-Hop-K237/238/239A; Lane 7: GST-Hop-S189E; Lane 8: GST-Hop-T198E. 10 μL of the eluent containing varying concentrations of total protein was loaded in each lane.

### 4.3.3 The Interaction of GST-Hop and Derivative Proteins With Hsp90 Using SPR Analysis

SPR analysis was used to monitor the biomolecular interactions of GST-Hop and various derivatives of this protein with Hsp90. Concentration-dependent SPR signals (0.2, 1 and 5 μM) were recorded for specific protein interactions. Apparent dissociation constants ($K_D$ values) were determined and taken as apparent affinities of binding. The binding curves of three concentrations of GST-Hop to immobilized Hsp90 showed a dose-dependent binding pattern as seen in figure 4.4 A. The binding of the phosphorylation mimics, GST-Hop-S189E and GST-Hop-T198E to immobilized Hsp90 also showed similar dose-dependent patterns (figure 4.4 D and E) in contrast to the NLS mutants, GST-Hop-K239A and GST-Hop-K237/238/239A (figure 4.4 B and C), which showed similar binding patterns to Hsp90 as that of the negative control, GST (figure 4.5 A). The $K_D$ of binding of the full-length unmodified Hop (GST-Hop) to immobilized Hsp90 was calculated to be 1.4 μM. This value correlates with $K_D$ values reported in the literature (Brinker *et al.*, 2002; Odunuga *et al.*, 2003). $K_D$ values for GST-Hop-K239A and GST-Hop-K237/238/239A could not be calculated due to the low levels of interaction with Hsp90. The $K_D$ of binding of GST-Hop-S189E with Hsp90 was calculated to be 1 μM and that of GST-Hop-T198E with Hsp90, 2.5 μM. GST-Hop-T198E showed reduced binding to Hsp90 compared to the unmodified protein, GST-Hop (figure 4.5 B). These experiments have been repeated independently by immobilizing the GST-Hop constructs on a sensor chip and passing purified Hsp90. Similar results were obtained (data not shown).

### 4.3.4 The Interaction of GST-Hop Derivative Proteins With Hsp90 Using GST-Co-Precipitation Assays

GST-co-precipitation assays using equivalent concentrations (0.3 μM) of GST-fusion proteins (confirmed by Coomassie staining; data not shown) were carried out to confirm the results obtained using SPR analysis. The results showed that all mutant derivatives of GST-Hop, GST- Hop-T198E, GST-Hop-K239A and GST-Hop-K237/238/239A, showed minimal and possibly non-specific binding to purified Hsp90, compared to the positive control, GST-C334 and the negative control, GST.

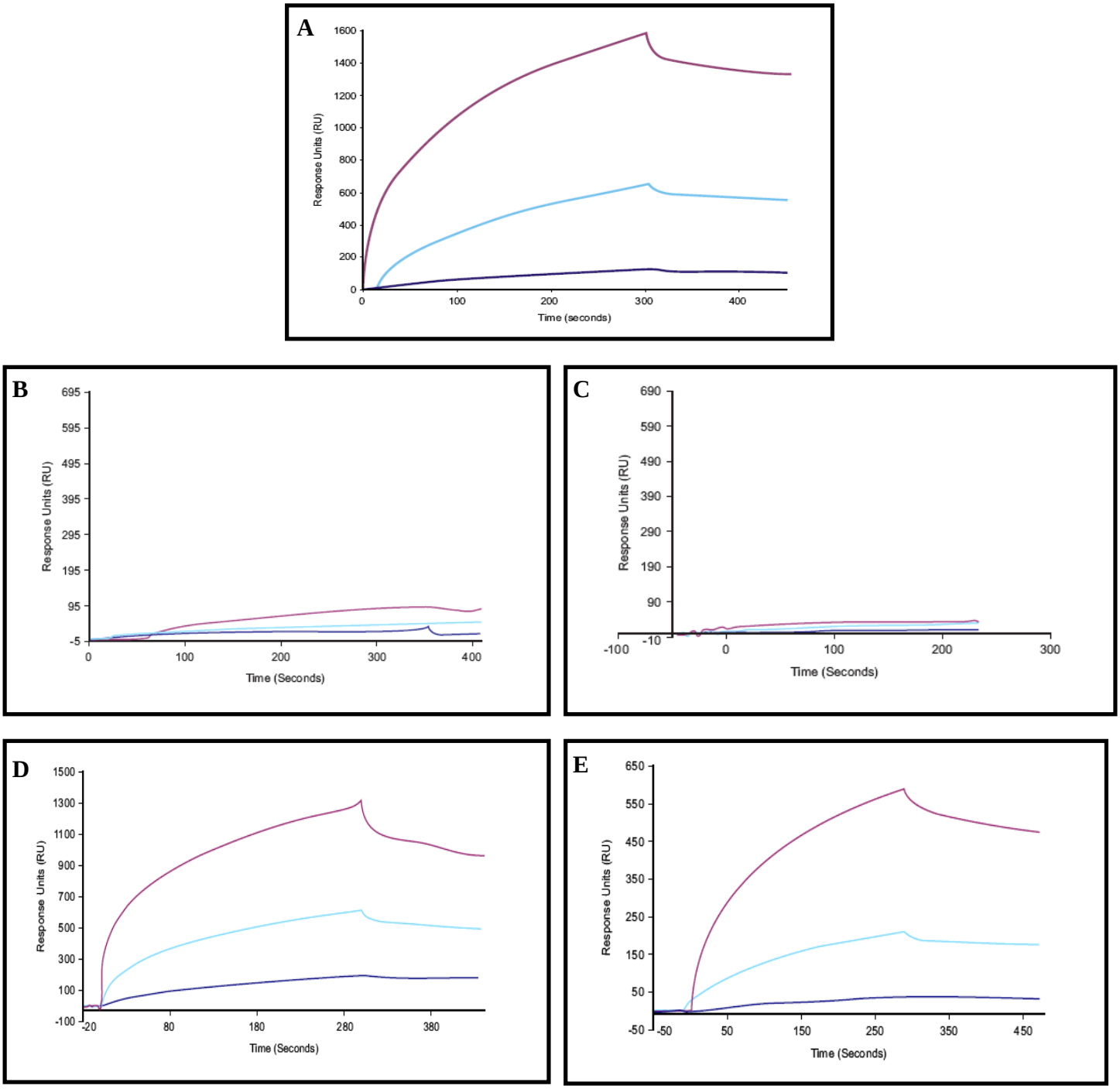


**Figure 4.4: Surface plasmon resonance (SPR) spectroscopy was used to determine the apparent affinity of GST-Hop and its derivative proteins for purified Hsp90.** Approximately 9165 response units (RU) of Hsp90 was immobilized on a sensor chip, and three varying concentrations of each GST-Hop protein (purple: 5 µM, light blue: 1 µM and dark blue: 0.2 µM) was passed over the chip at a continuous flow rate of 10 µL/minute. The response units obtained were plotted against time (in seconds) to obtain the binding response curves. **A:** GST-Hop-Hsp90 binding; **B:** GST-Hop-K239A-Hsp90 binding; **C:** GST-Hop-K237/238/239A-Hsp90 binding; **D:** GST-Hop-S189E-Hsp90 binding; **E:** GST-Hop-T198E-Hsp90 binding.

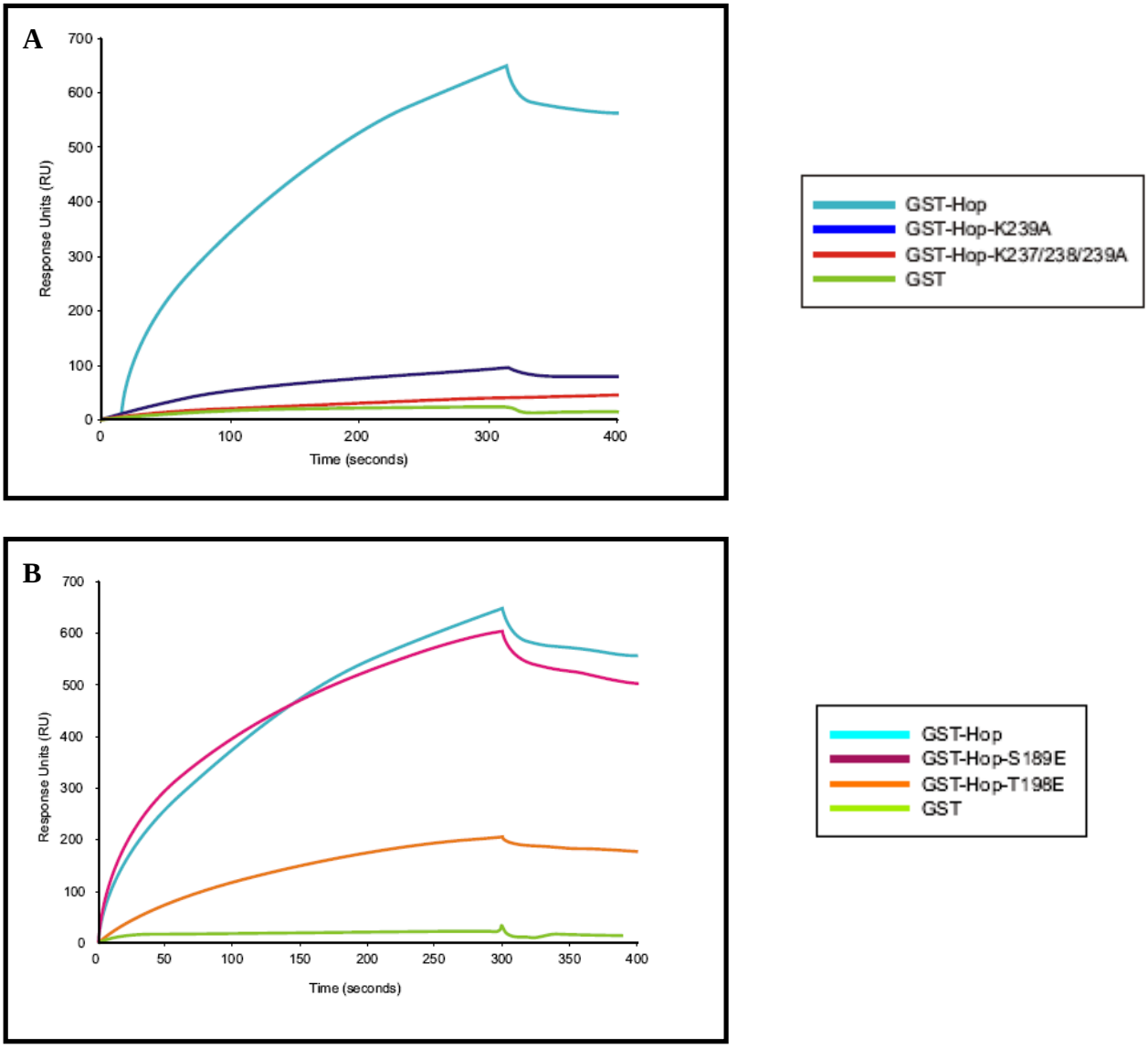


**Figure 4.5 Mutations in the major arm of the NLS abrogated Hop-Hsp90 binding whereas cdc2-kinase phosphorylation of Hop may disrupt binding of Hop to Hsp90.** A summary of the relative binding response curves of GST-Hop and its derivative proteins (1 μM) with purified Hsp90 generated by surface plasmon resonance (SPR) spectroscopy. Color codes are indicated to the right and the left of each graph. **A:** GST-Hop and the NLS mutants (GST-Hop-K239A and GST-Hop-K237/238/239A) with Hsp90. GST alone was used as the negative control. Relative binding curves shown by both NLS mutants were comparable to GST and thus showed negative binding to Hsp90. **B:** GST-Hop and the phosphorylation mimics (GST-Hop-S189E and GST-Hop-T198E) with Hsp90. GST-Hop-S189E showed a similar binding response pattern to Hsp90 as did unmodified GST-Hop. However, GST-Hop-T198E showed comparatively reduced binding to Hsp90. GST was used as the negative control.

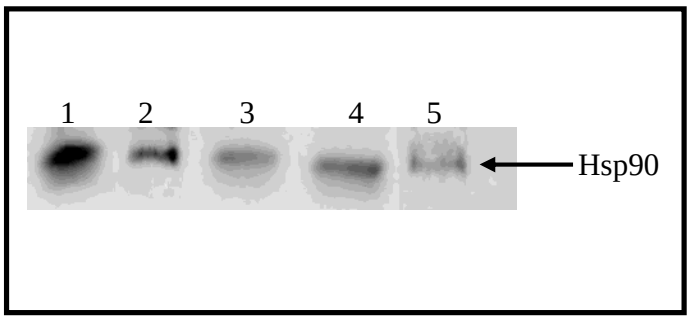


**Figure 4.6: Interaction of GST-Hop derivative proteins with purified Hsp90.** Co-precipitation assays were used to confirm the extent of interaction between various GST-Hop derivatives (0.3 μM) and purified Hsp90 (0.2 μM). GST-Hop proteins that were previously coupled to glutathione agarose beads were incubated with purified Hsp90 for three hours at 4$^{o}$C. After extensive washes to remove unbound proteins, the bound proteins were solubilized in SDS sample buffer and resolved by SDS-PAGE. Western analysis was carried out to detect the co-precipitation of Hsp90 with the GST-Hop proteins by using an antibody specific for Hsp90 α and β. Lane 1: GST-C334 (positive control); Lane 2: GST (negative control); Lane 3: GST-Hop-K239A; Lane 4: GST-Hop-K237/238/239A; Lane 5: GST-Hop-T198E. This figure is representative of two independently conducted experiments.

## 4.4 DISCUSSION

Residues, K237, K238 and K239, which constitute the major arm of the proposed bipartite NLS, were shown to be critical for Hop-Hsp90 interactions by SPR and GST-co-precipitation studies. Mutation of these amino acid residues abrogated binding to Hsp90, and the results were comparable to that of the negative control, GST (figure 4.5 A). Three different concentrations of each mutant were passed over immobilized Hsp90 on a chip, in order to calculate the mutant/Hsp90 affinity constants. However, since binding of the mutant Hop proteins to Hsp90 were below detection, it was impossible to calculate $K_D$ values (figure 4.4 B and C). The effects of phosphorylation at two sites previously described, S189 and T198 (Longshaw *et al.*, 2004), on Hop-Hsp90 interactions were also investigated. SPR analysis of the phosphorylation mimics, GST-Hop-S189E and GST-Hop-T198E with Hsp90 showed that mimicking phosphorylation at position S189 did not alter Hop-Hsp90 interactions (figure 4.5 B) and showed similar affinity values to unmodified Hop (figure 4.4 D compared to A). GST-Hop-T198E on the other hand, showed a diminished affinity for Hsp90 compared to that of unmodified Hop (figure 4.5 B). GST-co-precipitation assays confirmed the low affinity binding of GST-Hop-T198E to Hsp90 (figure 4.6), with similar levels of Hsp90 co-precipitating for this GST-Hop mutant as was observed for the negative control, GST.

Interestingly SPR analysis showed partial disruption of Hsp90-GST-Hop-T198E interactions whereas the co-precipitation analysis suggested that mimicking phosphorylation at T198 completely abolished interactions of Hop with Hsp90. This may reflect the transient nature of interactions between Hsp90 and the phosphorylated mimic of Hop, since the SPR technique can generally detect weak protein-protein interactions which are not always detectable using GST-co-precipitation analysis. It must also be noted that the $K_D$ values were calculated by artificially fitting the binding response curves obtained onto a Langmuir binding curve, and is therefore not exact, but rather an apparent value reflecting the affinity between the two proteins. Moreover, a number of differences in technicalities between the two methods may have given rise to slight differences in results obtained. In the SPR studies conducted, Hsp90 was immobilized on the surface of a chip and GST-Hop proteins were passed over it, whereas in the co-precipitation

analysis, although GST was bound to the matrix, neither Hop nor Hsp90 was immobilized. Immobilization of Hsp90 may have allowed for stronger interactions with GST-Hop-T198E, thereby portraying a less realistic illustration of its interactions with GST-Hop-T198E. The SPR analysis cannot be completely disregarded on the basis of this however, since binding of Hop to Hsp90 showed results comparable to previously published work in which Hsp90 was not immobilized (Brinker *et al.*, 2002; Odunuga *et al.*, 2003). Moreover, the experiments conducted by immobilizing Hsp90 were repeated using immobilized anti-GST, followed by GST-Hop binding, and then passing Hsp90 over the immobilized GST-Hop. Similar trends were obtained (data not shown).

Taking into consideration the results from the previous chapter together with the present chapter, disruption of Hop-Hsp90 binding accounted for increased incidences of nuclear localization of Hop. These data suggested that the major arm of the proposed NLS of Hop contributed to the network of interactions between Hop and Hsp90, and that these interactions may modulate the subcellular localization of Hop by sequestering Hop in the cytosol. A three dimensional (3D) representation of the structure of the TPR2A domain of Hop, shown in space fill with the NLS residues that were mutated, illustrates the proximity of these NLS residues to the methionine of the Hsp90 peptide (figure 4.7). It is therefore proposed that one or more of the NLS residues are involved in direct interactions with Hsp90.

Mimicking phosphorylation at T198, a site that was earlier shown to be phosphorylated by cdc2-kinase *in vitro*, appeared to disrupt Hop-Hsp90 interaction. Previously, immunoprecipitation assays using Hop-T198E-EGFP and NIH 3T3 cell lysate showed that Hsp90 co-immunoprecipitated with the phosphorylation mimic in mouse fibroblast lysate (Longshaw *et al.*, 2004). This could be attributed to the dimerization of Hop (Prodromou *et al.*, 1999; Carrigan *et al.*, 2004) *in vivo*, resulting in the binding of mutated Hop with endogenous unmutated Hop within the cell lysate and thereby masking the functional effects of the mutations on Hop. In the present study conducted, no cell lysate was introduced into the SPR analysis system and the GST-co-precipitation assay, thereby eliminating the possibility of GST-Hop interacting with endogenous Hop.

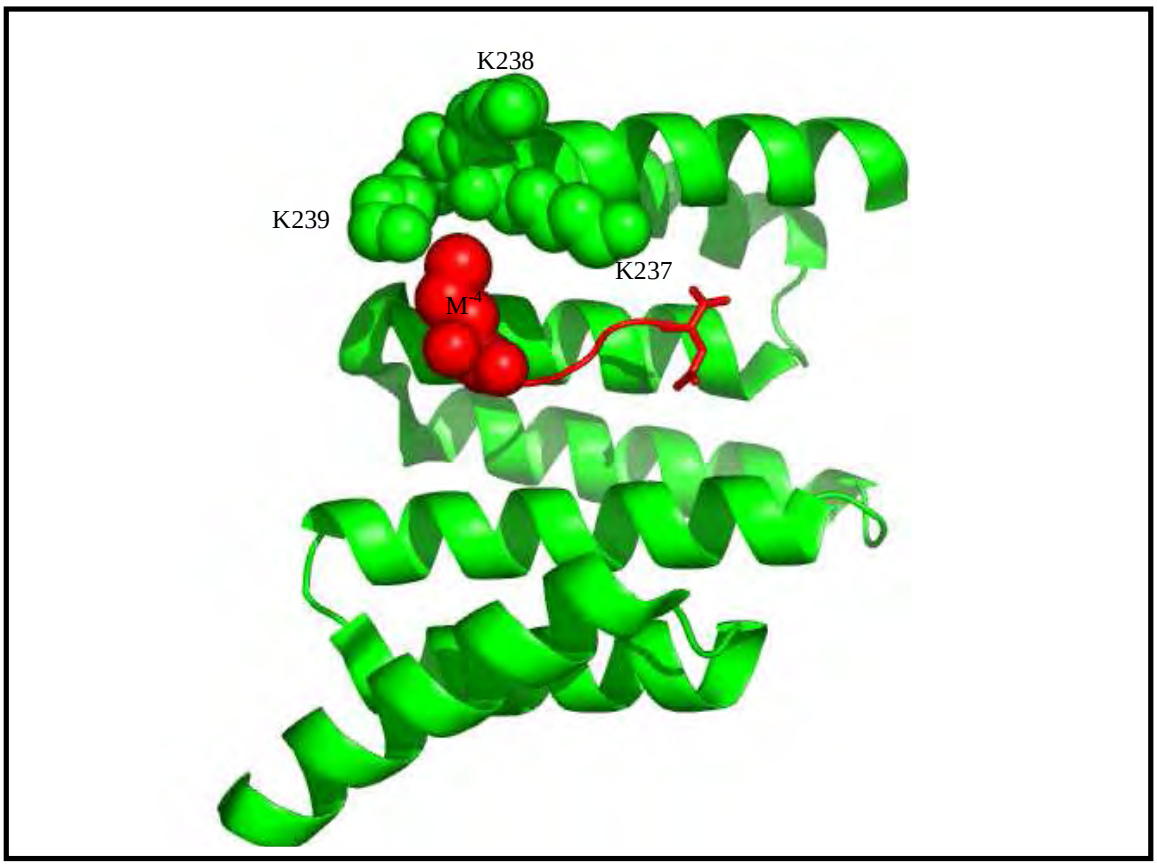


**Figure 4.7: Ribbon representation of the structure of TPR2A of Hop and the C-terminal TPR acceptor motif of Hsp90**. The structure of the TPR2A (green) of human Hop with the C-terminal MEEVD motif of Hsp90 shown in red (1ELR; Scheufler *et al*., 2000). The space filled residues in green, K237, K238 and K239 form the major arm of the predicted NLS, and these are shown relative to the space filled residue in red, methionine, which forms part of the pentapeptide MEEVD of Hsp90. This figure was generated using Pymol Molecular Graphics Software (http://pymol.sourceforge.net).

A predicted homology model of Hop showing the positions of the phosphorylation sites T198 and S189 in conjunction with the first motif of TPR2A domain of Hop depicted the positioning of T198 directly opposite K229 (Longshaw, 2002). Phosphorylation at T198 would induce a negative charge to this residue and this may result in weak ionic interactions with a positively charged K229, which in turn, may partially disrupt the binding of Hop to Hsp90. The partial disruption of Hop-Hsp90 binding, upon mimicking phosphorylation at T198, is indicative of a possible role of phosphorylation in regulating Hop-Hsp90 interactions.

Previous studies mapped out residues in TPR2A domain of Hop, K229, N233, N264, K301 and R305, which form a carboxylate clamp with the MEEVD motif of the TPR acceptor site of Hsp90 (Scheufler *et al.*, 2000; Odunuga *et al.*, 2003). Interestingly, the phosphorylation site T198, falls outside of the TPR2A domain. A number of other residues have been identified in Hop which are not part of the TPR2A domain but which are necessary for Hop-Hsp90 interaction (Flom *et al.*, 2006; Flom *et al.*, 2007). Moreover, although the MEEVD sequence of Hsp90 is mainly involved in interaction with Hop (Chen *et al.*, 1998), there are multiple binding sites within Hsp90 that are necessary for Hop interaction and which are not necessarily part of the MEEVD motif. For example, mutations of residues Glu-651 and Asp-653 in Hsp90 not only decreased the extent of Hop binding, but also diminished chaperone activity of Hsp90 (Ramsey *et al.*, 2000). There are a host of other co-chaperones other than Hop that interact with Hsp90 through their TPR domains; mutation of the above mentioned residues in Hsp90 did not appear to affect their interactions with Hsp90 (Ramsey *et al.*, 2000). The simplest conclusion would be that the TPR domain interactions between Hsp90 and Hop serve as a targeting site, and that the differences in biological significance of interactions between the TPR containing co-chaperone, Hop, with Hsp90 may lie within the sites of interaction that are outside the TPR domains.

# CHAPTER 5

# CONCLUSION

*"Science …never solves a problem without creating ten more"*

*- George Bernard Shaw*

## 5.1 CHAPTER 2

2D gel electrophoretic analysis of 120 µg protein of total cell lysate resolved on a non-linear pI strip of 3-10 confirmed the presence of a major and minor isoform of Hop under normal conditions. However, the addition of tyrosine and serine/threonine phosphatase inhibitors to the cell lysate, and resolution of the isoforms on a pI strip range of 4-7 showed that apart from the two isoforms detected initially, there were at least three more relatively acidic isoforms. Dephosphorylation of the cell lysate with SAP showed a considerable decrease in levels of two of the relatively more acidic isoforms, thereby providing evidence of *in vivo* phosphorylation of at least two subpopulations of Hop under normal conditions. Heat shock caused a decrease in the amounts of the major isoform and the presence of a number of minor acidic isoforms. Dephosphorylation of the heat shocked lysate caused various changes to the isoform composition, with a particular decrease in amounts of one of the minor acidic isoforms, which were present after the heat shock exposure. This data was suggestive of phosphorylation being a modification of Hop under normal conditions, and that Hop was differently phosphorylated after heat stress.

## 5.2 CHAPTER 3

Previous literature has shown a varied subcellular localization pattern for the various homologues of Hop under different conditions. A mouse Hop-EGFP protein construct was predominantly cytosolic under normal conditions but showed higher nuclear, but not nucleolar, localization when the cells were subjected to heat stress. The arrest of the cells in the G1/S transition showed a higher incidence of nuclear accumulation of Hop-EGFP, confirming that Hop indeed translocates to the nucleus under G1/S phase arrest. Since heat stress is known to cause cell cycle arrest in the G1/S phase (Khandijan, 1995; Kuhl and Rensing, 2000) it was concluded that Hop's nuclear localization was possibly primarily regulated by heat stress and secondarily regulated by the cell cycle events.

Biochemical fractionation of the cells confirmed the cytosolic localization of endogenous Hop, but also showed that Hop localized to the membranes and to a smaller extent, the cytoskeletal fractions, under normal and heat shocked conditions. The presence of

endogenous Hop in the nucleus under heat-shocked conditions was detected using the *in vitro* fractionation method and suggested that the nuclear translocation of Hop was of a highly dynamic nature and could not be captured with this invasive technique.

Mutation of the residues, K237, K238 and K239, which formed the major arm of the putative NLS, did not disrupt the nuclear localization of Hop under heat shock or G1/S arrest. Thus unlike classical bipartite NLS's, the major arm of this NLS did not contribute directly to its nuclear translocatory function but may have an alternative regulatory role in Hop localization.

Biochemical fractionation of the cells also showed that Hsp70 but not Hsp90 co-fractionated with Hop to the nucleus under heat stress. Mammalian Hsp90 is known to translocate dynamically to the nucleus under heat stress, and it was concluded that this method of fractionation was not sufficient to detect Hsp90 in the nucleus and more conclusive *in vivo* techniques would have to be used to confirm this result. Both heat shock proteins were shown to localize with Hop in the membranes and cytoskeletal fractions of the cells after heat shock.

## 5.3 CHAPTER 4

GST-Hop and its various derivatives were successfully constructed and their interactions with Hsp90 analyzed using SPR analysis and GST-co-precipitation studies. GST-Hop-K239A and GST-Hop-K237/238/239A did not bind to Hsp90 and were comparable to the negative control, indicating that these residues found within the putative NLS were critical for Hop-Hsp90 binding. Mimicking phosphorylation at S189 did not alter Hop-Hsp90 interactions, but a phosphorylation mimic at T198 showed partial disruption of Hop-Hsp90 binding. This suggested that phosphorylation of Hop by cdc2-kinase could possibly disrupt this complex formation.

## 5.4 DISCUSSION

This study of mammalian Hop has shown, for the first time that Hop is a phosphoprotein *in vivo* and that one of the modifications that Hop undergoes when the cell is stressed may be phosphorylation. Work done in BHK-21 cells showed that exogenous and endogenous Hop was primarily localized to the cytosol and membranes under normal conditions. However, under heat stress and/or conditions that may lead to the arrest of the cell in the G1/S transitory phase of the cell cycle, mouse Hop-EGFP was localized to the nucleus. This supports previously published reports of mouse Hop translocating to the nucleus of NIH 3T3 mouse fibroblast cells under conditions of G1/S arrest (Longshaw *et al.*, 2004) and provides novel evidence of the subcellular localization of Hop possibly being primarily regulated by stress events.

A bipartite NLS within the amino acid sequence of mouse Hop was earlier shown to be functional when fused to EGFP by successfully translocating EGFP into the nucleus (Longshaw *et al.*, 2004). When the localization of Hop-EGFP NLS mutants was assessed, contrary to expectations, there was an increased incidence of nuclear localization of the NLS mutants. This suggested that the residues of the major arm of this putative NLS were not directly responsible for nuclear translocation of Hop. However mutation of the NLS in Hop abrogated binding of Hop to Hsp90, as was shown by the *in vitro* studies conducted. A ribbon representation of the 3D structure of TPR2A domain of Hop in association with the Hsp90 pentapeptide shown in figure 4.7 demonstrated the proximity of the residues of the major arm of the NLS to methionine of Hsp90. This shows the potential of Hop-Hsp90 interactions in regulating the localization of Hop. Hop-Hsp90 binding may act as a cytosolic retention factor for Hop. Based on the results from this study, as well as what is currently known about Hop's subcellular localization particularly in terms of its nucleocytosolic shuttling capabilities, and its functions within the cell, we propose a model shown in figure 5.1. Various aspects of this model are further discussed in this section.

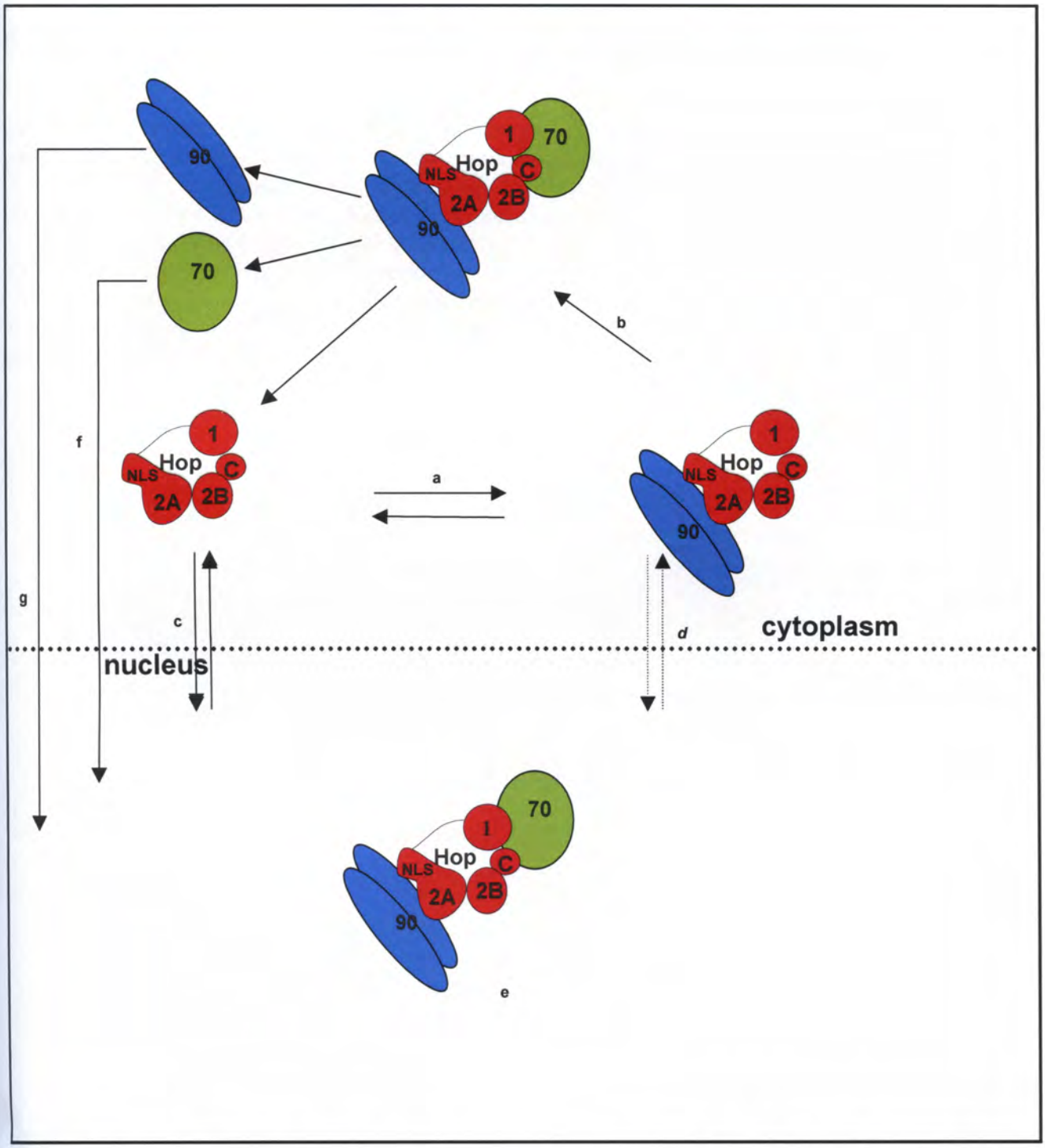


**Figure 5.1: Predicted model for Hop's interaction as an Hsp70-Hsp90 co-chaperone.** Hop exists on its own or in complex with Hsp90, in the cytosol under normal conditions. This may be regulated by phosphorylation (a). Interaction of Hop with Hsp90 is known to facilitate a number of other interactions, of which the most well established one is the interaction of Hop-Hsp90 complex

**(Figure 5.1 contd)**

with Hsp70 in order to facilitate substrate transfer from Hsp70 to Hsp90 (b). This multichaperone complex then dissociates, freeing its various components. Hop is known to translocate to the nucleus (c) under stress conditions and its nuclear localization mechanism may be regulated by phosphorylation by CKII and cdc2 kinase. It is already known that both Hsp70 and Hsp90 translocate to the nucleus under heat shock (f and g respectively). Hop may also be capable of moving into the nucleus in concert with Hsp90 (d) as a complex (arrows shown in dotted lines) using its putative NLS (222-239), or through the functioning of multiple NLSs. Within the nucleus Hop may have a number of functions, of which we propose that it is capable of its basic function of interacting with Hsp70 and/or Hsp90 to form nuclear complexes (e).

The possibility that binding of Hop to Hsp90 may serve to sequester Hop in the cytosol (figure 5.1) is consistent with the finding that the majority of Hop under normal conditions is cytosolic and complexed to Hsp90 (Smith *et al.*, 1993; Chang *et al.*, 1997; Prodromou *et al.*, 1999). Ligand-Hsp90 interactions sequestering the ligand within the cytosol has previously been reported in the case of the GR which when bound to Hsp90 restricted its localization to the cytosol (Guiochon-Mantel *et al.*, 1996). A protein-protein interaction regulating the subcellular localization of one or both partners is also seen in the case of ICAP-1 (integrin cytoplasmic domain-associated protein 1), a protein involved in cell proliferation processes and possessing a functional NLS. The cytosolic retention of ICAP-1, which shuttles between the nucleus and the cytoplasm, was shown to be through the specific interaction of this protein with β-1 integrin (Fournier *et al.*, 2005).

In the case of Hop, however, we suggest that not only does binding of Hop to Hsp90 regulate its cytosolic retention, but also that the Hop-Hsp90 interaction could involve residues of the proposed bipartite NLS of Hop. Therefore, within the bipartite NLS, the minor arm could be the functional nuclear localization signal, whereas the major arm, in binding to Hsp90, promotes cytosolic retention of Hop-Hsp90 under normal conditions. Despite the apparent logic of this suggested mechanism of cytosolic retention by NLS-protein interaction, surprisingly few reports of such interactions are available. Li *et al*. (1999) showed that the breast cancer-associated protein, BCRA1, which is previously described in section 1.1.3, is sequestered in the cytosol by binding of its NLS to a cytosolic retention protein, BRAP2 (BCRA1-associated protein 2). The BRCA1 protein is a nucleo-cytosolic shuttling protein that is ordinarily targeted to the nuclei by two functional NLS motifs, which bind to importin α. Its exclusive retention in the cytosol or the nucleus has been observed in many breast cancer cell lines; however this was suggested to be due to problems in its nucleo-cytosolic transport regulation rather than due to mutations within BRCA1 (Chen *et al.*, 1996a; Li *et al.*, 1999; Fabbro *et al.*, 2002).

The cytosolic retention protein BRAP2 showed a higher affinity for NLS motifs of BRCA1 than does importin-α. It was speculated that phosphorylation of BRCA1 may

serve to dissociate it from the BRCA1-BRAP2 complex, and allow for binding to importin-α and consequent nuclear translocation. Interestingly, BRAP2 also recognized the NLS motifs of SV40 large T-ag and the bipartite NLS found in mitosin. The role of BRAP2 was suggested to be exclusive to regulation of nuclear transport of a number of shuttling proteins by serving as a cytosolic retention protein (Li *et al.*, 1999). This was confirmed more recently by reports showing the interaction of BRAP2 with the NLS of cell cycle inhibitory protein p21 during monocyte differentiation, causing the cytosolic arrest of p21 (Asada *et al.*, 2004). p21 expressed in the cytosol is known to inhibit apoptosis as well as promote the assembly and nuclear translocation of cyclinD/Cdk4 complexes (LaBaer *et al.*, 1997; Asada *et al.*, 1999). Thus its interaction with BRAP2 appears to be a mode of regulation of its nucleo-cytosolic trafficking.

Reports showing the interaction of the prion protein $PrP^c$ with Hop mapped out residues on TPR2A of Hop to be crucial for this interaction (Coitinho *et al.*, 2007). Since a number of residues on TPR2A are also crucial for Hop-Hsp90 interactions, it is possible that $PrP^c$ may compete with Hsp90 for binding to Hop. Wild-type $PrP^c$ is not detected in the cytosol and is localized predominantly on cell surfaces or synaptosomal fractions (Martins *et al.*, 2001; Zanata *et al.*, 2002). Since a portion of Hop has been shown to be localized at the cell membranes, it is also possible that $Prp^c$-Hop binding through residues within the TPR2A of Hop which may include those found in the NLS region, could allow for the retention of a subpopulation of Hop at the plasma membrane.

A second potential NLS in mouse Hop was detected downstream (amino acids 337-351), shown in figure 5.2, which appeared to be 'buried' within the protein conformation (Blatch *et al.*, 1997). The possibility exists that both NLSs are functional *in vivo*. It is already known that multiple copies of an NLS are more efficient than single copies, for example, the maize R protein requires two of three NLS-functioning sequences to be nuclear (Shieh *et al.*, 1993). Also, in the case of the APC protein, two monopartite NLSs were identified. Although either NLS was found to be sufficient to function on its own, optimal nuclear import of APC required both NLS functioning (Zhang *et al.*, 2000).

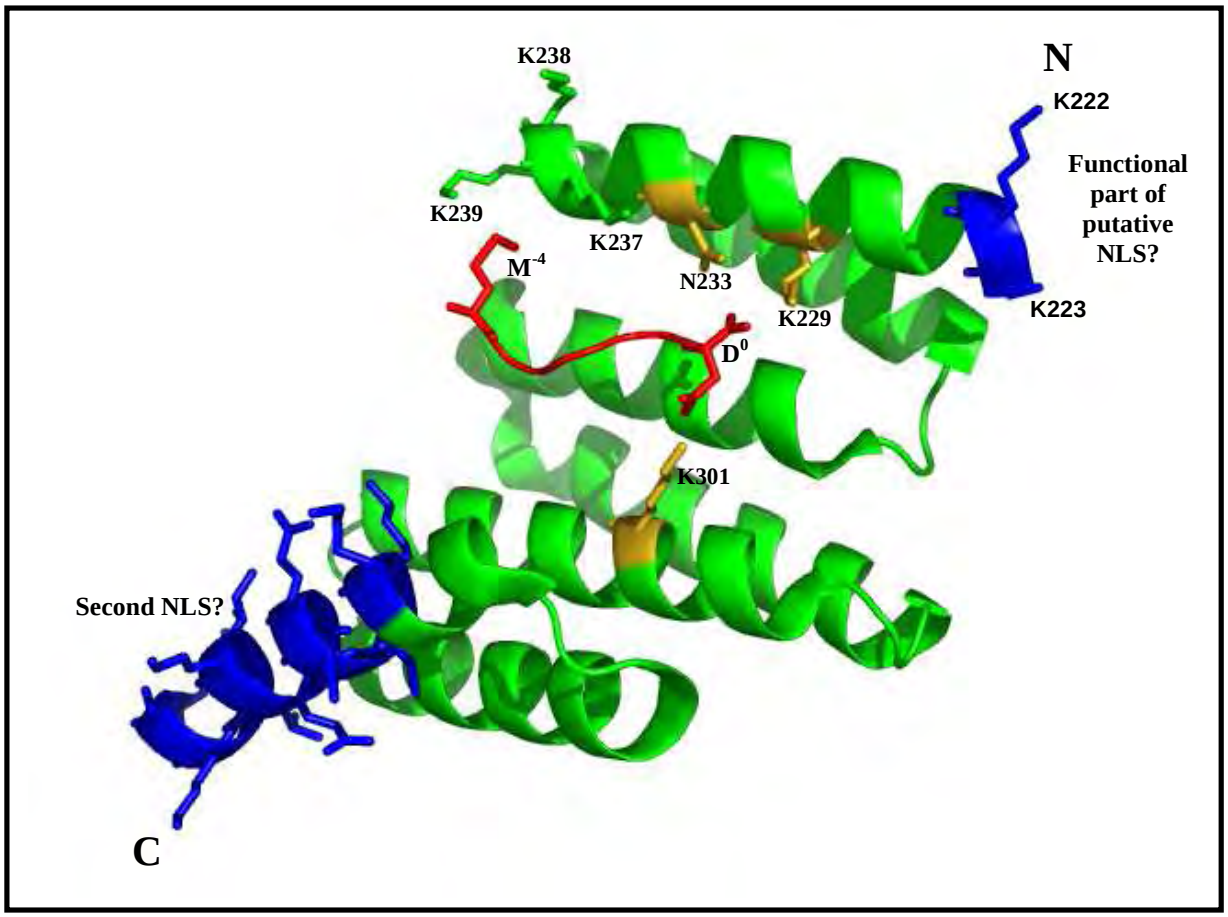


**Figure 5.2: Minor arm of the putative NLS acts as a Monopartite NLS with a second possible NLS downstream?** A ribbon representation of the structure of TPR2A (green) of human Hop with the C-terminal MEEVD motif of Hsp90 shown in red (1ELR; Scheufler *et al*., 2000). The minor arm of the predicted bipartite NLS (residues K222 and K223, shown in blue) may be responsible for the functionality of the NLS, with the major arm acting as a cytosolic retention factor by interacting with Hsp90. There also exists the possibility of a second NLS found downstream of the first NLS, also shown in blue (residues 337-351), which could be acting in concert with the predicted bipartite NLS. Residues shown in gold are those that form part of the carboxylate clamp of Hop, which is important for interaction with Hsp90 (Odunuga *et al*., 2003). This figure was generated using Pymol Molecular Graphics Software (http://pymol.sourceforge.net).

If both NLSs found in mouse Hop are indeed functional, mutation of the major arm of the first NLS could result in a modification of the structure of Hop such that the second NLS may be better positioned and exposed to importin binding, facilitating more efficient nuclear localization than that obtained for unmutated Hop.

Hsp90 is cytosolic under normal conditions but has been shown to translocate to the nucleus as shown in figure 5.1g (Perdew *et al.*, 1993), and has also been implicated in the dynamic nuclear trafficking of SR and p53 (Pratt, 1997; Galigniana *et al.*, 2004). Hsp90 translocates into the nucleus under heat shock and although a number of potential NLS's have been identified within its amino acid sequence, none of them have been shown to be functional *in vivo* (Biggiogera *et al.*, 1996; Bharadwaj *et al.*, 1999; Langer *et al.*, 2003). It has been proposed, however, that certain conditions, which alter the conformation of Hsp90, may allow for the presentation of its NLSs such that they become functional (Langer *et al.*, 2003). The interaction of Hop with Hsp90 is one in which the conformation of one or both partners is altered (Prodromou *et al.*, 1999; Murphy *et al.*, 2001; Hernandez *et al.*, 2002).

Thus although the Hop-Hsp90 complex is cytosolic under normal conditions, it is tempting to speculate that a sub-population of Hop and Hsp90 may be directed to the nucleus as a complex under heat stress, either by the combined effort of NLSs found within both proteins, or by Hsp90 'piggy-backing' on Hop (figure 5.1d). However, this does not exclude the translocation of a population of Hop into the nucleus on its own (figure 5.1c). This is inferred by the finding that mutations in Hop that were seen to disrupt Hop-Hsp90 binding *in vitro*, were also seen to promote the nuclear translocation of Hop *in vivo*.

The nuclear translocation of both Hop, and Hsp90 have been described as dynamic (Langer *et al.*, 2003; Longshaw *et al.*, 2004) and it was proposed that Hop was constantly shuttling between the nucleus and the cytosol but that the nuclear export of Hop occurred at a faster rate than its nuclear import (Longshaw *et al.*, 2004). The results of the *in vitro* fractionation studies supports this theory because of the difficulty in detecting Hop in the

nuclear extracts of heat stressed cells, despite the evident detection of its nuclear localization under heat stress and cell cycle arrest, using confocal microscopic analysis. Moreover Hsp90, which is known to translocate to the nucleus under stressful conditions like heat shock (Perdew *et al.*, 1993; Biggiogera *et al.*, 1996; Bharadwaj *et al.*, 1999; Langer *et al.*, 2003) was not detected in the heat shocked nuclear fractions obtained by biochemical fractionation (chapter 3). Thus, although this method was sufficient to detect the nuclear localization of proteins such as Hsp70 after heat shock, the time delays involved in various steps of fractionation were not necessarily conducive to detecting the subcellular localization of dynamically shuttling proteins.

Hop was found to co-fractionate with Hsp70 in the nucleus after heat shock; this was not unexpected, as Hsp70 has been shown to migrate to the nucleus and the nucleolus, particularly during stress (figure 5.1f), where it is involved in stress-related cytoprotection (Bharadwaj *et al.*, 1999; Nollen *et al.*, 2001). Hsp70 not only participated in the holding and refolding of heat unfolded nuclear proteins, but also stimulated the translocation of unfolded proteins into the nucleolus during stress. Storage of these unfolded proteins in the nucleolus during stress was associated with preventing random aggregation with other nuclear proteins and temporarily halting protein synthesis by interfering with the assembly of ribosomes (Nollen *et al.*, 2001).

The detection of Hop in the nucleus under stress conditions allows for various speculations on its possible roles within the nucleus, particularly with regards to its scaffolding properties as an Hsp70-Hsp90 co-chaperone. It is already known that Hsp70 is involved in the import of various proteins into the nucleus such as the SV 40 large T-ag and nucleoplasmin (Tsukahara and Maru, 2004), as well as being involved in the regulation of the activity of certain nuclear DNA-binding transcription factors (Diehl *et al.*, 2003). Thus, the question arises as to whether Hop forms heterocomplexes with Hsp70 and Hsp90 in the nucleus under stressed conditions as it does in the cytosol (figure 5.1e). A role for nuclear Hop together with Hsp70 was previously proposed in maintaining a transcriptionally potent form of the OCA-S complex, a multicomponent transcription activator complex in the S phase (Zheng *et al.*, 2003).

Various studies suggest that the regulation of HSF under stress and non-stress conditions is mediated by constituents of the Hsp70-Hsp90 multichaperone heterocomplex in a similar manner to that of SR complexes (Nair *et al.*, 1996; Bharadwaj *et al.*, 1999). Reconstitution experiments in a cell-free system showed that Hop, in addition to Hsp90, Hsp70, FKBP51, FKBP52, CyP40 and p23, were capable of forming a heterocomplex with HSF (Nair *et al.*, 1996). In an amphibious system (*Xenopus* oocytes) where HSF is an entirely nuclear protein, a role for Hop along with Hsp70 and Hsp90 was proposed in the disassembly of the HSF homotrimer within the nucleus (Bharadwaj *et al.*, 1999).

The possibility of Hop translocating into the nucleus as a complex with Hsp90 implies that there may be specific functions for this complex within the nucleus. Hop may be involved in Hsp90 complexes that have been shown to stably associate and participate in the chaperoning of telomerase complexes (Forsythe *et al.*, 2001). Hop, in both the yeast and mammalian system, has been detected within protein complexes involving Hsp90 and Ssl2, a DNA helicase required for transcription and DNA repair. These results have suggested roles for Hop and Hsp90 in mediating the function of Ssl2, and in so doing, ultimately being involved in DNA repair and transcription (Flom *et al.*, 2005). However, it must be noted that yeast Hop does not appear to have an NLS, and has thus far, not been shown to localize to the nucleus.

Hop, Hsp70 and Hsp90 were also found to co-fractionate in the membranes under normal and stress conditions, and in the cytoskeleton under heat shocked conditions. This implies that Hop interacts as a scaffolding protein with both these major heat shock proteins, not only in the cytosol, and possibly nucleus, but also in the membranous and cytoskeletal structures of the cell. Further studies in the form of live cell imaging of various fluorophore-tagged proteins (i.e. Hop and it's chaperone partners, Hsp70 and 90) and using techniques such as FRAP (Fluorescence Recovery After Photobleaching) and FRET (Fluorescence Resonance Energy Transfer) would be required to characterize such interactions within these cellular compartments. The function(s) of the possible membranous and cytoskeletal Hsp70-Hop-Hsp90 heterocomplexes may not be restricted

to those conventionally known of, because of the variation in types of proteins and their roles within the various compartments of the cell.

Although this study showed direct evidence of the differential phosphorylation of Hop, the residues at which it is phosphorylated have only been mapped *in vitro* (Longshaw *et al*., 2000). Future studies using antibodies that are developed against phosphorylated residues of Hop, such as S189 and T198 (Longshaw *et al*., 2000) have to be conducted to further charecterize the phosphorylation of Hop *in vivo*. It was postulated that the phosphorylation of Hop may regulate its subcellular localization (Longshaw *et al.*, 2000; Longshaw *et al.*, 2004) and this hypothesis is supported by this study. The various isoforms of Hop seen in the 2D gel electrophoretic study and the change in isoform profile after dephosphorylation, confirmed the presence of differentially phosphorylated isoforms of Hop under normal as well as stressed conditions; each of these isoforms may be differentially localized within the cell. We propose that the major isoform of Hop under normal conditions was cytosolic, and that the majority of this isoform was complexed to Hsp90 (figure 5.1).

The treatment of mouse fibroblast cells with a CKII inhibitor caused a cytosolic distribution of Hop similar to normal conditions. Moreover, a CKII-phosphorylation mimic of Hop showed increased incidences of nuclear localization compared to the unmodified Hop (Longshaw *et al.*, 2004). Mimicking phosphorylation at the *in vitro* CKII phosphorylation site of Hop had no significant effect on Hop-Hsp90 binding implying that phosphorylation of Hop by CKII did not disrupt Hop-Hsp90 interaction. Interestingly Hsp90 also associates with CKII and not only enhances its kinase activity (Miyata and Yahara, 1992) but is itself phosphorylated by this kinase (Lees-Miller and Anderson, 1989). Thus CKII phosphorylation may regulate the nuclear import of Hop, whether it is on its own, or in complex with Hsp90 (figure 5.1c,d).

The inhibition of cdc2-kinase in mouse fibroblast cells resulted in a marked nuclear accumulation of Hop (Longshaw *et al.*, 2004). In this study, a cdc2-kinase phosphorylation mimic of Hop disrupted Hop-Hsp90 interactions *in vitro* and implied

that phosphorylation of Hop by cdc2-kinase was unfavourable for Hop-Hsp90 interactions *in vivo*. We speculate that the regulation of the complexation state of Hop within the cytosol may be carried out by cdc2-kinase phosphorylation (figure 5.1a). A Hop isoform phosphorylated at T198 by cdc2-kinase *in vivo* may not be associated with Hsp90, and be involved in various cytosolic functions that do not involve Hsp90, such as Hop-Hsp104 interactions (Abbas-Terki *et al.*, 2001), and the interaction of Hop with TRiC which is involved in folding of actins and tubulins (Gebauer *et al.*, 1998).

Dephosphorylation of free Hop at T198 and its subsequent phosphorylation by CKII at S189, may enable it to move into the nucleus with or without Hsp90. This may not be the only mode of regulation of nuclear translocation. Based on the data presented in this study however, we propose that one of the mechanisms that regulates Hop's interactions with Hsp90 and its subcellular localization, both as free Hop and the Hop-Hsp90 complex, is phosphorylation. Phosphorylation-dephosphorylation events have also been implicated in SR-Hsp90 interactions and subcellular trafficking, with studies suggesting that under normal physiological conditions a dephosphorylation event, particularly relating to serine/threonine phosphorylation sites, may be required for the loss of high affinity binding to Hsp90 (Galigniana *et al.*, 1999).

Phosphorylation-dependent subcellular localization of heat shock proteins is not uncommon. Hsp25, a small heat shock protein induced by various kinds of cell stress conditions, was shown to be phosphorylated by MAPK and ERK signal transduction pathways in hippocampal HiB5 cells during heat shock. Although a population of phosphorylated Hsp25 remained in the cytosol, a large portion of the phosphorylated Hsp25 translocated into the nucleus where it was implicated in various thermoprotective roles (Geum *et al.*, 2002). Interestingly, the bacterial homolog of Hsp70, DnaK, showed a decrease in electrophoretic mobility and isoelectric point, upon heat shock at 42$^{o}$C for 30 minutes. This heat-induced modification was attributed to phosphorylation, and the phosphorylated form of DnaK was shown to possess an enhanced affinity for unfolded proteins (Sherman and Goldberg, 1993). Although it is known that Hsp70 translocates to the nucleus under heat shock, it is not yet known whether phosphorylation of Hsp70

plays a functional role in its subcellular localization. Thus it is tempting to speculate that heat-induced phosphorylation may be a general mechanism in regulation of the subcellular localization, and consequently, function of heat shock proteins and/or their co-chaperones.

Further research in this field is necessary to elucidate the mechanism by which Hop translocates to the nucleus, specifically with regard to its NLS. Guidelines to establishing whether a putative NLS is truly functional *in vivo* are reviewed by Lange *et al*. (2007). Four main specifications have been elaborated, namely:
(a). The proposed NLS sequence must be shown to be sufficient to target an unrelated protein into the nucleus.
(b) The transport of the protein into the nucleus must be shown to be dramatically hindered upon modification or deletion of the proposed NLS.
(c) The putative NLS must be shown to directly interact with its putative import receptor.
(d) Disabling the proposed nuclear import pathway *in vivo* must be shown to disrupt the nuclear import of the protein carrying the proposed NLS.

Thus far, the proposed NLS of Hop has been shown to be functional only with respect to the first specification mentioned (Longshaw *et al.*, 2004). Although the transport of the protein into the nucleus was shown to be enhanced upon mutation of the major arm of the proposed NLS this appeared to be an indirect effect. The results of this study appear to be pointing at the minor arm of the putative NLS as being directly responsible for its nuclear translocation. However, this has to be established by mutation or deletion of these residues and analyzing the subcellular localization of such modified Hop proteins.

The proposed bipartite NLS of Hop has not yet been analyzed with respect to its interactions with any nuclear transport machinery, in particular, importin-α and β. Several isoforms of importin-α have been described in eukaroytes, including importin-α1/Rch1, importin-α5/hSRP1, importin-α3/Qip, importin-α4/hSRP1, importin-α6 and importin-α7. There are 14 putative members of the importin-β family in the yeast system and possibly more than 22 in the mammalian system (Köhler *et al.*, 1999; Ström and

Weis, 2001). Previously bipartite NLS sequences have shown to bind to both the major and the minor binding site on importin-α, with the major binding site of importin-α recognizing the major arm of the NLS and the minor binding site of importin-α recognizing the minor arm of the NLS (Conti *et al.*, 1998; Kobe, 1999; Fontes *et al.*, 2000; Fontes *et al.*, 2005; Lange *et al.*, 2007). Binding of the NLS to the major binding site of importin-α appears to be more physiologically relevant to nuclear transport than its minor binding site and furthermore, the auto-inhibitory domain on importin-α is found on its major NLS-binding site (Conti *et al.*, 1998; Conti and Kuriyan, 2000; Fanara *et al.*, 2000; Catimel *et al.*, 2001).

Therefore the possibility of the minor arm and not the major arm, of this putative NLS, acting as the functional nuclear localization signal is interesting in the context of how it interacts with importin-α and needs to be investigated further. Moreover, the results of this study raise questions as to whether the second NLS found downstream of the first NLS is involved in nuclear translocation, either on its own, or in concert with the first NLS. Treating cells with a nuclear export inhibitor such as leptomycin B (Longshaw *et al.*, 2004) and analyzing the subcellular localization of various NLS mutants of Hop after different time intervals could prove to be a useful kinetic study in determining the nature of its NLS's and subsequently, its nuclear localization. The inhibition of export of mouse Hop-EGFP by leptomycin B (Longshaw *et al.*, 2004) suggested a CRM-1 export pathway mediated by a nuclear export signal (NES). The NES may be working together with the cytosolic retention factor (Hop-Hsp90 interactions) in regulating the export of Hop from the nucleus, and its characterization may prove to be vital in further understanding the dynamics of Hop's subcellular localization.

Traditionally, the function of Hop has been restricted to that of Hsp70-Hsp90 scaffolding protein, but various studies now indicate that Hop plays a greater role within this system, as a modulator of their chaperone activities and is even involved in their protein folding pathways. Moreover, other research has also shown that Hop interacts with a variety of other proteins that may or may not be linked with Hsp70 or Hsp90. The work presented here may be regarded as novel data demonstrating the phosphorylation status of Hop, its

subcellular localization patterns under stressful conditions, and its mechanism of interaction with Hsp90 as well as the possibility of all three aspects of Hop being mechanistically linked. The presence of the various isoforms of Hop including a number of differentially phosphorylated isoforms, and its varied subcellular localization patterns are an indication of the complex roles that Hop plays in numerous systems and under a variety of cellular conditions. Understanding these processes would help to elucidate the integral aspects of chaperone-mediated processes within the cell, particularly with regards to the assembly of the Hsp70-Hsp90 heterochaperone complex.

# REFERENCES


Abbas-Terki, T., Briand, P.A., Donze, O., and Picard, D. (2002). The Hsp90 co-chaperone cdc37 and STI1 interact physically and genetically. Biol Chem 383, 1335-1342.

Abbas-Terki, T., Donze, O., Briand, P.A., and Picard, D. (2001). Hsp104 interacts with Hsp90 cochaperones in respiring yeast. Mol Cell Biol 21, 7569-7575.

Acconcia, F., Barnes, C.J., Singh, R.R., Talukder, A.H., and Kumar, R. (2007). Phosphorylation-dependent regulation of nuclear localization and functions of integrin-linked kinase. Proc Natl Acad Sci U S A 104, 6782-6787.

Adams, M.D., Celniker, S.E., Holt, R.A., Evans, C.A., Gocayne, J.D., Amanatides, P.G., Scherer, S.E., Li, P.W., Hoskins, R.A., Galle, R.F., et. al. (2000). The genome sequence of Drosophila melanogaster. Science 287, 2185-2195.

Agarraberes, F.A., and Dice, J.F. (2001). A molecular chaperone complex at the lysosomal membrane is required for protein translocation. J Cell Sci 114, 2491-2499.

Akakura, S., Yoshida, M., Yoshihiro, Y., and Horinouchi, S. (2001). A role for Hsc70 in regulating nucleocytoplasmic transport of a temperature-sensitive p53 (p53Val-135). J Biol Chem 276, 14649-14657.

Alberts, B. (1998). The cell as a collection of protein machines: preparing the next generation of molecular biologists. Cell 92, 291-294.

Alberts, B., Bray, D., Lewis, J., Raff, M., Roberts, K., and Watson, J.D. (1994). Molecular biology of the cell Garland Publishing Inc.: New York.

Alberts, B., Bray, D., Lewis, J., Raff, M., Roberts, K., and Watson, J.D. (1998). Essential Cell Biology. Garland Publishing, Inc.: New York.

Ali, M.M.U., Roe, S.M., Vaughan, C., Meyer, P., Panaretou, B., Piper, P.W., Prodromou, C., and Pearl, L.H. (2006). Crystal structure of an Hsp90–nucleotide–p23/Sba1 closed chaperone complex. Nature 440, 1013-1017.

Allen, T.D., Cronshaw, J.M., Bagley, S., Kiseleva, E., and Goldberg, M.W. (2000). The nuclear pore complex: mediator of translocation between nucleus and cytoplasm. J Cell Sci 113, 1651-1659.

Amici, C., Giorgi, C., Rossi, A., and Santoro, M.G. (1994). Selective inhibition of virus protein synthesis by prostaglandin A: A translational block associated with HSP70 synthesis. J Virol 68, 6890-6899.

Arispe, N., and De Maio, A. (2000). ATP and ADP modulate a cation channel formed by Hsc70 in acidic phospholipid membranes. J Biol Chem 275, 30839-30843.

Asada, M., Ohmi, K., Delia, D., Enosawa, S., Suzuki, S., Yuo, A., Suzuki, H., and Mizutani, S. (2004). Brap2 functions as a cytoplasmic retention protein for p21 during monocyte differentiation. Mol Cell Biol 24, 8236-8243.

Asada, M.T., Yamada, H., Ichijo, D., Miyazono, D.K., Fukumuro, K., and Mizutani, S. (1999). Apoptosis inhibitory activity of cytoplasmic p21(Cip1/WAF1) in monocytic differentiation. EMBO J 18, 1223-1234.

Bagi, G., and Hidvegi, E.J. (1990). Protein phosphorylation and kinase activities in tumour cells after hyperthermia. Int J Radiat Biol 58, 633-650.

Behrens, S., Maier, R., de Cock, H., Schmid, F.X., and Gross, C.A. (2001). The SurA periplasmic PPIase lacking its parvulin domains functions in vivo and has chaperone activity. EMBO J 20, 285-294.

Bharadwaj, S., Ali, A., and Ovsenek, N. (1999). Multiple components of the HSP90 chaperone complex function in regulation of heat shock factor 1 In vivo. Mol Cell Biol 19, 8033-8041.

Bianchini, L., Woodside, M., Sardetll, C., Pouyssegurll, J., Takaill, A., and Grinstein, S. (1991). Okadaic acid, a phosphatase inhibitor, induces activation and phosphorylation of the Na+/H+ antiport. J Biol Chem 266, 15406-15413.

Biggiogera, M., Tanguay, R.M., Marin, R., Wu, Y., Martin, T.E., and Fakan, S. (1996). Localization of heat shock proteins in mouse male germ cells: an immunoelectron microscopical study. Exp Cell Res 229, 77-85.

Blatch, G.L., and Lassle, M. (1999). The tetratricopeptide repeat: a structural motif mediating protein-protein interactions Bioessays 21, 932-939.

Blatch, G.L., Lässle, M., Zetter, B.R., and Kundra, V. (1997). Isolation of a mouse cDNA encoding mSTI1, a stress-inducible protein containing the TPR motif. Gene 194, 277-282.

Bosc, D.G., Slominski, E., Sichler, C., and Litchfield, D.W. (1995). Phosphorylation of casein kinase II by p34cdc2. J Biol Chem 270, 25872-25878.

Breeuwer, M., and Goldfarb, D.S. (1990). Facilitated nuclear transport of histone H1 and other small nucleophilic proteins. Cell 60, 999-1008.

Brinker, A., Scheufler, C., von der Mulbe, F., Fleckenstein, B., Herrmann, C., Jung, G., Moarefi, I., and Hartl, F.U. (2002). Ligand discrimination by TPR domains. Relevance and selectivity of EEVD-recognition in hsp70.hop.hsp90 complexes. J. Biol. Chem. 277, 19265-19275.

Bukau, B., and Horwich, A.L. (1998). The Hsp70 and Hsp60 chaperone machines. Cell 92, 351-366.

Burg, M.B. (2000). Macromolecular crowding as a cell volume sensor. Cell Physiol Biochem 10, 251-256.

Bursac, D., and Lithgow, T. (2006). The evolution and function of co-chaperones in mitochondria. In: The Networking of Chaperones by Co-chaperones, ed. G.L. Blatch: Landes Bioscience, 99-108.

Carrigan, P.E., Nelson, G.M., Roberts, P.J., Stoffer, J., Riggs, D.L., and Smith, D.F. (2004). Multiple domains of the co-chaperone Hop are important for Hsp70 binding. J Biol Chem 279, 16185-16193.

Carrigan, P.E., Riggs, D.L., Chinkers, M., and Smith, D.F. (2005). Functional comparison of human and drosophila Hop reveals novel role in steroid recepter maturation. J Biol Chem 280, 8906-8911.

Catelli, M.G., Binart, N., Jung-Testas, I., Renoir, J.M., Baulieu, E.E., Feramisco, J.R., and Welch, W.J. (1985). The common 90-kd protein component of non-transformed '8S' steroid receptors is a heat-shock protein. EMBO J 4, 3131-3135.

Catimel, B., Teh, T., Fontes, M.R.M., Jennings, I.G., Jans, D.A., Howlett, G.J., Nice, E.C., and Kobe, B. (2001). Biophysical charecterization of interactions involving importin-α during nuclear import. J Biol Chem 276, 34189-34198.

Chang, H.C.J., and Lindquist, S. (1994). Conservation of Hsp90 macromolecular complexes in saccharomyces cerevisiae. J Biol Chem 1994, 24983-24988.

Chang, H.C.J., Nathan, D.F., and Lindquist, S. (1997). In vivo analysis of the hsp90 cochaperone sti1 (p60). Mol Cell Biol 17, 318-325.

Chen, C.-F., Shang, L., Chen, Y.H., Chen, P.-L., Sharp, Z.D., and Lee, W.-H. (1996a). The nuclear localization sequences of the BRCA1 protein interact with the importin-α subunit of the nuclear transport signal receptor. J Biol Chem 271, 32863–32868.

Chen, F., Torres, M., and Duncan, R.F. (1995). Activation of mitogen-activated protein kinase by heat shock treatment in Drosophila. Biochem J 312 341–349.

Chen, S., and Smith, D.F. (1998). Hop as an adaptor in the heat shock protein 70 (Hsp70) and Hsp90 chaperone machinery. J Biol Chem 273, 35194-35200.

Chen, S., Prapapanich, V., Rimerman, R.A., Honore, B., and Smith, D.F. (1996). Interactions of p60, a mediator of progesterone receptor assembly, with heat shock proteins hsp90 and hsp. Mol Endocrinol 10, 682 – 693.

Chen, S.Y., Sullivan, W.P., Toft, D.O., and D.F., S. (1998). Differential interactions of p23 and the TPR-containing proteins Hop, Cyp40, FKBP52 and FKBP51 with Hsp90 mutants. Cell Stress Chap 3, 118-129.

Cheng, C.H., Liu, S.M., Chow, T.Y., Hsiao, Y.Y., Wang, D.P., Huang, J.J., and Chen, H.H. (2002). Analysis of the complete genome sequence of the Hz-1 virus suggests that it is related to members of the Baculoviridae. J Virol 76, 9024-9034.

Cheung, J., and Smith, D.F. (2000). Molecular chaperone interactions with steroid receptors: an update. Mol Endocrinol 14, 939-946.

Cheung, M.S., Garcia, A.E., and Onuchic, J.N. (2002). Protein folding mediated by solvation: water expulsion and formation of the hydrophobic core occur after the structural collapse. Proc Natl Acad Sci U S A 99, 685-690.

Chook, Y.M., and Blobel, G. (2001). Karyopherins and nuclear import. Curr Opin Struct Biol 11, 703-715.

Chu, A., Matusiewicz, N., and Stochaj, U. (2001). Heat-induced nuclear accumulation of hsc70s is regulated by phosphorylation and inhibited in confluent cells. FASEB J 15, 1478-1480.

Chun, J., Hyun, S., Kwon, T., Lee, E.J., Hong, S.K., and Kang, S.S. (2005). The subcellular localization control of integrin linked kinase 1 through its protein-protein interaction with caveolin-1. Cell Signal 17, 751-760.

Coitinho, A.S., Lopes, M.H., Hajj, G.N.M., Rossato, J.I., Freitas, A.R., Castro, C.C., Cammarota, M., Brentani, R.R., Izquierdo, I., and Martins, V.R. (2007). Short-term memory formation and long-term memory consolidation are enhanced by cellular prion association to a stress-inducible protein 1. Neurobiol Dis 26, 282-290.

Conti, E., and Kuriyan, J. (2000). Crystallographic analysis of the specific yet versatile recognition of distinct nuclear localization signals by karyopherin alpha. Structure 8, 329-338.

Conti, E., Uy, M., Leighton, L., Blobel, G., and Kuriyan, J. (1998). Crystallographic analysis of the recognition of a nuclear localization signal by the nuclear import factor karyopherin alpha. Cell 94, 193-204.

Csermely, P., and Kahn, C.R. (1991). The 90-kDa heat shock protein (hsp-90) possesses an ATP binding site and autophosphorylating activity. J Biol Chem 266, 4943-4950.

Csermely, P., Kajtar, J., Hollosi, M., Jalsovszky, G., Holly, S., Kahn, C.R., Gergely, P., Jr., Soti, C., Mihaly, K., and Somogyi, J. (1993). ATP induces a conformational change of the 90-kDa heat shock protein (hsp90). J Biol Chem 268, 1901-1907.

Czar, M.J., Galigniana, M.D., Silverstein, A.M., and Pratt, W.B. (1997). Geldanamycin, a heat shock protein 90-binding benzoquinone ansamycin, inhibits steroid-dependent translocation of the glucocorticoid receptor from the cytoplasm to the nucleus. Biochemistry 36, 7776-7785.

Czar, M.J., Welsh, M.J., and Pratt, W.B. (1996). Immunofluorescence localization of the 90-kDa heat shock protein to cytoskeleton. Eur J Cell Biol 70, 322-330.

Dai, Q., Zhang, C., Wu, Y., McDonough, H., Whaley, R.A., Godfrey, V., Li, H.-H., Madamanchi, N., Xu, W., Neckers, L., Cyr, D., and Patterson, C. (2003). CHIP activates HSF1 and confers protection against apoptosis and cellular stress. EMBO J 22, 5446-5458.

Daniel, S., Söti, C, Csermely, P., Bradley, G. and Blatch, G.L. (2006) Hop: an Hsp70/90 co-chaperone that functions within and beyond Hsp70-Hsp90 protein folding pathways. In: Networking of chaperones by co-chaperones, ed. G.L. Blatch: Landes Bioscience; New York: Springer Science + Business Media, 23-37.

Demand, J., Luders, J., and Hohfeld, J. (1998). The carboxy-terminal domain of Hsc70 provides binding sites for a distinct set of chaperone cofactors. Mol Cell Biol 18, 2023-2028.

Diehl, J.A., Yang, W., Rimerman, R.A., Xiao, H., and Emili, A. (2003). Hsc70 regulates accumulation of cyclin D1 and cyclin D1-dependent protein kinase. Mol Cell Biol 23, 1764-1774.

Dingwall, C., and Laskey, R.A. (1991). Nuclear targetting sequences: a consensus? Trends Biochem Sci 16, 478-481.

Dittmar, K.D., Hutchison, K.A., Owens-Grillo, J.K., and Pratt, W.B. (1996). Reconstitution of the steroid receptor.hsp90 heterocomplex assembly system of rabbit reticulocyte lysate. J Biol Chem 271, 12833-12839.

Dobson, C.M. (2003). Protein folding and misfolding. Nature 426, 884-890.

Dudek, J., Jung, M., Weitzmann, A., Greiner, M., and Zimmermann, R. (2006). Co-chaperones of the endoplasmic reticulum. In: Networking of chaperones by co-chaperones, ed. G.L. Blatch: Landes Bioscience; New York: Springer Science + Business Media, 88-98.

Duncan, R.F., and Hershey, J.W.B. (1989). Protein synthesis and protein phosphorylation during heat stress, recovery and adaptation. J Cell Biol 109, 1467-1481.

Ellis, R.J. (1998). Steric chaperones. Trends Biochem Sci 23, 43-45.

Ellis, R.J. (2001a). Macromolecular crowding: an important but neglected aspect of the intracellular environment. Curr Opin Struct Biol 11, 114-119.

Ellis, R.J. (2001b). Macromolecular crowding: obvious but underappreciated. Trends Biochem Sci 26, 596-604.

Ellis, R.J. (2007). Protein misassembly: Macromolecular crowding and molecular chaperones. In: Molecular aspects of the stress response : chaperones, membranes and networks eds. P. Csermely and L. Vígh, New York: Landes Bioscience.

Elowitz, M.B., Surette, M.G., Wolf, P.E., Stock, J.B., and Leibler, S. (1999). Protein mobility in the cytoplasm of Escherichia coli. J Bacteriol 181, 197-302.

Fabbro, M., Rodriguez, J.A., Baer, R., and Hendersen, B.R. (2002). BARD1 induces BRCA1 intranuclear foci formation by increasing RING-dependent BRCA1 nuclear import and inhibiting BRCA1 nuclear export. J Biol Chem 277, 21315-21354.

Fanara, P., Hodel, M.R., Corbett, A.H., and Hodel, A.E. (2000). Quantitative analysis of nuclear localization signal (NLS)-importin alpha interaction through fluorescence depolarization. Evidence for auto-inhibitory regulation of NLS binding. J Biol Chem 275.

Fersht, A.R. (2000). Transition-state structure as a unifying basis in protein-folding mechanisms: contact order, chain topology, stability, and the extended nucleus mechanism Proc Natl Acad Sci U S A 97, 1525-1529.

Fink, A.L. (1999). Chaperone-mediated protein folding. Physiol Rev 79, 425-449.

Flom, G., Behal, R.H., Rosen, L., Cole, D.G., and Johnson, J.L. (2007). Definition of the minimal fragments of Sti1 required for dimerization, interaction with Hsp70 and Hsp90 and in vivo functions. Biochem J 404, 158-167.

Flom, G., Weekes, J., and Johnson, J.L. (2005). Novel interaction of the Hsp90 chaperone machine with Ssl2, an essential DNA helicase in Saccharomyces cerevisiae. Curr Genet 47, 368-380.

Flom, G., Weekes, J., Williams, J.J., and Johnson, J.L. (2006). Effect of mutation of the tetratricopeptide repeat and asparatate-proline 2 domains of Sti1 on Hsp90 signaling and interaction in Saccharomyces cerevisiae. Genetics 172, 41-51.

Flower, A.M. (2007). The SecY translocation complex: convergence of genetics and structure. Trends Microbiol 15, 203-210.

Fontes, M.R., Teh, T., and Kobe, B. (2000). Structural basis of recognition of monopartite and bipartite nuclear localization sequences by mammalian importin-alpha. J Mol Biol 297, 1183-1194.

Fontes, M.R., Teh, T., Riell, R.D., Parkd, S.B., Standaert, R.F., and Kobe, B. (2005). Crystallization and preliminary X-ray diffraction analysis of importin-α complexed with NLS peptidomimetics. Biochim Biophys Acta 1750, 9-13.

Fontes, M.R., Teh, T., Toth, G., John, A., Pavo, I., Jans, D.A., and Kobe, B. (2003). Role of flanking sequences and phosphorylation in the recognition of the simian-virus-40 large T-antigen nuclear localization sequences by importin-α. Biochem J 375, 339-349.

Forsythe, H.L., Jarvis, J.L., Turner, J.W., Elmore, L.W., and Holt, S.E. (2001). Stable association of Hsp90 and p23, but not Hsp70, with active human telomerase. J Biol Chem 276, 15571-15574.

Fostinis, Y., Theodropoulos, P.A., Gravanis, A., and Stournaras, C. (1992). Heat shock protein HSP90 and its association with the cytoskeleton:a morphological study. Biochem Cell Biol 70:779–786. Biochem Cell Biol 70, 779-786.

Fournier, H.-N., Dupe-Manet, S., Bouvard, D., Luton, F., Degani, S., Block, M.R., Retta, S.F., and Albiges-Rizo, C. (2005). Nuclear translocation of integrin cytoplasmic domain associated protein 1 stimulates cellular proliferation. Mol Biol Cell 16, 1859-1871.

Freeman, B.C., Myers, M.P., Schumacher, R., and Morimoto, R.I. (1998). Identification of a regulatory motif in Hsp 70 that affects ATPase activity, substrate binding and interaction with HDJ-1. EMBO J 14, 2281-2292.

Friedrich, B., Quensel, C., Sommer, T., Hartmann, E., and Köhler, M. (2006). Nuclear localization signal and protein context mediate importin α specificity of nuclear import substrates. Mol Cell Biol 26, 8697-8709.

Frydman, J. (2001). Folding of newly translated proteins in vivo: the role of molecular chaperones. Annu Rev Biochem 70, 603-647.

Fujihara, S., and Nadler, S.G. (1999). Intranuclear targeted delivery of functional NF-kB by 70 kDa heat shock protein EMBO J 18, 411-419.

Galigniana, M.D., Harrell, J.M., O'Hagen, H.M., Ljungman, M., and Pratt, W.B. (2004). Hsp90-binding immunophilins link p53 to dynein during p53 transport to the nucleus. J Biol Chem 279, 22483-22489.

Galigniana, M.D., Housley, P.R., DeFranco, D.B., and Pratt, W.B. (1999). Inhibition of glucocorticoid receptor nucleocytoplasmic shuttling by okadaic acid requires intact cytoskeleton. J Biol Chem 274, 16222-16227.

Garnier, C., Lafitte, D., Jorgensen, T.J., Jensen, O.N., Briand, C., and Peyrot, V. (2001). Phosphorylation and oligomerization states of native pig brain HSP90 studied by mass spectrometry. Eur J Biochem 268, 2402-2407.

Gebauer, M., Melki, R., and Gehring, U. (1998). The chaperone cofactor hop/p60 interacts with the cytosolic chaperonin-containing TCP-1 and affects its nucleotide exchange and protein folding activities. J Biol Chem 273, 29475-29480.

Geum, D., Son, G.H., and Kim, K. (2002). Phosphorylation-dependent cellular localization and thermoprotective role of heat shock protein 25 in hippocampal progenitor cells. J Biol Chem 277, 19913-19921.

Gidalevitz, T., Ben-Zvi, A.P., Ho, K.H., Brignull, H.R., and Morimoto, R.I. (2006). Progressive disruption of cellular protein folding in models of polyglutamine diseases. Science 311, 1471-1474.

Glover, J.R., and Lindquist, S. (1998). Hsp104, Hsp70, and Hsp40: a novel chaperone system that rescues previously aggregated proteins. Cell 94, 73-82.

Gragerov, A.I., Martin, E.S., Krupenko, M.A., Kashlev, M.V., and Nikiforov, V.G. (1991). Protein aggregation and inclusion body formation in Escherichia coli rpoH mutant defective in heat shock protein induction. FEBS Lett 291, 222-224.

Guiochon-Mantel, A., Delabre, K., Lescop, P., and Milgrom, E. (1996). Intracellular traffic of steroid hormone receptors. J Steroid Biochem Mol Biol 56, 3-9.

Harreman, M.T., Kline, T.M., Milford, H.G., Harben, M.B., Hodel, A.E., and Corbett, A.H. (2004). Regulation of nuclear import by phosphorylation adjacent to nuclear localization signals. J Biol Chem 279, 20613-20621.

Harris, S.F., Shiau, A.K., and Agard, D.A. (2004). The crystal structure of the carboxy-terminal dimerization domain of htpG, the Escherichia coli Hsp90, reveals a potential substrate binding site. Structure 12, 1087-1097.

Harst, A., Hongying, L., and Obermann, M.J. (2005). Aha1 competes with hop, p50 and p23 for binding to the molecular chaperone hsp90 and contributes to kinase and hormone receptor activation. Biochem J 387, 789-796.

Hartl, F.U. (1996). Molecular chaperones in protein folding. Nature 381, 571-580.

Hartl, F.U., and Hayer-Hartl, M. (2002). Molecular chaperones in the cytosol: from nascent chain to folded protein. Science 295, 1852-1858.

Helmbrecht, K., Zeise, E., and Rensing, L. (2000). Chaperones in cell cycle regulation and mitogenic signal transduction: a review. Cell Prolif 33, 341-365.

Henderson, B.R., and Fagotto, F. (2002). The ins and outs of APC and β-catenin nuclear transport. EMBO Rep 3, 834-839.

Hennessy, F., Nicoll, W.S., Zimmermann, R., Cheetham, M.E., and Blatch, G.L. (2005). Not all J domains are created equal: Implications for the specificity of Hsp40–Hsp70 interactions. Protein Sci 14, 1697-1709.

Hernandez, M.P., Sullivan, W.P., and Toft, D.O. (2002). The assembly and intermolecular properties of the hsp70-Hop-hsp90 molecular chaperone complex. J Biol Chem 277, 38294-38304.

Hohfeld, J. (1998). Regulation of the heat shock cognate Hsc 70 in the mammalian cell: The characterization of the anti-apoptotic protein BAG-1 provides novel insights (Review) 379, 269-274.

Hong, Y., Rogers, R., Matunis, M.J., Mayhew, C.N., Goodson, M., Park-Sarge, O.-K., and Sarge, K.D. (2001). Regulation of Heat Shock Transcription Factor 1 by Stress-induced SUMO-1 Modification. J Biol Chem 276, 40263-40267.

Honoré, B., Leffers, H., Madsen, P., Rasmussen, H.H., Vandekerckhove, J., and Celis, J.E. (1992). Molecular cloning and expression of a transformation-sensitive human protein containing the TRP motif and sharing identity to the stress-inducible yeast protein STI1. J Biol Chem 267, 8485–8491.

Hoogenraad, N.J., Ward, L.A., and Ryan, M.T. (2002). Import and assembly of proteins into mitochondria of mammalian cells. Biochim Biophys Acta 1592, 97-105.

Horwich, A. (2002). Protein aggregation in disease: a role for folding intermediates forming specific multimeric interactions. J Clin Invest 110, 1221-1232.

Huyer, G., Liu, S., Kelly, J., Moffat, J., Payette, P., Kennedy, B., Tsaprailis, G., Gresser, M.J., and Ramachandran, C. (1996). Mechanism of inhibition of protein-tyrosine phosphatases by vanadate and pervanadate. J Biol Chem 272, 843-851.

Iida, K., Matsumoto, S., and Yahara, I. (1992). The KKRKKSequence is Involved in Heat Shock-Induced Nuclear Translocation of the 18-kDa Actin-Binding Protein, Cofilin. Cell Struct Func 17, 39-46.

Inoue, A., Torigoe, T., Sogahata, K., Kamiguchi, K., Takahashi, S., Sawada, Y., Saijo, M., Taya, Y., Ishii, S., Sato, N., and Kikuchi, K. (1995). 70-kDa Heat shock cognate protein interacts directly with the N-terminal region of the retinoblastoma gene product pRB. Am Soc Biochem Mol Biol 270, 22571-22576.

Jacquier-Sarlin, M.R., Fuller, K., Dinh-Xuan, A.T., Richard, M.J., and Polla, B.S. (1994). Protective effects of hsp70 in inflammation. Experientia 50, 1031-1038.

Jana, N.R., Tanaka, M., Wang, G.-U., and Nukina, N. (2000). Polyglutamine length-dependent interaction of Hsp40 and Hsp70 family chaperones with N-terminal huntingtin: their role in suppression of aggregation and cellular toxicity. Human Mol Gen 9, 2009-2018.

Jans, D.A., and Hubner, S. (1996). Regulation of protein transport to the nucleus: central role of phosphorylation. Physiol Rev 76, 651-685.

Jansen, C., M., H., Tommassen, J., and de Cock, H. (2000). The assembly pathway of outer membrane protein PhoE of Escherichia coli. Eur J Biochem 267, 3792-3800.

Jin, P., Hardy, S., and Morgan, D.O. (1998). Nuclear localization of cyclin B1 controls mitotic entry after DNA damage. J Cell Biol 141, 875-885.

Johnson, B.D., Schumacher, R.J., Ross, E.D., and Toft, D.O. (1998). Hop modulates Hsp70/Hsp90 interactions in protein folding. J Biol Chem 273, 3679-3686.

Johnson, J.L., Halas, A., and Flom, G. (2007). Nucleotide-dependent interaction of Saccharomyces cerevisiae Hsp90 with the cochaperone proteins Sti1, Cpr6, and Sba1. Mol Cell Biol 27, 768-776.

Kaffman, A., and O'Shea, E.K. (1999). Regulation of nuclear localization: a key to a door. Annu Rev Cell Dev Biol 15, 291-339.

Kanelakis, K.C., Shewach, D.S., and Pratt, W.B. (2002). Nucleotide binding states of hsp70 and hsp90 during sequential steps in the process of glucocorticoid receptor·hsp90 heterocomplex assembly J Biol Chem 277, 33698-33703.

Kao, H.P., Abney, J.R., and Verkman, A.S. (1993). Determinants of the translational mobility of a small solute in cell cytoplasm. J Cell Biol 1993, 175-184.

Karasuyama, H., and Melchers, F. (1988). Establishment of mouse cells which constitutively secrete large quantities of interleukin 2, 3, 4, or 5, using modified cDNA expression vectors. Eur J Immunol 18, 97-104.

Kato, M. (2005). An overview of the CCAAT-box binding factor in filamentous fungi: assembly, nuclear translocation and transcriptional enhancement. Biosci Biotechnol Biochem 69, 663-672.

Kehlenbach, R.H., and Gerace, L. (2000). Phosphorylation of the nuclear transport machinery down-regulates nuclear protein import in vitro. J Biol Chem 275, 17848-17856.

Khandijan, E.W. (1995). Heat treatment induces dephosphorylation of pRb and dissociation of T-antigen pRb complex during transforming infection withSV40. oncogene 10, 359–367.

Khokhlatchev, A.V., Canagarajah, B., Wilsbacher, J., Robinson, M., Atkinson, M., and al., e. (1998). Phosphorylation of the MAP kinase ERK2 promotes its homodimerization and nuclear translocation. Cell 93, 605-615.

Kiang, J.G., and Tsokos, G.C. (1998). Heat Shock Protein 70 kDa: molecular biology, biochemistry, and physiology. Pharmacol Ther 80, 183-201.

King, K.L., and Cidlowski, J.A. (1998). Cell cycle regulation and apoptosis. Annu Rev Physiol 60, 601-617.

Klucken, J., Shin, Y., Masliah, E., Hyman, B.T., and McLean, P.J. (2004). Hsp70 reduces α-Synuclein aggregation and toxicity. J Biol Chem 279, 25497-25502.

Kobe, B. (1999). Autoinhibition by an internal nuclear localization signal revealed by the crystal structure of mammalian importin alpha. Nat Struct Biol 6, 388-397.

Köhler, M., Speck, C., Christiansen, M., Bischoff, F.R., Prehn, S., Haller, H., Görlich, D., and Hartmann, E. (1999). Evidence for distinct substrate specificities of importin α family members in nuclear protein import. Mol Cell Biol 19, 7782-7791.

Kohn, K.W. (1999). Molecular interaction map of the mammalian cell cycle control and DNA repair systems. Mol Biol Cell 10, 2703-2734.

Kong, M., Barnes, E.A., Ollendorff, V., and Donoghue, D.J. (2000). Cyclin F regulates the nuclear localization of cyclin B1 through a cyclin–cyclin interaction EMBO J 19, 1378-1388.

Kosano, H., Stensgard, B., Charlesworth, M.C., McMahon, N., and Toft, D. (1998). The assembly of progesterone receptor-Hsp90 complexes using purified proteins. J Biol Chem 273, 32973-32979.

Kovarova, H., Hajduch, M., Livingstone, M., Dzubak, P., and Lefkovits, I. (2003). Analysis of state-specific phosphorylation of proteins by two-dimensional gel electrophoresis approach. J Chromatogr B Analyt Technol Biomed Life Sci 787, 53-61.

Krebber, H., and Silver, P.A. (2000). Directing proteins to nucleus by fusion to nuclear localization signal tags.

Kudo, N., Matsumori, N., Taoka, H., Fujiwara, D., Schreiner, E.P., Wolff, B., Yoshida, M., and Horinouchi, S. (1999). Leptomycin B inactivates CRM1/exportin 1 by covalent modification at a cysteine residue in the central conserved region. Proc Natl Acad Sci U S A 96, 9112-9117.

Kuhl, N.M., and Rensing, L. (2000). Heat shock effects on cell cycle progression. Cell Mol Life Sci 57, 450-463.

LaBaer, J., Garrett, M.D., Stevenson, L.F., Slingerland, J.M., Sandhu, C., Chou, H.S., Fattaey, A., and Harlow, E. (1997). New functional activities for the p21 family of CDK inhibitors. Genes Dev 11, 847-862.

Laemmli, U.K. (1970). Cleavage of structural proteins during the assembly of the head of bacteriophage T4. Nature 227, 680-685.

Lange, A., Mills, R.E., Lange, C.J., Stewart, M., Devine, S.E., and Corbett, A.H. (2007). Classical Nuclear Localization signals: definition, function, and interaction with importin α. J Biol Chem 282, 5101-5105.

Langer, T., Rosmus, S., and Fasold, H. (2003). Intracellular localization of the 90 kDA heat shock protein (HSP90alpha) determined by expression of a EGFP-HSP90 alpha-fusion protein in unstressed and heat stressed 3T3 cells. Cell Biol Int 27, 47-52.

Lässle, M., Blatch, G.L., Kundra, V., Takatori, T., and Zetter, B.R. (1997). Stress-inducible, murine protein mSTI1. Characterization of binding domains for heat shock proteins and in vitro phosphorylation by different kinases. J Biol Chem 272, 1876-1884.

Lazar, S.W., and Kolter, R. (1996). SurA assists the folding of Escherichia coli outer membrane proteins. J Bacteriol 178, 1770-1773.

Lee, K.-H., Lee, C.-T., Kim, Y.W., Han, S.K., Shim, Y.-S., and Yoo, C.-G. (2005). Preheating accelerates mitogen-activated protein (MAP) kinase inactivation post-heat shock via a heat shock protein 70-mediated increase in phosphorylated MAP kinase phosphatase-1. J Biol Chem 280, 13179-13186.

Lee, P., Shabbir, A., Cardozo, C., and Caplan, A.J. (2004). Sti1 and cdc37 can stabilize hsp90 in chaperone complexes with a protein kinase. Mol Biol Cell 15, 1785-1792.

Lees-Miller, S.P., and Anderson, C.W. (1989). Two human 90-kDa heat shock proteins are phosphorylated in vivo at conserved serines that are phosphorylated in vitro by casein kinase II. J Biol Chem 264, 2431-2437.

Lei, H., Venkatakrishnan, A., Yu, S., and Kazlauskas, A. (2007). Protein Kinase A-dependent Translocation of Hsp90a Impairs Endothelial Nitric-oxide Synthase Activity in High Glucose and Diabetes. J Biol Chem 282, 9364-9371.

Li, S., Ku, C.-Y., Farmer, A.A., Cong, Y.-S., Chen, C.-F., and Lee, W.-H. (1999). Identification of a novel cytoplasmic protein that specifically binds to nuclear localization signal motifs. J Biol Chem 273, 6183-6189.

Liang, S.-H., and Clarke, M.F. (1999a). A bipartite nuclear localization signal is required for p53 nuclear import regulated by a carboxy-terminal domain. J Biol Chem 274, 32699-32703.

Liang, S.-H., and Clarke, M.F. (1999b). The nuclear import of p53 is determined by the presence of a basic domain and its relative position to the nuclear localization signal. Oncogene 18, 2163-2166.

Lindquist, S., and Craig, E.A. (1988). The heat shock proteins. Annu Rev Genet 22, 631-667.

Longshaw, V.M. (2002). The phosphorylation and nuclear localization of the co-chaperone murine stress-inducible protein 1, Rhodes University, Grahamstown.

Longshaw, V.M., Chapple, J.P., Balda, M.S., Cheetham, M.E., and Blatch, G.L. (2004). Nuclear translocation of the Hsp70/Hsp90 organizing protein mSTI1 is regulated by cell cycle kinases. J Cell Sci 117, 701-710.

Longshaw, V.M., Dirr, H.W., Blatch, G.L., and Lässle, M. (2000). The in vitro phosphorylation of the co-chaperone mSTI1 by cell cycle kinases substantiates a predicted casein kinase II-p34cdc2-NLS (CcN) motif. Biol Chem 381, 1133-1138.

Martins, V.R., Mercadante, A.F., Cabral, A.L.B., Freitas, A.R.O., and Castro, R.M. (2001). Insights into the physiological function of cellular prion protein. Braz J Med Biol Res 34, 585-595.

Mattaj, I.W., and Englmeier, L. (1998). Nucleocytoplasmic transport: the soluble phase. Annu Rev Biochem 67, 265-306.

McLaughlin, S.H., and Jackson, S. (2002). Folding and stability of the ligand-binding domain of the glucocorticoid receptor. Protein Sci 11, 1926-1936.

McLaughlin, S.H., Smith, H.W., and Jackson, S.E. (2002). Stimulation of the weak ATPase activity of human hsp90 by a client protein. J Mol Biol 315, 787-798.

McLaughlin, S.H., Sobott, F., Yao, Z., Zhang, W., Nielsen, P.R., Grossmann, J.G., Laue, E.D., Robinson, C.V., and Jackson, S.E. (2006). The Co-chaperone p23 Arrests the Hsp90 ATPase Cycle to Trap Client Proteins. J Mol Biol 356, 746-758.

McLaughlin, S.H., Ventouras, L.-A., Lobbezoo, B., and Jackson, S.E. (2004). Independent ATPase activity of Hsp90 subunits creates a flexible assembly platform. J Mol Biol 344, 813-826.

Mestril, R., Chi, S.H., Sayen, M.R., O'Reilly, K., and Dillmann, W.H. (1994). Expression of inducible stress protein 70 in rat heart myogenic cells confers protection against stimulated ischemia-induced injury. J Clin Invest 93, 759-767.

Meyer, P., Prodromou, C., Hu, B., Vaughan, C., Roe, S.M., Panaretou, B., Piper, P.W., and Pearl, L.H. (2003). Structural and functional analysis of the middle segment of hsp90: implications for ATP hydrolysis and client protein and cochaperone interactions. Mol Cell 11, 647-658.

Michael, W.M., Choi, M., and Dreyfuss, G. (1995). A nuclear export signal in hnRNP Al: a signal-mediated, temperature-dependent nuclear protein export pathway. Cell 83, 415-422.

Michael, W.M., Eder, P.S., and Dreyfuss, G. (1997). The K nuclear shuttling domain: a novel signal for nuclear import and nuclear export in the hnRNP K protein. EMBO J 16, 3587-3598.

Miyata, Y., and Yahara, I. (1992). The 90-kDa heat shock protein, HSP90, binds and protects casein kinase II from self-aggregation and enhances its kinase activity. J Biol Chem 267, 7042-7047.

Moll, T., Tebb, G., Surana, U., Robitsch, H., and Nasmyth, K. (1991). The role of phosphorylation and the CDC28 protein kinase in cell cycle regulated nuclear import of the S. cerevisiae transcription factor SWI5. Cell 66, 743-758.

Moreno, S., and Nurse, P. (1990). Substrates for p34cdc2. In vivo Veritas? Cell 61, 549-551.

Morishima, Y., Kanelakis, K.C., Silverstein, A.M., Dittmar, K.D., Estrada, L., and Pratt, W.B. (2000). The hsp organizer protein hop enhances the rate of but is not essential for glucocorticoid receptor folding by the multiprotein Hsp90-based chaperone system. J Biol Chem 275, 6894-6900.

Moroianu, J., Blobel, G., and Radu, A. (1995). Previously identified protein of uncertain function is karypherin α and together with karyopherin β docks import substrate at nuclear pore complexes. Proc Natl Acad Sci U SA 92, 2008-2011.

Muesch, A., Hartmann, E., Rohde, K., Rubartelli, R., Sitia, R., and Rapoport, T.A. (1990). A novel pathway for secretory proteins? . Trends Biochem Sci 15, 86-88.

Mulner-Lorillon, O., Cormier, P., Labbe, J.C., Doree, M., Poulhe, R., Osborne, H., and Belle, R. (1990). M-phase-specific cdc2 protein kinase phosphorylates the b subunit of casein kinase II and increases casein kinase II activity. Eur J Biochem 193, 529-534.

Multhoff, G., Botzler, C., and Issels, R. (1998). The role of the heat shock proteins in the stimulation of an immune response. Biol Chem 379, 295-300.

Munoz, M.J., and Jimenez, J. (1999). Genetic interactions between Hsp 90 and the Cdc2 mitotic machinery in the fission yeast Schizosaccharomyces pombe. Mol Gen Genet 261, 242-250.

Murphy, P.J., Kanelakis, K.C., Galigniana, M.D., Morishima, Y., and Pratt, W.B. (2001). Stoichiometry, abundance, and functional significance of the hsp90/hsp70-based multiprotein chaperone machinery in reticulocyte lysate. J Biol Chem 276, 30092-30098.

Nair, S.C., Toran, E.J., Rimerman, R.A., Hjermstad, S., Smithgall, T.E., and Smith, D.F. (1996). A pathway of multi-chaperone interactions common to diverse regulatory proteins: estrogen receptor, Fes tyrosine kinase, heat shock transcription factor Hsf1, and the aryl hydrocarbon receptor. Cell Stress Chap 1, 237-250.

Nakamura, S., Tatuno, I., Noguchi, Y., Kitagawa, M., Kohn, L.D., Saito, Y., and Hirai, A. (1999). 73-kDa Heat shock cognate protein interacts directly with $P27^{Kip1}$, a cyclin-dependent kinase inhibitor, during G1/S transition. Biochem Biophys Res Commun 257, 340-343.

Nicolet, C.M., and Craig, E.A. (1989). Isolation and characterization of STI1, a stress-inducible gene from Saccharomyces cerevisiae. Mol Cell Biol 9, 3638-3646.

Nollen, E.A., Salomons, F.A., Brunsting, J.F., Want, J.J., Sibon, O.C., and Kampinga, H.H. (2001). Dynamic changes in the localization of thermally unfolded nuclear proteins associated with chaperone-dependent protection. Proc Natl Acad Sci U SA 98, 12038-12043.

Nylandsted, J., Rohde, M., Brand, K., Bastholm, L., Elling, F., and Jäättelä, M. (2000). Selective depletion of heat shock protein 70 (Hsp70) activates a tumor-specific death program that is independent of caspases and bypasses Bcl-2. . Proc Natl Acad Sci U S A 97, 7871-7876.

Odunuga, O.O., Hornby, J.A., Bies, C., Zimmermann, R., Pugh, D.J., and Blatch, G.L. (2003). Tetratricopeptide repeat motif-mediated Hsc70-mSTI1 interaction. Molecular characterization of the critical contacts for successful binding and specificity. J Biol Chem 278, 6896-6904.

Odunuga, O.O., Longshaw, V.M., and Blatch, G.L. (2004). Hop: more than an Hsp70/Hsp90 adaptor protein. Bioessays 26, 1058-1068.

Osborne, A.R., Rapoport, T.A., and Berg, v.d.B. (2005). Protein translocation by the sec61/secY channel. Annu Rev Cell Dev Biol 21, 529-550.

Palleros, D.R., Welch, W.J., and Fink, A.L. (1991). Interaction of hsp 70 with unfolded proteins: effects of temperature and nucleotides on the kinetics of binding. Proc Natl Acad Sci USA 88, 5719-5723.

Panaretou, B., Prodromou, C., Roe, S.M., O'Brien, R., Ladbury, J.E., Piper, P.W., and Pearl, L.H. (1998). ATP binding and hydrolysis are essential to the function of the Hsp90 molecular chaperone in vivo. EMBO J 17, 4829-4836.

Panaretou, B., Siligardi, G., Meyer, P., Maloney, A., Sullivan, J.K., Singh, S., Millson, S.H., Clarke, P.A., Naaby-Hansen, S., Stein, R., Cramer, R., Mollapour, M., Workman, P., Piper, P.W., Pearl, L.H., and Prodromou, C. (2002). Activation of the ATPase activity of hsp90 by the stress-regulated cochaperone aha1. Mol Cell 10, 1307-1318.

Pauwels, K., Molle, V.I., Tommassen, J., and Gelder, V.P. (2007). Chaperoning Anfisen: the steric foldases. Mol Microbiol 64, 917-922.

Pearl, L.H., and Prodromou, C. (2006). Structure and mechanism of the Hsp90 molecular chaperone machinery. Annu Rev Biochem 75, 271-294.

Perdew, G.H., Hord, N., Hollenback, C.E., and Welsh, M.J. (1993). Localization and characterization of the 86- and 84-kDa heat shock proteins in Hepa 1c1c7 cells. Exp Cell Res 209, 350-356.

Picard, D., Khursheed, B., Garabedian, M.J., Fortin, M.G., Lindquist, S., and Yamamoto, K.R. (1990). Reduced levels of Hsp90 compromise steroid-receptor action in vivo. Nature 346, 166-168.

Pirkkala, L., Nykanen, P., and Sistonen, L. (2001). Roles of the heat shock transcription factors in regulation of the heat shock response and beyond. FASEB J 15, 1118-1131.

Pockley, A.G. (2003). Heat shock proteins as regulators of the immune response. Lancet 362, 469-476.

Polla, B.S., Bachelet, M., Elia, G., and Santoro, M.G. (1998). Stress proteins in inflammation. Annu NY Acad Sci 851, 75-85.

Porter, L.A., and Donoghue, D.J. (2003). Cyclin B1 and CDK1: nuclear localization and upstream regulators. In: Progress in Cell Cycle Research, vol. 5, eds. L. Meijer, A. Jézéquel, and M. Roberge, California, 335-347.

Prapapanich, V., Chen, S., and Smith, D.F. (1998). 6Mutation of Hip's carboxy-terminal region inhibits a transitional stage of progesterone receptor assembly. Mol Cell Biol 1998; 18:944-952. Mol Cell Biol 18, 944-952.

Pratt, W.B. (1993). The role of heat shock proteins in regulating the function, folding, and trafficking of the glucocorticoid receptor. J Biol Chem 268, 21455-21458.

Pratt, W.B. (1997). The role of the hsp90-based chaperone system in signal transduction by nuclear receptors and receptors signaling via MAP kinase. Annu Rev Pharmacol Toxicol 37, 297-326.

Pratt, W.B., and Toft, D.O. (1997). Steroid receptor interactions with heat shock protein and immunophilin chaperones. Endocr Rev 18, 306-360.

Pratt, W.B., and Toft, D.O. (2003). Regulation of signaling protein function and trafficking by the hsp90/hsp70-based chaperone machinery. Exp Biol Med (Maywood) 228, 111-133.

Pratt, W.B., Galigniana, M.D., Harrell, J.M., and DeFranco, D.B. (2004a). Role of hsp90 and the hsp90-binding immunophilins in signalling protein movement. Cell Signal 16, 857-872.

Pratt, W.B., Galigniana, M.D., Morishima, Y., and Murphy, P.J. (2004b). Role of molecular chaperones in steroid receptor action. Essays Biochem 40, 41-58.

Pratt, W.B., Krishna, P., and Olsen, J.J. (2001). Hsp 90-binding immunophilins in plants: the protein movers. Trends Plant Sci 6, 54-58.

Pratt, W.B., Silverstein, A.M., and Galigniana, M.D. (1999). A model for the cytoplasmic trafficking of signalling proteins involving the hsp90-binding immunophilins and p50cdc37. Cell Signal 11, 839-851.

Prodromou, C., Roe, S.M., O'Brien, R., Ladbury, J.E., Piper, P.W., and Pearl, L.H. (1997). Identification and structural characterization of the ATP/ADP-binding site in the Hsp90 molecular chaperone. Cell 90, 65-75.

Prodromou, C., Siligardi, G., O'Brien, R., Woolfson, D.N., Regan, L., Panaretou, B., Ladbury, J.E., Piper, P.W., and Pearl, L.H. (1999). Regulation of Hsp90 ATPase activity by tetratricopeptide repeat (TPR)-domain co-chaperones. EMBO J 18, 754-762.

Pyerin, W. (1994). Human casein kinase II: structures, genes, expression and requirement in cell growth stimulation. Advn Enzym Regul 34, 225-246.

Radford, S.E., and Dobson, C.M. (1999). From computer simulations to human disease: emerging themes in protein folding. Cell 97, 291-298.

Ramsey, A.J., Russel, L.C., Whitt, S.R., and Chinkers, M. (2000). Overlapping sites of tetratricopeptide repeat protein binding and chaperone activity in heat shock protein 90. J Biol Chem 275, 17857-17862.

Richter, K., Muschler, P., Hainzl, O., Reinstein, J., and Buchner, J. (2003). Sti1 is a non-competitive inhibitor of the Hsp90 ATPase. Binding prevents the N-terminal dimerization reaction during the ATPase cycle. J Biol Chem 278, 10328-10333.

Roberts, B., Richardson, W.D., and Smith, A.E. (1997). The effect of protein context on nuclear location signal function. Cell 50, 465-475.

Rohde, M., Daugaard, M., Jensen, M.H., Helin, K., Nylandsted, J., and Jäättelä, M. (2005). Members of the heat-shock protein 70 family promote cancer cell growth by distinct mechanisms. Genes Dev. 19: 570–582. Genes Dev 19, 570-582.

Rosin-Arbesfeld, R., Cliffe, A., Brabletz, T., and Bienz, M. (2003). Nuclear export of the APC tumour suppressor controls -catenin function in transcription EMBO J 22, 1101-1113.

Rosser, M.F.N., and Cyr, D. (2006). Do Hsp40's act as chaperones or co-chaperones? In: Networking of chaperones by co-chaperones, ed. G.L. Blatch, Texas: Landes Bioscience; New York: Springer Science + Business Media, 38-51.

Rouse, J., Cohen, P., Trigon, S., Morange, M., and Alonso-Llamazares, A. (1994). A novel kinase cascade triggered by chemical stress and heat shock which stimulates MAP kinase-activated protein kinase-2 and phosphorylation of the small heat shock proteins. Cell 78, 1027-1037.

Rudiger, S., Buchberger, A., and Bukau, B. (1997). Interaction of Hsp 70 chaperone with substrates. Nat Struct Biol 4, 342-349.

Sabio, G., Arthur, J.S.C., Kuma, Y., Peggie, M., Carr, J., Murray-Tait, V., Centeno, F., Goedert, M., Morrice, N.A., and Cuenda, A. (2005). p38g regulates the localisation of SAP97 in the cytoskeleton by modulating its interaction with GKAP. EMBO J 24, 1134-1145.

Sanchez, E.R., Redmond, T., Scherrer, L.C., Bresnick, E.H., Welsh, M.J., and Pratt, W.B. (1988). Evidence that the 90-kilodalton heat shock protein is associated with tubulin-containing complexes in L cell cytosol and in intact PtK cells. Mol Endocrinol 2, 756-760.

Santoro, M.G. (2000). Heat shock factors and the control of the stress response. Biochem Pharmacol 59, 55-63.

Schafer, K.A. (1998). The cell cycle: a review. Vet Path 35, 461-478.

Scheufler, C., Brinker, A., Bourenkov, G., Pegoraro, S., Moroder, L., Bartunik, H., Hartl, F.U., and Moarefi, I. (2000). Structure of TPR domain-peptide complexes: critical elements in the assembly of the Hsp70-Hsp90 multichaperone machine. Cell 101, 199-210.

Schiene, C., and Fischer, G. (2000). Enzymes that catalyse the restructuring of proteins. Curr Opin Struct Biol 10, 40-45.

Schüchner, S., Tembe, V., Rodriguez, J.A., and Hendersen, B.R. (2005). Nuclear Targeting and Cell Cycle Regulatory Function of Human BARD1. J Biol Chem 280, 8855-8861.

Sheilds, D. (2001). Gunter Blobel - still passionate after all these years. Trends Cell Biol 11, 349-350.

Sherman, M.Y., and Goldberg, A.L. (1993). Heat shock of Escherichia coli increases binding of dnaK (the hsp70 homolog) to polypeptides by promoting its phosphorylation. Proc Natl Acad Sci U S A 90, 8648-8652.

Shi, Y., Mosser, D.D., and Morimoto, R.I. (1998). Molecular chaperones as HSF1-specific transcriptional repressors. Genes Dev 12, 654-666.

Shieh, M.W., Wesser, S.R., and Raikhel, N.V. (1993). Nuclear targeting of the maize R protein requires two nuclear localization sequences. Plant Physiol. 101, pp. 353 – 361. Plant Physiol 101, 353-361.

Siligardi, G., Panaretou, B., Meyer, P., Singh, S., Woolfson, D.N., Piper, P.W., Pearl, L.H., and Prodromou, C. (2002). Regulation of Hsp90 ATPase activity by the co-chaperone Cdc37p/p50cdc37. J Biol Chem 277, 20151-20159.

Simon, S.M., and Blobel, G. (1991). A protein-conducting channel in the endoplasmic reticulum. Cell 65, 371-380.

Smith, D.F. (2000). Chaperones in progesterone receptor complexes. Semin Cell Dev Biol 11, 45-52.

Smith, D.F., Sullivan, W.P., Marion, T.N., Zaitsu, K., Madden, B., McCormick, D.J., and Toft, D.O. (1993). Identification of a 60-kilodalton stress-related protein, p60, which interacts with hsp90 and hsp70. Mol Cell Biol 13, 869-876.

Smith, D.F., Whitesell, L., and Katsanis, E. (1998). Molecular chaperones: biology and prospects for pharmacological intervention. Pharm Rev 50, 493-514.

Somero, G.N. (1995). Proteins and temperature. Annu Rev Physiol 57, 43-68.

Song, Y., and Masison, D.C. (2005). Independent regulation of Hsp70 and Hsp90 chaperones by Hsp70/90 organizing protein STI1 (Hop1). J Biol Chem (in press) 2005; M505420200. J Biol Chem 280, 34178-34185.

Sørensen, J.G., Kristensen, T.N., and Loeschcke, V. (2003). The evolutionary and ecological role of heat shock proteins. Ecol Lett 6, 1025-1037.

Söti, C., Racz, A., and Csermely, P. (2002). A Nucleotide-dependent molecular switch controls ATP binding at the C-terminal domain of Hsp90. N-terminal nucleotide binding unmasks a C-terminal binding pocket. J Biol Chem 277, 7066-7075.

Söti, C., Radics, L., Yahara, I., and Csermely, P. (1998). Interaction of vanadate oligomers and permolybdate with the 90-kDa heat-shock protein, Hsp90. Eur J Biochem 255, 611-617.

Stebbins, C.E., Russo, A.A., Schneider, C., Rosen, N., Hartl, F.U., and Pavletich, N.P. (1997). Crystal Structure of an Hsp90–Geldanamycin Complex: Targeting of a Protein Chaperone by an Antitumor Agent. Cell 89, 239-250.

Steidl, S., Tüncher, A., Goda, H., Guder, C., Papadopoulou, N., Kobayashi, T., Tsukagoshi, N., Kato, M., and Brakhage, A.A. (2004). A single subunit of a heterotrimeric CCAAT-binding complex carries a nuclear localization signal: piggy back transport of the pre-assembled complex to the nucleus. J Mol Biol 342, 515-524.

Stommel, J.M., Marchenko, N.D., Jimenez, G.S., Moll, U.M., Hope, T.J., and Wahl, G.M. (1999). A leucine-rich nuclear export signal in the p53 tetramerization domain: regulation of subcellular localization and p53 activity by NES masking. EMBO J 18, 1660-1672.

Ström, A.C., and Weis, K. (2001). Importin-β-like nuclear transport receptors. Gene Biol 2, 3008.3001-3008.3009.

Sullivan, W., Stensgard, B., Caucutt, G., Bartha, B., McMahon, N., Alnemri, E.S., Litwack, G., and Toft, D. (1997). Nucleotides and two functional states of hsp90. J Biol Chem 272, 8007-8012.

Suntharalingam, M., and Wente, S.R. (2003). Peering through the Pore:Nuclear Pore Complex Structure, Assembly, and Function. Dev Cell 4, 775-789.

Takayama, S., Bimston, D.N., Matsuzawa, S., Freeman, B.C., Aime-Sempe, C., Xie, H., and Morimoto, R.I. (1997). BAG-1 modulates the chaperone activity of Hsp70/Hsc70. EMBO J 16, 4887-4896.

Tamm, L.K., Hong, H., and Liang, B. (2004). Folding and assembly of β-barrel membrane proteins. Biochim Biophys Acta 1666, 250-263.

Tavaria, M., Gabriele, T., Kola, I., and Anderson, R.L. (1996). A hitchhiker's guide to the human Hsp70 family. Cell Stress Chap 1, 23-28.

Thomas, P.J., Qu, B.H., and Pedersen, P.L. (1995). Defective protein folding as a basis of human disease. Trends Biochem Sci 20, 456-459.

Towbin, H., Staehelin, T., and Gordon, J. (1979). Electrophoretic transfer of proteins from polyacrylamide gels to nitrocellulose sheets: procedure and some applications. Proc Natl Acad Sci U S A 76, 4350-4354.

Tsukahara, F., and Maru, Y. (2004). Identification of novel nuclear export and nuclear localization signals in human heat shock cognate protein 70. J Biol Chem 279, 8867-8872.

Tutar, Y., Song, Y., and Masison, D.C. (2006). Primate chaperones Hsc70 (Constitutive) and Hsp70 (induced) differ functionally in supporting growth and prion propagation in Saccharomyces cerevisiae. Genetics 172, 851-861.

van der Spuy, J., Cheetham, M.E., Dirr, H.W., and Blatch, G.L. (2001). The cochaperone murine stress-inducible protein 1: overexpression, purification, and characterization. Protein Expr Purif 21, 462-469.

van der Spuy, J., Kana, B.D., Dirr, H.W., and Blatch, G.L. (2000). Heat shock cognate protein 70 chaperone-binding site in the co-chaperone murine stress-inducible protein 1 maps to within three consecutive tetratricopeptide repeat motifs. Biochem J 345 645-651.

Wada, A., Fukuda, M., Mishima, M., and Nishida, E. (1998). Nuclear export of actin: a novel mechanism regulating the subcellular localization of a major cytoskeletal protein. EMBO J 17, 1635–1641.

Wandinger, S.K., Suhre, M.H., Wegele, H., and Buchner, J. (2006). The phosphatase Ppt1 is a dedicated regulator of the molecular chaperone Hsp90. EMBO J 25, 367-376.

Webb, J.R., Campos-Neto, A., Skeiky, Y.A.W., and Reed, S.G. (1997). Molecular characterization of the heat-inducible LmSTI1 protein of Leishmania major. Mol Biochem Parasitol 89, 179-193.

Wegele, H., Haslbeck, M., Reinstein, J., and Buchner, J. (2003). Sti1 is a novel activator of the Ssa proteins. J Biol Chem 278, 25970-25976.

Welch, W.J., Garrels, J.L., Thomas, G.P., Lin, J.J., and Feramisco, J.R. (1983). Biochemical charecterisation of the mammalian stress proteins and identification of stress proteins as glucose and $Ca^{2+}$ ionophore-regulated proteins. J Biol Chem 258.

Williams, R.S., Thomas, J.A., Fina, M., German, Z., and Benjamin, I.J. (1993). Human heat shock protein 70 (hsp70) protects murine cells from injury during metabolic stress. J Clin Invest 92, 503-508.

Yang, J., and DeFranco, D.B. (1996). Assessment of glucocorticoid receptor heat shock protein 90 interactions in vivo during nucleocytoplasmic trafficking. Mol Endocrinol 10, 3-13.

Yang, J., Hebok, S., Walsh, S., Bardes, E.S.G., and Kornbluth, S. (2001). Combinatorial control of cyclin B1 nuclear trafficking through phosphorylation at multiple sites. J Biol Chem 276, 3604-3609.

Yasuhara, N., Takeda, E., Inoue, H., Kotera, I., and Yoneda, Y. (2004). Importin α/β-mediated nuclear protein import is regulated in a cell cycle-dependent manner. Exp Cell Res 297, 285-293.

Yoneda, Y. (1997). How proteins are transported from cytoplasm to the nucleus. J. Biochem 121, 811-817.

Yoneda, Y. (2000). Nucleocytoplasmic protein traffic and its signifcance to cell function. Genes Cell 5.

Yoshihiro, M., Kanelakis, K.C., Silverstein, A.M., Dittmar, K.D., Estrada, L., and Pratt, W.B. (1999). The Hsp organizer protein Hop enhances the rate of but is not essential for glucocorticoid receptor folding by the multiprotein Hsp 90-based chaperone system. J Biol Chem 275, 6894-6900.

Young, J.C., and Hartl, F.U. (2000). Polypeptide release by Hsp90 involves ATP hydrolysis and is enhanced by the co-chaperone p23. EMBO J 19, 5930-5940.

Young, J.C., Hoogenraad, N.J., and Hartl, F.U. (2003). Molecular chaperones Hsp90 and Hsp70 deliver Preproteins to the mitochondrial import receptor Tom70 Cell 112, 41-50.

Young, J.C., Moarefi, I., and Hartl, F.U. (2001). Hsp90: a specialized but essential protein-folding tool. J Cell Biol 154, 267-273.

Young, J.C., Obermann, W.M., and Hartl, F.U. (1998). Specific binding of tetratricopeptide repeat proteins to the C-terminal 12-kDa domain of hsp90. J Biol Chem 273, 18007-18010.

Zanata, S.M., Lopes, M.H., Mercadante, A.F., Hajj, G.N.M., Chiarini, L.B., Nomizo, R., Freitas, A.R.O., Cabral, A.L.B., Lee, K.S., Juliano, M.A., de Oliveira, E., Jachieri, S.G., Linden, R., Brentani, R.R., and Martins, V.R. (2002). Stress-inducible protein 1 is a cell surface ligand for cellular prion that triggers neuroprotecti. EMBO J 21, 3307-3316.

Zennadi, R., Hines, P.C., De Castro, L.M., Cartron, J.-P., Parise, L.V., and Telen, M.J. (2004). Epinephrine acts through erythroid signaling pathways to activate sickle cell adhesion to endothelium via LW-avb3 interactions. Blood 104, 3774-3781.

Zhang, F., White, R.L., and Neufeld, K.L. (2000). Phosphorylation near nuclear localization signal regulates nuclear import of adenomatous polyposis coli protein. Proc Natl Acad Sci U S A 97, 12577-12582.

Zhang, Z., Quick, M.K., Kanelakis, K.C., Gijzen, M., and Krishna, P. (2003). Characterization of a plant homolog of Hop, a cochaperone of Hsp90. Plant Physiol 131, 525-535.

Zhao, Y.G., Gilmore, R., Leone, G., Coffey, M.C., Weber, B., and Lee, P.W. (2001). Hsp90 phosphorylation is linked to its chaperoning function. Assembly of the reovirus cell attachment protein. J Biol Chem 276, 32822-32827.

Zheng, L., Roeder, R.G., and Luo, Y. (2003). S phase activation of the histone H2B promoter by OCA-S, a coactivator complex that contains GAPDH as a key component. Cell 114, 255-266.

Zhu, D., Dix, D.J., and Eddy, E.M. (1997). Hsp70 is required for cdc2 kinase activity at 37 degrees C and after heat shock. Development 124, 3007-3014.

Zimmermann, R., Muller, L., and Wullich, B. (2006). Protein transport into the endoplasmic reticulum: mechanisms and pathologies. Trends Mol Med 12, 567-573.

Zimmermann, S.B., and Minton, A.P. (1991). Estimation of macromolecule concentrations and excluded volume effects for the cytoplasm of Escherichia coli. J Mol Biol 222, 599-620.

Zou, J., Guo, Y., Guettouche, T., Smith, D.F., and Voellmy, R. (1998). HSF1 Activation by HSP90 (HSP90 complex) that forms a stress-sensitive complex with HSF1 Cell 94, 471-480.

# APPENDIX

## A1 Special Reagents and Chemicals

| Reagent | Supplier |
|---|---|
| 24 Magnet Plate | IBA BioTAGnology, Germany (Cat. No. 7-2006-000) |
| 2D Clean-Up Kit | Amersham Biosciences, USA (Cat. No. 80-6484-51) |
| 2D Quant Kit | Amersham Biosciences, USA (Cat. No. 80-6483-56) |
| Agarose | Sigma, USA |
| All reagents such as Ethanol, Methanol, Acetic acid | Chemistry Stores, Rhodes University |
| Aprotinin | Sigma, USA |
| BHK-21 (Baby Hamster Kidney) cells | Dr. Martin Ryan, University of St. Andrews, Scotland |
| BigDye V3.1 | ABI, USA |
| Bradford Reagent | Sigma-Aldrich Inc, USA |
| Bradford Reagent | Sigma Aldrich, USA |
| Carbon dioxide | Afrox, South Africa |
| DakoCytomation Fluorescent mounting medium | DakoCytomation, Denmark |
| Deoxyribonuclease I (Rnase free) | Fermentas Life Sciences, USA (Cat. No. EN0521) |
| Dithiothreitol (DTT) | Amersham Biosciences, USA |
| DNA Clean and Concentrator-5 | Zymo research, USA |
| Dulbecco's Modified Eagle Medium (DMEM) | Cambrex; USA |
| *Eag* I | Amersham Pharmacia Biotech |
| ECL Advance western blotting detection kit | Amersham Biosciences, UK |
| ECL anti-mouse $IgG_1$ horseradish peroxidase-linked species specific whole antibody (from sheep) | Amersham Biosciences, UK |
| Fetal calf serum | Highveld Biologicals PTY LTD. South Africa |
| Glutathione agarose | Sigma-Aldrich Inc, USA |
| High-range rainbow molecular weight | Amersham Biosciences, UK |

| | |
|---|---|
| markers | |
| *Hind* III | Amersham Pharmacia Biotech |
| Hybond-C extra supported nitrocellulose membrane | Amersham International, UK |
| IBAfect | IBA BioTAGnology, Germany (Cat. No. 7-2005-020) |
| IPTG | Promega Corporation, USA |
| MA Lipofection Enhancer | IBA BioTAGnology, Germany (Cat. No. 7-2003-020) |
| Mouse monoclonal anti-Hsp70 | StressGen, Canada |
| Mouse monoclonal anti-Hsp72/73 | StressGen, Canada |
| Mouse monoclonal anti-β-actin | Sigma, USA |
| N-hydroxy-succinimide and 1-ethyl-3 –[3-dimethylaminopropyl] carbodiimide (NHS/EDC) | BIACORE, Sweden |
| NIH 3T3 mouse fibroblast cells | Highveld Biologicals PTY LTD. South Africa |
| *Not* I | Amersham Pharmacia Biotech, USA |
| *Nsi* I | New England BioLabs Inc., UK |
| Okadeic acid | Sigma, USA |
| Penicillin/Streptomycin | Highveld Biologicals PTY LTD. South Africa |
| Peroxidase-conjugated AffiniPure F(ab')$_2$ fragment goat anti-human IgG$_1$ Fragment | Jackson ImmunoResearch Laboratories INC. USA (Cat. No. 109-036-097) |
| ProteoExtract® Subcellular Proteome Extraction Kit (S-PEK) | Calbiochem, USA |
| QIAprep Spin Miniprep kit | Qiagen, USA |
| Quickchange Site-Directed Mutagenesis kit | Stratagene, USA |
| Rat Liver Hsp90 | Purified by Csaba Soti (Hungary) |
| Rat monoclonal anti-Hsp90 | Sigma, USA |
| Recombinant antibodies against Hop | Morphosys® (Antibodies by Design) Germany. Final concentration used: 2 ug/mL |
| Sensor Chip CM5 (Research Grade) | BIACORE, Sweden |
| Shrimp alkaline phosphatase (SAP) | |
| Sodium orthovanadate | Sigma, USA |
| Supercompetent *E. coli* JM109 cells | Promega Corporation, USA |
| Supercompetent *E. coli* XL1Blue cells | Promega Corporation, USA |
| T4 DNA Ligase | Promega Corporation, USA |
| Urea | Amersham Biosciences, USA |
| *Xho* I | Amersham Pharmacia Biotech, USA |
| Zoom® Carrier Ampholytes 3-10 | Invitrogen Life technologies, UK (Cat. No. ZM0021) |
| Zoom® Carrier Ampholytes 4-7 | Invitrogen Life technologies, UK (Cat. No. |

| | |
|---|---|
| | ZM0022) |
| Zoom® IPGRunner™ Cassette | Invitrogen Life technologies, UK (Cat. No. ZM0003) |
| Zoom® Strip pH 3-10NL | Invitrogen Life technologies, UK (Cat. No. ZM0011) |
| Zoom® Strip pH 4-7 | Invitrogen Life technologies, UK (Cat. No. ZM0012) |

## A2

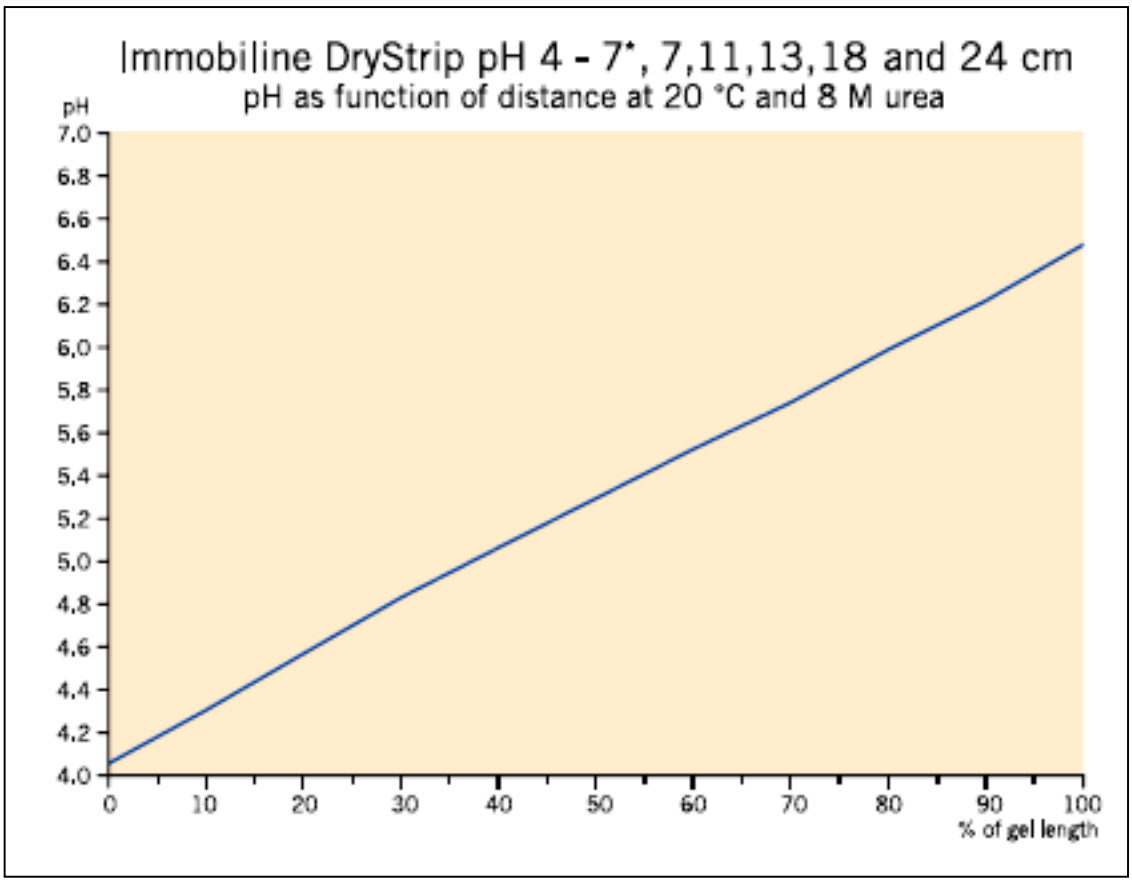


**Appendix A2:** Technical data obtained from Amersham at www.amershambiosciences.com. When IPG strips with a linear pI range were used, the approximate pI's of the spots resolved by 2D gel electrophoresis were estimated by calculating the distance migrated by the spot as a percentage of gel length and reading off the pI from a graph of pH vs percentage of gel length generated by Amersham.

## A3 Preparation of Supercompetent Cells

A colony of *E.coli* cells was selected from a 2 x Yeast-Trpytone (YT) agar plate (1.6 g tryptone, 1 g yeast, 1.5 g agar, 0.5 g NaCl in 100 mL deionized water, prepared and sterilized before use) and used to inoculate 25 mL of 2 x YT broth (1.6 g tryptone, 1 g yeast, 0.5 g NaCl in 100 mL deionized water, prepared and sterilized before use). The culture was allowed to grow overnight at 37$^{o}$C. The following day, the culture was diluted in fresh 250 mL of 2 x YT broth in a ration of 1:10 and allowed to grow for three hours until the culture reached log phase ($A_{600}$ = 0.3-0.6). The cells were collected by centrifugation at 5000 g for 15 minutes at 4$^{o}$C in sterile centrifuge tubes. The cell pellet was then resuspended in 25 mL of ice-cold $MgCl_2$ (0.1 M) and left to stand in ice for 20 minutes. The cell suspension was centrifuged as before and pellet resuspended in in 12.5 mL of ice-cold $CaCl_2$ (0.1 M). The suspensions were incubated on ice for 2 hours and the cells were again collected by centrifugation as before and cel pellet was resuspended in 2.5 mL $CaCl_2$. 100 μL of cell suspension was mixed with equal volume of sterile 30% glycerol, and stored at –80$^{o}$C for future use.

## A4 Transformation of Supercompetent Cells

Separate aliquots of supercompetent *E.coli* cells (100 μL) were incubated with aliquots of ligation products or appropriate plasmids (2 μL of 50 ng/μL) or sterile deionized triple-distilled water (2 μL) as a negative transformation control. The reactions were incubated on ice for 30 minutes. Each transformation reaction was then heat pulsed for 30 seconds at 42$^{o}$C in a dry heating block, and then placed on ice for 2 minutes. Sterile 2 x YT broth (800 μL of 1.6% tryptone, 1 % yeast extract, 0.5% NaCl) preheated to 42$^{o}$C was added to each transformation reaction, before incubation at 37 $^{o}$C for 1-3 hours with shaking. The transformation reactions were then centrifuged at 5000 g for 1 minute, the supernatent partially removed (800 μL) and the cell pellets resuspended in the remaining supernatent

(100 μL) and plated out onto sterile 2 x YT agar plates containing 0.1 mg/mL ampicillin. The plates were then incubated at 37 $^{o}$C for 16 hours.

## A5 Induction Studies

A colony of *E.coli* cells successfully transformed with the desired plasmid, was selected from a 2 x YT agar plate and used to inoculate 25 mL of 2 x YT broth containing 0.1 mg/mL ampicillin, with shaking, overnight at 37$^{o}$C. Overnight cultures were then diluted 1:10 into sterile 2 x YT broth (225 mL) containing 0.1 mg/mL ampicillin and incubated at 37$^{o}$C with shaking until mid-log phase was reached ($A_{600}$=0.6-1). The cultures were then induced with the addition of isopropyl-1-thio-β-D-galactopyranoside (IPTG; final concentration of 1 mM) and allowed to grow for another five hours. Samples (1 mL) were taken hourly before induction, as well as for the five hours after induction. Each 1 mL sample was centrifuged at 13000 rpm on a benchtop centrifuge for 1 minute, and resuspended in 150 uL of PBS for every 0.5 absorbance unit at $A_{600}$. The samples were then treated with SDS-PAGE sample loading buffer and resolved by SDS-PAGE for visual anaysis.

## A6 Expression and Purification of GST-Tagged Proteins

Exponentially growing *E.coli* cells carrying pGEX3X derived plasmid constructs were induced for 5 – 6 hours at 37°C with 1 mM IPTG. The cells were harvested by centrifuging at 3000 g for 10 minutes and resuspending the pellet in one-hundredth-culture volume of ice-cold phosphate-buffered saline (PBS; 137 mM NaCl, 2.7 mM KCl, 4.3 mM $Na_2HPO_4$, 1.4 mM $KH_2PO_4$, pH 7.3) containing PMSF (1 mM). This was followed by lysis of the cells by sonicating at 60 Amps for 30 seconds thrice, on ice. The lysis procedure was further enhanced by incubating the sonicate with Triton X-100 to 1%

final concentration and incubating at room temperature with gentle agitation for 30 minutes. The extracts were clarified by centrifugation at 12000 *g* for 30 minutes at 4°C.

Lyophilized glutathione agarose powder was allowed to swell in deionized water at a dilution of 2 mL / 10 mg overnight (4$^{o}$C). Aliquots of clarified cell extracts were added to 50 % (w/v) slurry of glutathione-agarose beads (250 µL for extracts obtained from an initial culture volume of 250 mL) previously equilibrated with PBS. Binding was allowed to occur for 1 hour at 4°C with gentle inversion. The beads were washed extensively with ice-cold PBS and then the bound GST fusion proteins were eluted by adding appropriate volume of the elution buffer (10 mM reduced glutathione in 50 mM Tris-HCl, pH 8.0). Eluted GST fusion proteins were analyzed by SDS-PAGE. Both unmodified GST-Hop and its mutant proteins were expressed and purified to typical yields of 1-3 mg/mL.

## A7 Bradfords Assay

A 96-well plate was used to contain the various protein samples diluted to 10 µL in each well. Bradfords reagent (200 µL) was added to the samples and allowed to stand for 5 minutes at room temperature. Absorbance values at A595 were then monitored and read against a standard curve constructed from known dilutions of BSA (2 mg/mL stock solution).

## A8 Site Directed Mutagenesis

All mutations were carried out by site-directed mutagenesis using a double-stranded whole plasmid linear amplification procedure (QuikChange mutagenesis kit; Stratagene). The following reagents were set up in 0.2 mL PCR tubes:

**Control Reaction**

| **Reagent** | **Volume (µL)** |
|---|---|
| Sterile deionized water | 39.5 |
| 10 x Reaction buffer | 5 |
| pWhitescript 4.5 kb control plasmid (5 ng/µL) | 2 |
| Oligonucleotide primer #1 (125 ng/µL) | 1.25 |
| Oligonucleotide primer #2 (125 ng/µL | 1.25 |
| DNTP mix | 1 |
| **Total Volume** | **50** |

**Test Reaction**

| **Reagent** | **Volume (µL)** |
|---|---|
| Sterile deionized water | 39.5 |
| 10 x Reaction buffer | 5 |
| Template DNA (100 ng/µL) | 1 |
| Forward primer (125 ng/µL) | 1 |
| Reverse primer (125 ng/µL) | 1 |
| DNTP mix | 1 |
| **Total volume** | **50** |

*PfuTurbo* DNA polymerase (1 μL) was added to final volumes of control and test reactions and submitted to the following cycling parameters for site directed mutagenesis:

| Segment | No. of cycles | Temperature ($^{o}$C) | Time |
|---|---|---|---|
| 1 | 1 | 95 | 30 seconds |
| 2 | 12-18 | 95 | 30 seconds |
| | | 52 | 1 minute |
| | | 68 | 1 minute / kb of plasmid length |

After cycling, the reaction was allowed to cool down on ice before 1 μL of *Dpn* I restriction enzyme (10 U) was added to each reaction tube to digest any contaminating parental plasmid DNA. The mixture was incubated at 37$^{o}$C for 2 hours and final products analyzed on a 0.8% agarose gel using 10 μL of each mutagenesis product.

## A9 Restriction Endonuclease Digestion of Double-Stranded DNA

For each single and double digestion reactions, the following protocol was used:

| **Reagents** | **Volume (μL)** |
|---|---|
| Sterile de-ionized water | 16 |
| 10 x Restriction buffer | 2 |
| ds DNA (100-500 ng) | 2 |

The addition of 2 U of restriction endonuclease started the reaction. The mixture was incubated for 2 hours or more at the recommended temperature for the enzyme and the reaction was stopped by the addition of 4 μL of 6 x DNA gel loading buffer (0.25% bromophenol blue and 30% glycerol). For double digestion, restriction endonuclease enzyme that required low ionic strength buffer or low temperature was first used to digest

the DNA before adding high ionic strength buffer, or incubating at higher temperature. All DNA digests were resolved by agarose gel electrophoresis.

## A10 Agarose Gel Electrophoresis

A 0.8% agarose gel was prepared in Tris-Borate-EDTA buffer (TBE: 0.045 M Tris, 0.045 M Borate, 0.001 M EDTA, pH 8.3) buffer to a total volume of 100 mL and containing 5 μL of 10 mg/mL stock solution of ethidium bromide. The agarose gel was cast and then lowered onto an electrophoretic tank. TBE buffer was added to a depth of about 3 mm above the gel. The DNA sample (20 μL) was added to agarose gel loading buffer (5 μL of 30% glycerol v/v, 0.25% w/v bromophenol blue). All air bubbles trapped in the wells were carefully removed before loading the DNA samples with a pipetteman. *Pst* I-digested lamda DNA was resolved as a molecular marker. The leads were set such that the negatively charged DNA would move towards the anode. A voltage of 100 V was applied and the samples were allowed to migrate to 75% of the length of the gel. The DNA was visualized and photographed under ultraviolet (UV) light using the Bio-Rad's VersaDoc$^{TM}$ Model 4000 imaging system.

## A11 DNA Sequencing

DNA sequencing was performed using the ABI 3100 Genetic Analyser with a capillary electrophoresis based system. DNA samples were prepared using the QIAprep Spin Miniprep kit, and then resuspended in sterilized ultra-pure water to reduce salt contamination that may interefere with the sequencing procedure. The reactions for thermocycling were conducted by preparing 250-500 ng of DNA mixed with 3.2 pmol of primer. The total volume of DNA and primer was made up to 12 μL using sterile triple distilled water. To this mixture, 8 μL of BigDye V3.1 was added prior to the amplification.

The amplification was carried out as follows:
Rapid thermal ramp to 96$^{o}$C, the temperature was held at 96$^{o}$C for 10 seconds, followed by thermal ramp at 50$^{o}$C and this temperature was held for 5 seconds. This was followed by a rapid thermal ramp to 60$^{o}$C, which was maintained for 4 minutes. This amplification was repeated 30 times. The temperature was dropped rapidly to 4$^{o}$C and the product held at this temperature for collection.

The product was then cleaned using the DNA Clean and Concentrator-5 columns according to the manufacturer's instructions (Zymo Research, California, USA). The product was vacuum dried and submitted to the Rhodes University DNA Sequencing Unit for electrophoresing.

# B1 Generation of a Recombinant Antibody against GST-C334 (C-Terminus of Hop)

## B1.1 Purification of GST-fusion protein GST-C334

A plasmid encoding the GST fusion of the N-terminal truncated (amino acid residues 1-208) mouse Hop protein (GST-C334) (Odunuga *et al.*, 2003), pGEX3X1400 was transformed into supercompetent *E. coli* XL1Blue cells (Appendix A3 and A4). GST-C334 was overproduced in *E.coli* XL1Blue (pGEX3X1400) by induction with IPTG (Appendix A5) and was purified by Glutathione (GSH) – Agarose affinity chromatography (Appendix A6).

Protein concentrations were estimated using a standard Bradford's protein analysis (Appendix A7) with a standard curve generated from known concentrations of a stock solution of bovine serum albumin (BSA; 2 μg/μL). 1 mg of total purified GST-C334 was lyophilized and sent to Morphosys-Antibodies by Design (Germany), for generation of recombinant antibodies using this protein as a target.

## B1.2 Generation of recombinant antibodies

Purified GST-C334 was lyophilized and sent to MorphoSys Antibodies by Design (Germany) to custom design a human recombinant mini-antibody fragment purified from *E.coli* specific for C-terminus of mouse Hop. Purified and lyophilised bivalent antibodies of the above-mentioned properties, and in addition, carrying a C-terminal myc / 6xHis combination were obtained. Sterile triple distilled water was used to reconstitute the lyophilised preparation (final concentration of 0.71 mg/mL), aliquoted into smaller volumes and stored at –80$^{o}$C. The antibodies received were tested against NIH 3T3 mouse fibroblast cell lysate, purified GST-C334 (positive control) and *E.coli* XL1Blue cell lysate (negative control).

### B1.3 Recombinant antibody against C-terminus of Hop was generated and successfully tested

GST-C334 was induced and purified (figure B 1) as the target for the process of 'panning' so as to enrich for binding antibodies within a pre-existing library of antibody genes. Successful antibody samples were isolated, by plating out the bacteria harbouring the specific antibody genes. Purified antibody samples were received and tested by Western blot analysis. The antibody sample that showed the best results were used for all further work conducted. Western analysis of the purified bivalent mini-antibodies received, showed a positive detection in NIH 3T3 mouse fibroblast lysate (figure B 1, lane 2), purified GST-C334 (figure B 1, lane 4). The negative control did not exhibit any detection, as was expected (figure B 1 lane 3).

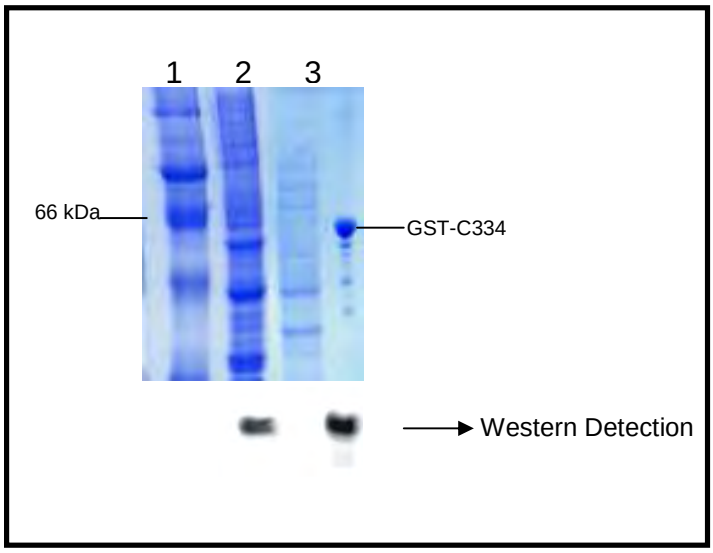


**Figure B 1: Antibody generated toward the C-terminus of Hop successfully detected Hop in positive controls.** Western detection of Hop using primary antibodies directed against C-terminus of Hop (lower panel, and indicated by an arrow) with the SDS-PAGE profile shown in the upper panel. Lane 1: Molecular weight markers; Lane 2: NIH 3T3 mouse fibroblast cell lysate; Lane 3: Cell lysate obtained from *E.col* XL1 Blue; Lane 4: purified GST-C334.

# C Oligonucleotide Primers

| Name | Sequence |
|---|---|
| mSTI1K239A (Fwd primer) | 5’ - GAG CTG GGA AAT GAT GCA TAC AAG AAG GCA GAT TTT GAC AAG – 3’ |
| mSTI1K239A (Rev primer) | 5’ - CTT GTC AAA ATC TGC CTT CTT GTA TGC ATC ATT TCC CAG CTC – 3’ |
| mSTI1K237/238/239A ( Fwd primer) | 5’ – CTG GGA AAT GAT GCA TAC GCA GCG GCA GAT TTT GAC AAG – 3’ |
| mSTI1K237/238/239A (Rev primer) | 5’ – CCT GTC AAA ATC TGC CGC TGC GTA TGC ATC ATT TCC CAG – 3’ |
| mSTI1S189E (Fwd primer) | 5’ – CCT CCT TGG GGT AGA CCT GGG CGA AAT GGA TGA AG – 3’ |
| mSTI1S189E (Rev. primer) | 5’ – CTT CAT CCA TTT CGC CCA GGT CTA CCC CAA GGA GG – 3’ |
| mSTI1T198E (Fwd primer) | 5’ – GAG GAA GAG GCG GCC GAA CCC CCA CCC CCA C – 3’ |
| mSTI1T198E (Rev. primer) | 5’ – GTG GGG GTC GGG GTT CGG CCG CCT CTT CCT C – 3’ |
| 3M SEQ FWD (sequencing primer) | 5’ - CCT AAT CTA TAC CAA AAG TTG – 3’ |
| 3M SEQ REV (sequencing primer) | 5’ – GAA TTT TCT CTG CCT GC – 3’ |